UNIVERSIDADE DE SÃO PAULO
FACULDADE DE FILOSOFIA, CIÊNCIAS E LETRAS DE RIBEIRÃO PRETO
PROGRAMA DE PÓS-GRADUAÇÃO EM BIOLOGIA COMPARADA

Estimates of body size and body mass in Caimaninae from the Miocene of South America, and contributions to their physiology

Estimativas de tamanho e massa corpórea em Caimaninae do Mioceno da América do Sul e contribuições para sua fisiologia

Ana Laura da Silva Paiva

Ribeirão Preto - SP

(2021)

UNIVERSIDADE DE SÃO PAULO
FACULDADE DE FILOSOFIA, CIÊNCIAS E LETRAS DE RIBEIRÃO PRETO
PROGRAMA DE PÓS-GRADUAÇÃO EM BIOLOGIA COMPARADA

Estimates of body size and body mass in Caimaninae from the Miocene of South America, and contributions to their physiology

Estimativas de tamanho e massa corpórea em Caimaninae do Mioceno da América do Sul e contribuições para sua fisiologia

Ana Laura da Silva Paiva

Orientadora: Profa. Dra. Annie Schmaltz Hsiou

Coorientador: Prof. Dr. Wilfried Klein

Dissertação apresentada à Faculdade de Filosofia, Ciências e Letras de Ribeirão Preto da Universidade de São Paulo, como parte das exigências para obtenção do título de Mestre em Ciências, obtido no Programa de Pós-Graduação em Biologia Comparada.

Ribeirão Preto - SP

(2021)

FICHA CATALOGRÁFICA

Paiva, Ana Laura da Silva

Estimates of body size and body mass of Caimaninae from the Miocene of South America, and contributions to their physiology.

157 p.

Dissertação de mestrado, apresentada ao Departamento de Biologia da Faculdade de Filosofia, Ciências e Letras de Ribeirão Preto/USP – Área de concentração: Biologia Comparada.

Orientadora: Hsiou, Annie Schmaltz

Coorientador: Klein, Wilfried

1. Gigantism. 2. Body proportions. 3. Ecomorphotypes. 4. Paleotemperature. 5.Body temperature.

Name: Paiva, Ana Laura da Silva

Title: Estimates of body size and body mass of Caimaninae from the Miocene of South America, and contributions to their physiology.

Dissertation presented at the Faculdade de Filosofia, Ciências e Letras de Ribeirão Preto da Universidade de São Paulo, to obtain a Master in Sciences degree, area of Comparative Biology.

Approved in:

Examination board

Prof. Dr.---------- Institution: ----------

Verdict: ----------

Prof. Dr.---------- Institution: ----------

Verdict: ----------

Prof. Dr.---------- Institution: ----------

Verdict: ----------

Acknowledgments

First, I would like to thank myself, for being so strong in hard moments, and even though keep this research working. Sometimes I thought I cannot handle this, but I managed.

Thank my supervisor Annie Hsiou, for having provided me this experience, for allowing me to begin a project in her lab, and to increase as a researcher in the academic area. Also, I want to thank my co-supervisor Wilfried Klein, for all the patience, support and help, contributing to the dissertation as a physiologist and researcher.

I want to thank Pedro Godoy, that even though he is not my supervisor, and even not meeting each other personally, showed all the availability to help. Additionally, thank you Marcos Bissaro and Giovanne Cidade, for also the support and some data which improved this dissertation.

Thanks to the Comparative Biology Program from Faculdade de Filosofia, Ciências e Letras de Ribeirão Preto, and I show my gratitude to Vera Cassia Cicilini de Lucca, for all the assistant, and being so patient with me. Thanks to the Coordenação de Aperfeiçoamento de Pessoal de Nível Superior (CAPES), for the financial support.

I am greatful to the Paleontology Laboratory, and all my friends: Bruna Farina, Fellipe Muniz, Flávia Servo, Francisco Neto, Gabriel Ferreira, Gabriel Mestriner, Guilherme Hermanson, Gustavo Darlim, João Kirmse, Julian Gonçalves, Mario Bronzati, Max Langer, Silvio Onari, Thiago Fachini. Thank you, guys, for all the talks, laughs, and help. All of you have a specific personality that makes you so unique, and I love to spend time with you. A special thank you to Wafa Alhalabi, for being so friendly with me in a hard time, for all the good moments with you, for your advice, and for all the teachings.

I would like to thank my friend Isabela Dias, for all the support and for being so friendly with me since the undergraduate, and to the friends of Ribeirão Preto Pamela Januario and Sabrina Alves for all the good moments with wines, talkings, and advice.

And finally, but not least important, to all my family (my mother, my father, brothers, sister, and grandmother), for all the patience with me, the support, and the good moments that we had as a family.

ABSTRACT

Crocodyliforms are a clade of Archosauria that originated in the late Triassic, containing a wide array of extinct and extant species, especially the crown-group Crocodylia, which diversified in the Cenozoic. The group includes the living gharials, crocodiles, alligators, and caimans, in addition to the extinct representatives. Among those, the Crocodylia species of the Miocene of South America are known for their peculiarities, such as cranial shape and greatly varying body size, as well as distinct behavioral and ecological niches. Regarding the crocodyliform lineage exist several studies about their evolutionary history, ecology, and body shape, mainly within Caimaninae. This group was morphologically diverse, which could be explained by biotic and abiotic factors in the middle and late Miocene, suggesting an opportunity to better study the evolutionary history. They can be found in three main geological units: Honda Group (Colombia), Solimões Formation (Brazil), and Urumaco Formation (Venezuela), which shared similar biodiversity and paleoenvironment. In particular, three species demonstrate this rich diversity of the group in the epoch: *Acresuchus*, *Mourasuchus*, and *Purussaurus*. Estimates of the total length and body mass of fossil Caimaninae are important to understand ecological and physiological factors that could have impacted their body size evolution. More than that, in many other groups of ectothermic animals, the body mass is correlated with abiotic factors. The first chapter of this dissertation will give a brief overview of the Crocodyliforms, especially Caimaninae, and their different morphotypes. In the second chapter, biotic factors related to body size and mass of three fossil caimanines will be analyzed, discussing their implications and comparing different methods for the estimation of body size and mass. The third chapter uses the abiotic factor of paleotemperature to discuss the thermophysiology of large extinct caimanine crocodilians.

Keywords: Gigantism; body proportions; ecomorphotypes; paleotemperature; body temperature.

RESUMO

Crocodyliformes é um clado de Archosauria que originou no fim do Triássico, contendo uma grande variedade de espécies extintas e viventes, em especial o grupo-coroa Crocodylia, que se diversificaram no Cenozoico. O grupo inclui os gaviais, crocodilos, aligátores e caimans viventes, além de representantes já extintos. Entre esses, as espécies de Crocodylia do Mioceno da América do Sul são conhecidas por suas peculiaridades, como formatos cranianos e tamanhos corpóreos variados, além de comportamentos e nichos ecológicos distintos. Em relação a linhagem dos crocodiliformes, existem diversos estudos sobre sua história evolutiva, ecologia e formas corpóreas, principalmente dentro de Caimaninae. Esse grupo era morfologicamente diverso o que poderia ser explicado por fatores bióticos e abióticos no Mioceno médio e superior, oferecendo uma oportunidade de se estudar melhor sua história evolutiva. São registrados em três unidades geológicas principais: Grupo Honda (Colômbia), Formação Solimões (Brasil) e Formação Urumaco (Venezuela), que compartilham uma paisagem paleoambiental e biodiversidade semelhantes. Em particular, três espécies demonstram a rica diversidade do grupo na época: *Acresuchus*, *Mourasuchus* e *Purussaurus*. Estimar o tamanho total e a massa corpórea desses fósseis Caimaninae é importante para entender os fatores ecológicos e fisiológicos que poderiam ter influenciado na evolução de seus tamanhos corpóreos. Mais do que isso, em diversos outros grupos de animais ectotérmicos, a massa corpórea está correlacionada com fatores abióticos. O primeiro capítulo desta dissertação será dado uma visão geral dos Crocodyliformes, em especial Caimaninae e seus diferentes morfótipos. No segundo capítulo, fatores bióticos relacionados ao tamanho e massa desses três fósseis caimanines serão analisados, discutindo suas implicações e comparando diferentes métodos para a estimativa de tamanho e massa. O terceiro capítulo utiliza os fatores abióticos de paleotemperatura para discutir a termofisiologia de grandes crocodilianos caimanines extintos.

Palavras-chave: Gigantismo; proporções corpóreas; ecomorfótipos; paleotemperatura; temperatura corpórea.

Summary of Contents

General background

The present Master dissertation comprises two chapters focusing on aspects of the body mass and body size of extinct caimanine crocodilians from the Miocene of South America. In summary, this study analyzed three peculiar caimanines: *Acresuchus*, *Mourasuchus,* and *Purussaurus*. Estimating the total length and body mass of these Caimaninae fossils is important to understand the ecological and physiological factors that drove their ecomorphological disparity, mainly within body size. Besides this, the temperature is important to infer issues regarding physiology, behavior, survival, and why they became so large. In this way, the present section aims to provide a brief overview of the fossil record of Caimaninae that introduces the main issues that permeate the next two chapters of the Dissertation.

CROCODYLIFORMES OVERVIEW

Together with birds (Aves), Crocodyliformes are the only lineage of Archosauria with living species, the group of reptiles that also includes non-avian dinosaurs and pterosaurs (Nesbitt, 2009). Although less diverse than birds today, Crocodyliformes are a group with a taxonomically rich fossil record, which is reflected in a great morphological disparity observed throughout the Mesozoic and the Cenozoic (Bronzati et al., 2015; Mannion et al., 2015). Due to the recent discovery of fossils, Crocodyliformes has become an excellent group for studies documenting evolutionary patterns (Bronzati et al., 2015; Godoy et al., 2019; Mannion et al., 2019; Gearty & Payne, 2020; Godoy, 2020) related to their extensive morphological changes in the deep past, since their origins in the Late Triassic, more than 200 million years (Ma) ago (Bronzati et al., 2015). Most crocodyliform species belong to the clade Mesoeucrocodylia, which is formed by two large subgroups: Notosuchia, comprised of predominantly terrestrial crocodyliforms, and Neosuchia, which were mostly aquatic or semi-aquatic (Bronzati et al., 2015), and their oldest fossil record dates from the Early Jurassic (Tykoski et al., 2002 *apud* Bronzati et

al., 2015). However, much of the diversity of Mesoeucrocodylia, along with many other non-crocodyliform groups, decreased throughout the Cenozoic, with surviving taxa belonging mostly to neosuchians, which includes the crown-group Crocodylia (Brochu, 1999; Bronzati et al., 2015; Cidade et al., 2019). Crocodylia originated in the Late Cretaceous, but diversified mostly throughout the Cenozoic, becoming the predominant crocodyliform group when considering number of species (Brochu, 2003; Cidade et al., 2019). This success in terms of diversity is also reflected in morphological variation, with great cranial morphological disparity, varying body dimensions, occupying distinct habitats and ecological niches, diverse diets, and complex behaviors (Cidade et al., 2019; Godoy et al., 2019).

Crocodylia (Figure 1) is defined as the group that includes the most recent common ancestor of *Alligator mississippiensis, Crocodylus niloticus,* and *Gavialis gangeticus* and all their descendants (Brochu, 2003), and its oldest fossil record dates from the Late Cretaceous (Mateus et al., 2019). This group includes three main lineages: Crocodyloidea, Gavialoidea, and Alligatoroidea, the last one being formed by all the crocodilians closer to *Alligator mississippiensis* than to *Crocodylus niloticus* and *Gavialis gangeticus* (Brochu, 1999; 2003). Alligatoroidea is a very diverse lineage throughout the Neogene, with the oldest fossil records dating from the Late Cretaceous of North America (Mook, 1942; Wu et al., 1996; Brochu, 1999). Alligatoroids spread out to almost all continents, with some important representatives including *Diplocynodon* (in Europe), *Protoalligator* (Asia), and many Caimaninae species (South America) (Brochu, 2003). The group consists of two subclades: Alligatorinae and Caimaninae (Figures 1 and 2), the last one being defined as the crocodilians closer to *Caiman crocodilus* than *Alligator mississippiensis* (Brochu, 1999; 2003). While Alligatorinae shows a Laurasian distribution (both in terms of fossils and living species), Caimaninae is predominant in South America (Brochu, 2003). It is suggested, however, that the fossil record of the group originated in North America and dispersed to the south of the continent during the Late Cretaceous or Early Paleocene (Brochu, 1996 *apud* Cidade et al., 2017; Cidade et al., 2019; Walter et al., 2021). The oldest fossil records come from

the Cretaceous-Paleogene of the United States (*Bottosaurus harlani* and probably *Chinatichampsus wilsonorum*; Cossette & Brochu, 2018; Stocker et al., 2021), followed by records in the Paleocene of Argentina (*Eocaiman palaeocenicus*, *Notocaiman stromeri*, *Necrosuchus ionensis*, *Protocaiman peligrensis*; Rusconi, 1937 *apud* Brochu, 2011; Simpson, 1937; Bona, 2007; Pinheiro et al., 2013; Bona et al., 2018), and records from the Paleocene of Brazil (*E. itaboraiensis*; Pinheiro et al., 2013). In the Eocene, South America caimanines are represented by the genus *Eocaiman* (Simpson, 1933), whereas more fossils are known from North America (e.g., *Orthogenysuchus olseni*, *Tsoabichi greenriverensis*, *Bottosaurus harlani*) and Central America (e.g., *Culebrasuchus* and *Centenariosuchus*) (Brochu, 2011; Hastings et al., 2013; Cidade, 2015; Cidade et al., 2020a).

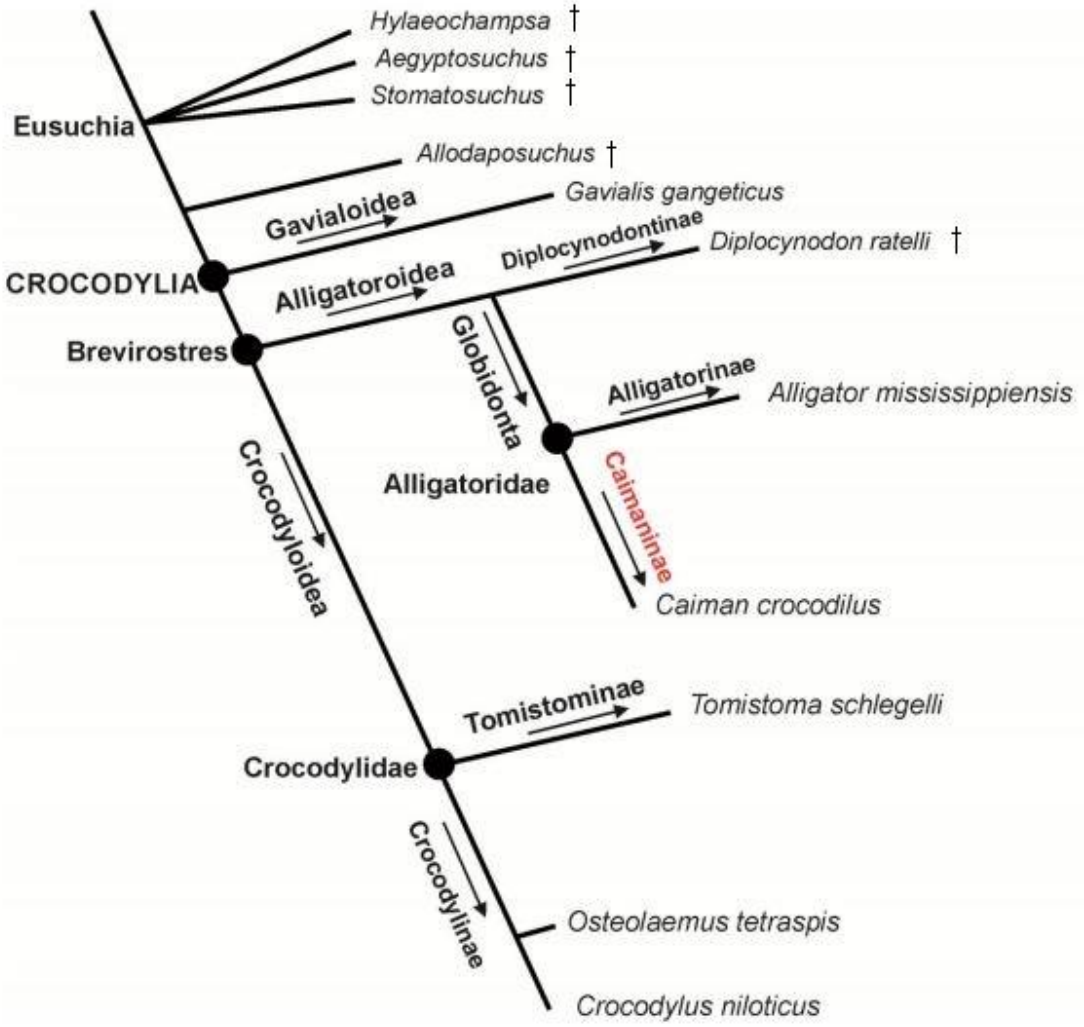

Figure 1 Phylogenetic relationship between Crocodylia groups. The extinct species are indicated by the symbol †. Taken and modified from Godoy (2014).

CAIMANINES FROM THE NEOGENE OF SOUTH AMERICA

The Neogene was marked by a seasonal climate (Flower & Kennett, 1994), between cooling and warming periods that had impacts on the diversity of the paleofauna, mainly during the Miocene of South America (Antoine et al., 2016). The diversity was mostly observed in the reptilian fauna, especially in fossil crocodyliforms, as the climatic conditions were favorable for their diversification. Caimanines are found in several fossiliferous deposits in northern South America (Riff et al., 2009). Many locations in that region have demonstrated the apex of the crocodyliforms diversity in different ecomorphotypes, such as Peru, Bolivia, Venezuela, Argentina, and Brazil, demonstrating the presence of a similar paleoenvironmental landscape composed by a large fluvial-lacustrine system, interpreted as being favorable for the group's survival during the Miocene (Hoorn et al., 2010a; 2010b; Latrubesse et al., 2010). According to Hoorn et al. (2010a; 2010b), Jaramillo et al. (2017), and Sá et al. (2020), the Andean uplift, the emergence of the current Amazon basin, and the marine incursions provided not only a complex ecosystem and a favorable climate but also abundant diversity of species in the Proto-Amazon landscape.

The Andes Cordillera uplift had its first peak in early Miocene, but its intensity happened in the middle Miocene, bringing together recurrent rainfall that, consequently, supplied water for a very large system of swamps and lakes, known as the Pebas Lake or Pebas System, resulting in a fluvial/continental paleoenvironment (Hoorn et al., 2010a; Latrubesse et al., 2010). This system was inhabited by small invertebrates serving as prey for many crocodyliforms. In addition, other abiotic factors may have contributed to this mega-diversity, such as the Cretaceous-Paleogene extinction (Riff et al., 2009; Cidade et al., 2019) and the increase in temperature during the middle Miocene, denominated as *Miocene Climatic Optimum*, in which there was a warming event in this epoch around 15.6 Ma, as suggested by low oxygen isotope ($\delta^{18}O$) levels (Böhme, 2003; Holbourn et al., 2015; Steinthorsdottir et al., 2021).

The Miocene (23.03 - 5.33 Ma) was an epoch rich in diversity of crocodylian caimanines (Cidade et al., 2019). Caimanines are a very abundant group (Figure 2) including several cranial shapes, great overall morphological disparity, reaching different body sizes (Bona et al., 2012; 2013; Cidade et al., 2019), from small to large sizes, occupying different habitats, food resources, niches (Aguilera et al., 2006; Riff et al., 2009; Cidade, 2015; Cidade et al., 2019) that are less present in recent groups (Cidade et al., 2019). Nowadays, the group comprises three living genera *Caiman*, *Melanosuchus*, and *Paleosuchus*, represented by six species: *C. latirostris*, *C. crocodilus*, *C. yacare*, *M. niger*, *P. palpebrosus*, and *P. trigonatus*, exclusive to South America, except *C. crocodilus*, which can be found in Central America and Mexico (Cidade et al., 2017; Cidade et al., 2019). However, the fauna of extant caimanines is incomparable with the diversity that existed during the middle and late Miocene.

Regarding the fossil record, caimanines are found in several fossiliferous localities concentrated mainly in the Middle Miocene of Colombia (Honda Group) and Peru (Fauna Fitzcarrald and Pebas Formation), and in the Late Miocene of Argentina (Ituzaingó Formation), Venezuela (Urumaco Formation) and Brazil (Solimões Formation). For the Middle Miocene, several caimanines have been recorded for the Honda Group (Colombia), showing a great diversity of crocodilians, such as *Caiman* sp., *Eocaiman* sp. (Langston, 1965), *Paleosuchus*, *Mourasuchus atopus* (Langston, 1965; Salas-Gismondi et al., 2015), and *Purussaurus neivensis* (Mook, 1942; Salas-Gismondi et al., 2015). Moreover, the Pebas Formation (Peru) also contains a diversity of caimanines, among them *Gnatusuchus*, *Kuttanacaiman*, and *Caiman wannlangstoni* (Scheyer et al., 2013; Fortier et al., 2014; Salas-Gismondi et al., 2015; Scheyer & Delfino, 2016). Along with these two localities, the Fitzcarrald Arch, Peru, exhibits a very similar fossil biota, rich in crocodyliforms, indicating a very diverse paleoenvironment (Salas-Gismondi et al., 2007; Negri et al., 2009).

However, the abundance of fossils is found mainly in the beginning of the Late Miocene localities. The Solimões (Brazil) and Urumaco (Venezuela) formations, all together, represent the greatest diversity of caimanine fauna from the Neogene of South America. The Ituzaingó Formation

(Argentina), the Pisco Formation (Peru), and Yecua Formation (Bolivia) are also represented by the group but are less diverse than in the previous ones (Cidade et al., 2019). These geological units represented a favorable environment for the evolution of these crocodyliforms since they share many taxa and contain an abundance of ecomorphotypes.

In the Ituzaingó Formation, *Mourasuchus arendsi*, *Caiman latirostris*, *C. australis*, *C. lutescens*, *Paleosuchus* species, and many other fossils have been described (Salas-Gismondi et al., 2007; Bona & Carabajal, 2013; Bona et al., 2013; Cidade et al., 2019). The Urumaco and Solimões localities are the largest geological units with several fossil records, represented by a very diverse fauna (Aguilera, 2004; Negri et al., 2009; Riff et al., 2009; Latrubesse et al., 2010; Cidade et al., 2019; Lacerda et al., 2020). The Urumaco Formation is constituted by *Caiman brevirostris* (Aguilera, 2004; Scheyer & Delfino, 2016), *C. latirotris* (Scheyer & Delfino, 2016), *Melanosuchus* sp. (Bona et al., 2015; Foth et al., 2018), *Globydentosuchus brachyrostris* (Scheyer et al., 2013; Scheyer & Delfino, 2016), *Acresuchus pachytemporalis* (Cidade & Rincón, 2021), *Purussaurus mirandai* (Aguilera et al., 2006), and *Mourasuchus arendsi* and *M. pattersoni* (Riff & Aguilera, 2008; Riff et al., 2009; Scheyer et al., 2013; Cidade et al., 2017; Cidade et al., 2019). In Brazil, the Solimões Formation is represented by small and medium-sized caimans, similar to those of the genus *Caiman* (*C. brevirostris*, *C. yacare*, Bona et al., 2012; Fortier et al., 2014), *Melanosuchus* (Souza-Filho et al., 2020; Lacerda et al., 2020), as well as the large caimanines *Mourasuchus arendsi*, *M. amazonensis*, and *Purussaurus brasiliensis* (Barbosa-Rodrigues, 1892; Price, 1967; Aguilera et al., 2006; Riff & Aguilera, 2008; Negri et al., 2009; Riff et al., 2009; Souza et al., 2016), in addition to the medium-sized *Acresuchus pachytemporalis* (Souza-Filho et al., 2018). For more details on the fossils found in the South American formations, see Cidade et al. (2019).

Hydrographic and sedimentary basins were formed during the Miocene and are currently located in the Acre and Amazonas states, giving rise to a huge and complex environment rich in biodiversity (Hoorn et al., 2010a; Lacerda et al., 2020; Sá et al., 2020), mainly in Crocodylia. Different morphotypes

including elongated, flattened, wide, or even generalized snout forms (Aguilera et al., 2006; Cidade et al., 2017), small to large body sizes, were evident due to several biotic and abiotic factors, giving rise to this species richness (Hoorn et al., 2010a). Thus, the different northern South American localities indicate the similarity of faunas (Cozzuol, 2006; Sanchez-Villagra & Aguilera, 2006; Latrubesse et al., 2010), and only the Ituzaingó Formation (Argentina) shares the same fauna outside of the Amazon basin (Riff et al., 2009), which raises interesting questions from a biogeographical point of view.

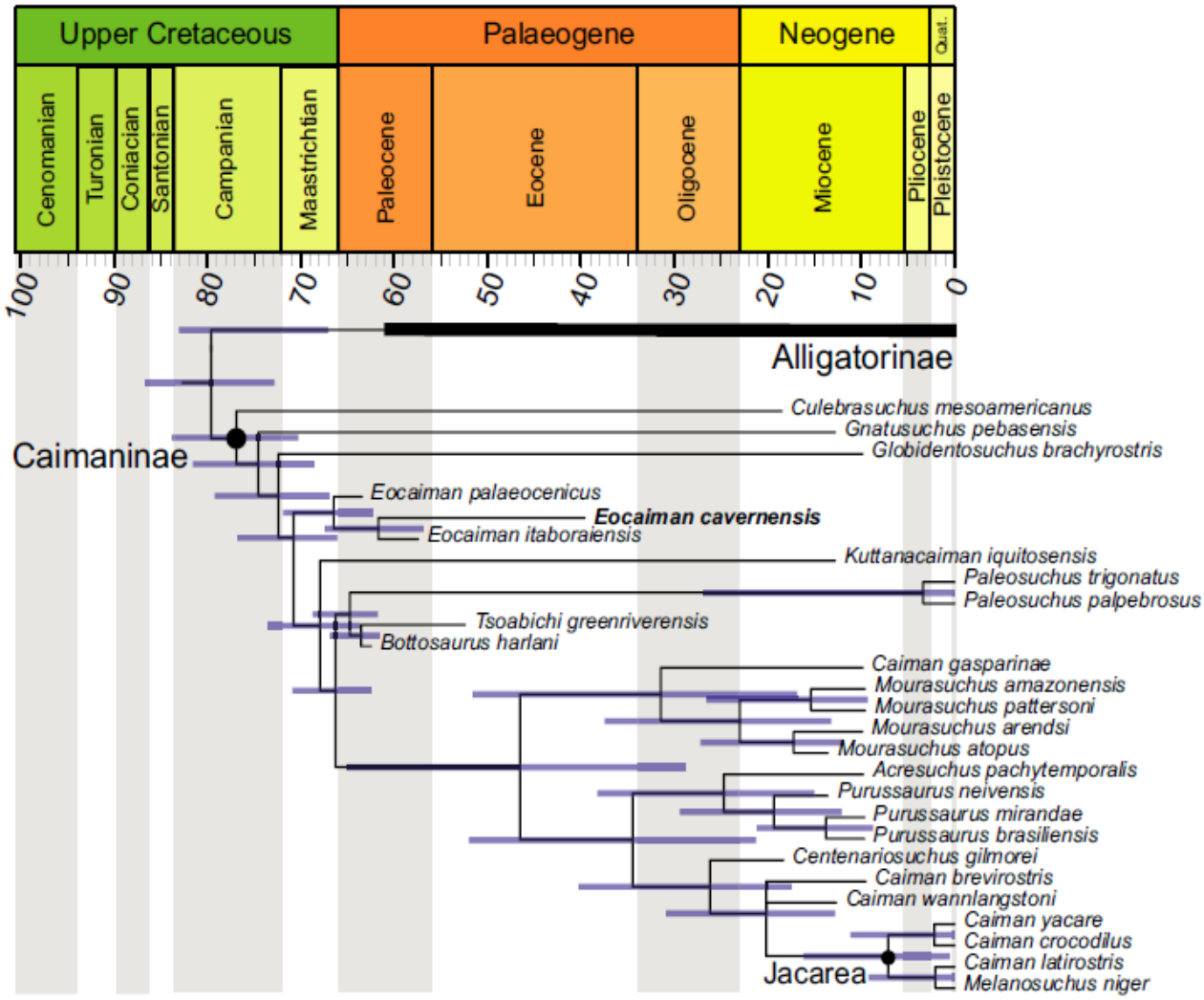

Figure 2 More recent relationship phylogeny within Caimaninae. Taken from Godoy et al. (2021).

ECOMORPHOTYPES AND GIGANTISM

Crocodyliforms have been interpreted by the characteristics that made them unique, due to morphological differences, food specializations, habitats, niches (Riff et al., 2009; Cidade et al., 2019), and in particular the cranial disparity (Wilberg, 2017; Godoy, 2020; Godoy et al., 2019). Most of these features are reflected by the shape of the snout, the result of an ecological specialization of each group, with an emphasis on the diet (Gignac & O'Brien, 2016; Godoy, 2020). This is quite evident during the Neogene, a period during which several large-sized taxa evolved, mainly between the middle and late Miocene (Riff et al., 2009; Scheyer et al., 2013). This is consistent with a recent survey by Godoy (2020), who analyzed cranial shapes in various crocodyliforms and noted high correlations with body sizes.

In general, there are six ecomorphotypes among crocodyliforms in the Miocene that are directly related to their habitat and/or their ecology: terrestrial predators, dominated by sebecids (Langston, 1965; Paolillo & Linares, 2007 *apud* Brochu, 2011); large and semi-aquatic top predators, such as *Purussaurus* (Aguilera, 2004; Aguilera et al., 2006; Aureliano et al., 2015); durophages, such as *Caiman wannlangstoni*, *C. brevirostris*, *Balanerodus*, *Kuttanacaiman*, *Globidentosuchus*, and *Gnatusuchus* (Langston, 1965; Salas-Gismondi et al., 2015); the semi-aquatic "gulp-feeder" *Mourasuchus* (Langston, 1965; Cidade et al., 2017; 2019); the piscivores gavialoids and some crocodyloids (Bocquentin-Villanueva & Buffetaut, 1981); and, finally, the small to medium-sized generalists like *Acresuchus*, some species of the genus *Caiman*, *Melanosuchus*, and *Paleosuchus* (Souza-Filho et al., 2018). Caimaninae predominates regarding different ecomorphotypes, representing four of the six types. On the other hand, body size issues are also quite curious within the group, with caimanines reaching between small, medium, and even gigantic proportions. In recent years, studies estimating body size of extinct crocodyliforms have been analyzed based on other body parameters with high correlations, such as the skull (Aureliano et al., 2015; O'Brien et al., 2019; Cidade et al., 2020b).

Three notable caimanines stand out composing this great diversity of the group (Figures 3 and 4), due to their huge body sizes and some atypical and very curious features that have raised the interest of several researchers in the last years (Aguilera et al., 2006; Aureliano et al., 2015; Souza- Filho et al., 2018; Cidade et al., 2020b; Solórzano et al., 2020). Among those, the extinct caimanine *Mourasuchus* shows a very peculiar skull morphology (Figure 3B) such as a long, wide, and dorsoventrally flattened rostrum, resembling a "duck's-face" (Langston, 1965; 2008; Bona et al., 2012; 2013; Riff et al., 2012; Cidade et al., 2017). Its delicate jaws showing small teeth indicate that this genus was not an active predator and that it could not feed on large preys (Langston 1965; 2008; Tineo et al., 2015), suggesting that it was an animal feeding by engulfment, recently denominated as "gulp-feeder" by Cidade et al. (2017). The hypothesis that it was not an active animal, that is, it is a sit-and-wait animal, could agree with the study of Cidade et al. (2020b). Based on their anteroposteriorly short cervical vertebrae, they estimated the "death-roll" ability, typical of crocodilians to subdue their prey, suggesting that *Mourasuchus* would not be capable of such an action. Their diet was based on small fish, bivalves, gastropods, and crustaceans (Langston, 1965; Cidade et al., 2017) that were "engulfed" in large quantities.

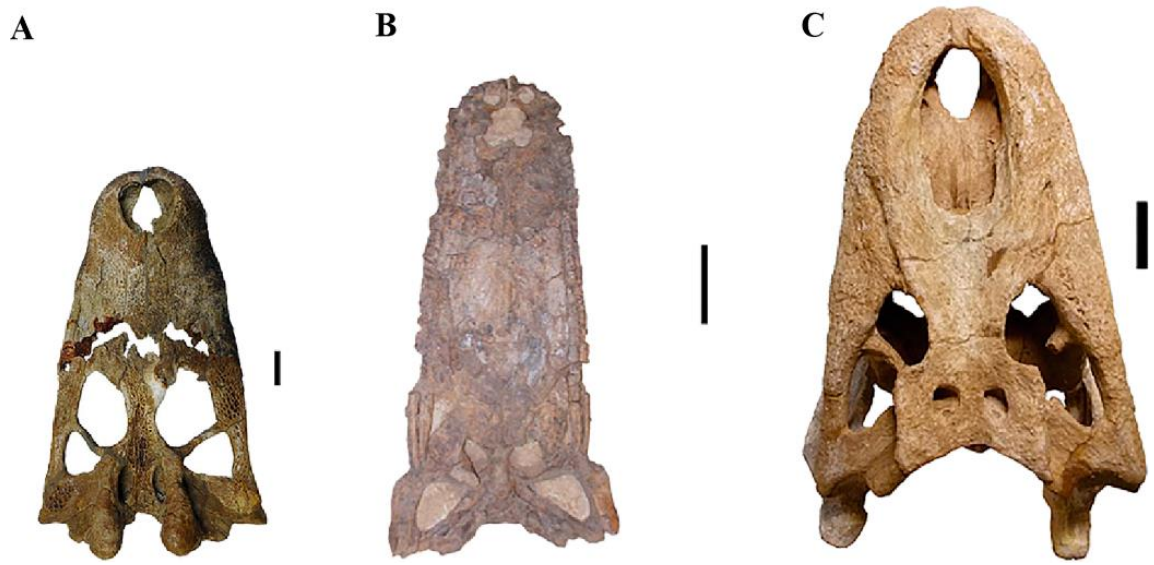

Figure 3 Skull of the three most peculiar caimanines from the Miocene of South America. A - represented by *Acresuchus pachytemporalis* (scale bar = 5 cm); B - represented by *Mourasuchus amazonensis* (scale bar = 20 cm); and C - represented by *Purussaurus brasiliensis* (scale bar = 20 cm). Taken and modified from Cidade (2019).

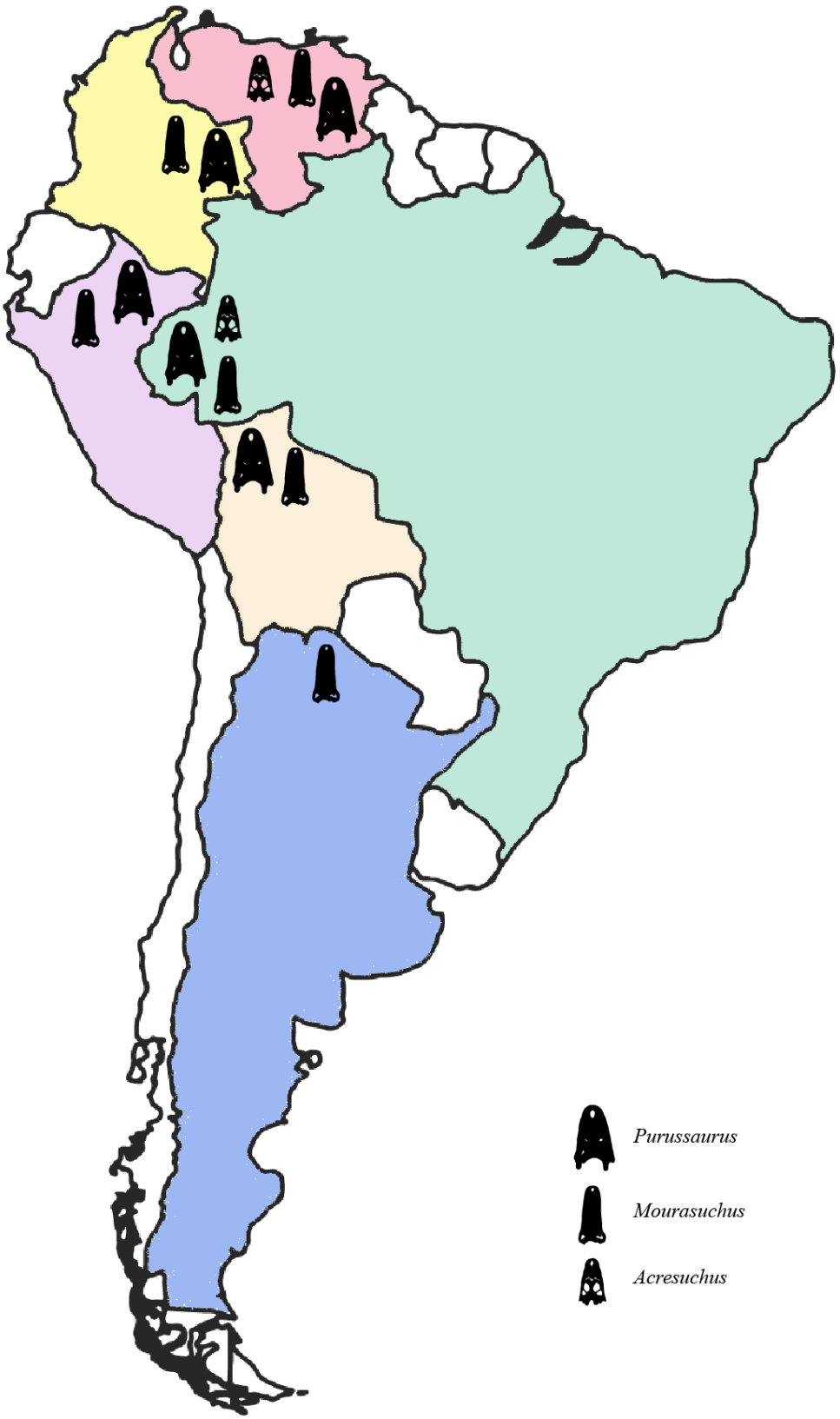

Figure 4 Occurrences of the three peculiar caimanines from the middle and late Miocene of South America: *Acresuchus* in Brazil (green) and Venezuela (pink); *Mourasuchus* in Argentina (blue), Brazil, Bolivia (beige), Colombia (yellow), Peru (purple), and Venezuela; and *Purussaurus* in Brazil, Bolivia, Colombia, Peru, and Venezuela.

In addition, recent studies have shown *Mourasuchus* as a giant caiman, measuring about 9 m and weighing 4 tons (Cidade et al., 2020b; Solórzano et al., 2020). Nowadays, *Mourasuchus* is comprised of four species: *M. amazonensis* from the late Miocene of Solimões Formation (Price, 1964); *M. atopus* from the middle Miocene of Honda Group and Pebas Formation (Langston, 1965; Salas-Gismondi et al., 2015); *M. arendsi* from the late Miocene of Ituzaingó, Solimões and Urumaco Formations (Bocquentin-Villanueva, 1984; Scheyer & Delfino, 2016); and *M. pattersoni* from the late Miocene of the Urumaco Formation (Cidade et al., 2017). Recently, *M. nativus* was considered a synonym for *M. arendsi* (Scheyer & Delfino, 2016). There are specimens also associated with the Castilletes Formation from the early Miocene of Colombia (Moreno-Bernal et al., 2016), Fitzcarrald Arch from the middle Miocene of Peru (Salas-Gismondi et al., 2007), Socorro Formation from the middle Miocene of Venezuela (Scheyer et al., 2013), and Yecua Formation from the late Miocene of Bolivia (Tineo et al., 2015). This wide distribution of the group demonstrates a great similarity in fauna shared in South American regions.

Purussaurus (Figure 3C) is considered to be one of the largest top predators ever and the largest Miocene Caimaninae in South America (Aguilera, 2004; Aguilera et al., 2006; Aureliano et al., 2015; Cidade et al., 2019; Souza et al., 2021). With a semi-aquatic habit, it could feed on other organisms of large body dimensions (e. g. large rodents such as *Neoplibema* and *Phoberomys*, turtles, and even other crocodilians), expressed by a robust dentition present in this taxon (Aureliano et al., 2015; Cidade et al., 2019). The skull of the referred material of the species *P. brasiliensis* Barbosa-Rodrigues (1892) measures about 1400 mm in dorsal length. Its total size has been estimated at over 12.5 m, with a body mass of 8 tons, and with a bite force of 69.000 N (Aureliano et al., 2015). However, even being a large crocodylian, Blanco et al. (2015) demonstrated that *P. brasiliensis* might not be able to do the "death-roll", as well as *Mourasuchus*, probably due to this robustness and large size, precluding them from making lateral movements. In addition to this species from the late Miocene of Brazil, *P. mirandai* was described from the Late Miocene of Venezuela (Aguilera et al., 2006; Scheyer & Delfino, 2016); *P. neivensis* from the middle Miocene of Colombia and Peru (Mook, 1942; Langston, 1965; Bocquentin-

Villanueva et al., 1989; Salas-Gismondi et al., 2015); and undetermined *Purussaurus* from the late Miocene of Venezuela (Aguilera, 2004). All these taxa also exhibit large and massive skulls, rounded snouts, and wide-open nostrils (Aguilera et al., 2006). There are also specimens of *Purussaurus* from the early Miocene of the Castillo Formation, Venezuela (Solórzano et al., 2019), the early/middle Miocene of the Castilletes Formation of Colombia (Moreno-Bernal et al., 2016), the middle Miocene of the Fitzcarrald Arch of Peru (Salas-Gismondi et al., 2007; 2015) and Socorro Formation, Venezuela (Scheyer et al., 2013), and to the late Miocene of Bolivia in Cobija Formation (Rusconi, 1931 *apud* Cidade et al., 2019; Fortier, 2011).

Acresuchus Souza-Filho et al. (2018) was originally described for the Solimões Formation, Brazil, and it was recently found in the Urumaco Formation, Venezuela (Cidade & Rincón, 2021). The holotype (UFAC-2505) has a well-preserved skull, large orbits, and a circular external nostril. Additionally, it is different from other caimanines due to the presence of an eminence in the squamosals that forms a "horn" in the posterior portion of the cranial roof, which could be used as a “social display” (Souza-Filho et al., 2018). *Acresuchus* is considered a generalist predator (Souza-Filho et al., 2018; Cidade & Rincón, 2021), feeding on small invertebrates to fish and small mammals, but the suspicion of being durophagous is not ruled out (Souza-Filho et al., 2018; Cidade & Rincón, 2021). A single species represents this genus, *A. pachytemporalis* (Figure 3A), being phylogenetically positioned as *Purussaurus* sister-group (Souza-Filho et al., 2018; Godoy et al., 2020; Souza et al., 2021), leading Souza-Filho et al. (2018) to affirm that the species would be an intermediate transitional form in the evolution of *Purussaurus* gigantism.

Several researchers have tried to explain the South American Miocene crocodilian diversity. Except for the Ituzaingó Formation (Argentina), the fossiliferous localities are concentrated in the northern portion of South America, related to tropical, warmer, and wetter paleoenvironments (Cidade et al., 2019). According to Hoorn et al. (2010a), the northern geological units were part of the ancient Pebas System, which provided sediments and nutrients, supplying a mega wetland system that allowed

the crocodilian diversification of distinct ecomorphotypes and the development of large body sizes. It is known that biotic and abiotic factors could explain larger body sizes and cranial morphology (Grigg & Kirshner, 2015; Godoy et al., 2019; Godoy & Turner, 2020; Stockdale & Benton, 2021). However, studies evaluating such correlations within the group are scarce, and a detailed analysis of the large crocodilians from the Miocene seems necessary, taking into account that this great diversity of shapes and sizes raises questions about the ecomorphotype that dominated the ecosystem in northern South America. Estimating the mass and size of these caimanines is essential to infer the ancient lifestyle of these animals and how the associated paleoenvironment was like (Aureliano et al., 2015; Godoy et al., 2019; O'Brien et al., 2019; Cidade et al., 2020b; Solórzano et al., 2020). Besides, which factors made these fossil crocodilians being so gigantic and diverse? Lastly, size and body mass are highly correlated with their physiology, taking into account that they are ectothermic animals. However, the gigantism in these crocodyliforms may have been influenced their thermal physiology (Grigg et al, 1998; Seebacher et al., 1999) and the paleotemperature (Godoy et al., 2019), but detailed data regarding thermal relations of crocodilians from the Pebas system are lacking.

In summary, the present dissertation addresses reconstructing body mass and size of caimanines from the Miocene of South America. In this way, first was made a review of the body mass/size estimates previously reported to the Miocene Caimaninae from northern South America (e.g., *Acresuchus*, *Mourasuchus,* and *Purussaurus*). Consequently, we generate new and more refined data, which will help estimate the body mass/size of species/specimens for which no previous estimates are available. Second, to investigate possible correlations between paleotemperature and body size of Miocene caimanines, testing the hypothesis that temperature is one of the main factors driving the evolution of large body dimensions in this group. Third, to estimate the body temperature of late Miocene crocodilians from South America and interpret the results from an ecological and physiological perspective.

Chapter I

Body size and body mass estimates in Caimaninae from the middle and late Miocene of South America

Abstract

Crocodyliforms have been increasingly well studied due to their peculiarities and different body dimensions and shapes observed in the fossil record. The lineage of Caimaninae showing diverse extinct forms during the Neogene of South America has not yet exhaustively been investigated. Their skull shape ranges from short to long snouts, robust and flattened rostrums, and serves as a proxy for many evolutionary studies in the group. Previous works have demonstrated that the skull is a good proxy to estimate the size and mass of extinct fossils, and it is known that they are highly correlated with ecology and physiology. Therefore, an extensive database of morphometric variables, such as head width, dorsal cranial length, snout-vent length, total length, and body mass, was compiled for extant Crocodylia, and three different methods were generated to comparative estimates: (1) based on DCL measurements; 2) based on HW measurements; and, 3) based on body proportions. All these parameters were used to estimate body mass and body dimensions in caimanine fossils from the Miocene of South America. Regression analysis was performed including or excluding juvenile specimens, observing that juveniles may significantly alter regressions, and in consequence, size estimates. We created a hypothetical crocodylian based on the body proportions of living crocodilians and compare if the estimates match with it. We concluded that a huge database containing as many living crocodilians as possible, constituted by adults, considering the DCL parameter, is the best model to estimate body sizes. Hence, *Acresuchus* could reach 4.5 m and 494 kg, *Mourasuchus* with an average of 7.7 m and 2.7 tons, and *Purussaurus* reaching 8.5 m and 3.8 tons on average. This is the first study to infer body mass and size in fossil and extant crocodilians performing a comparative approach, and it is important to discuss aspects about their ecology and physiology, which could have guided the evolution of big sizes. The Pebas System, where these animals lived, was the main contributor to the evolution of gigantism, proportionating long-surviving of the group, which is also provided good resources.

Keywords: Crocodylians; body proportions; ecology; Pebas System; physiology.

Introduction

In recent years, analyzes of size and body mass have been increasingly improved in paleontology, especially within Crocodyliforms, a group with a large morphological disparity and great diversity since the Mesozoic (Godoy et al., 2019; Godoy, 2020). Living adult crocodilians reach a mass of 5 to 1000 kg, ranging from 1 to 6 m in total length, while extinct ones could surpass these measures (Gearty & Payne, 2020). To estimate body size for extinct crocodyliforms, body measures are extrapolated from living organisms (Sereno et al., 2001; Farlow et al., 2005), using a morphometric measurement of a fossil as a proxy (Godoy & Turner, 2020). Several authors have used different proxies to infer estimates of size and mass in crocodyliforms, such as the femur (Farlow et al., 2005; Young et al., 2016), vertebrae (Iijima & Kubo, 2020), head width (O'Brien et al., 2019), orbital dorsal cranial length (Hurlburt et al., 2003; Scheyer et al., 2013; Godoy et al., 2019; Mannion et al., 2019), dorsal cranial length (Sereno et al., 2001; Hurlburt et al., 2003; Riff & Aguilera, 2008; Aureliano et al., 2015; Godoy et al., 2019; Solórzano et al., 2020; Cidade et al., 2020b), or a set of varied morphological characters (Stockdale & Benton, 2021).

The skull of crocodyliforms is well studied (Wilberg, 2017) and cranial measurements are commonly used since skulls are more easily preserved, and previous studies demonstrated that the correlation between skull *vs.* total size is quite robust (Godoy et al., 2019; O'Brien et al., 2019). Besides, the skull of some crocodilians is very big, indicating that these animals have reached extreme sizes in the past (Sereno et al., 2001; Riff & Aguilera, 2008; Aureliano et al., 2015; Grigg & Kirshner, 2015). Furthermore, the ratio of total size *vs.* body mass also demonstrated great correlations (Verdade, 2000; Aureliano et al., 2015; Grigg & Kirshner, 2015; O'Brien et al., 2019), allowing the mass of extinct animals to be estimated. Body mass is of great ecological and physiological importance for ectothermic crocodilians (Grigg et al., 1998; Seebacher et al., 1999; Hurlburt et al., 2003; Seymour et al., 2012;

2013), but few studies have explored the relations between fossil crocodilians and their paleoenvironment. Therefore, estimation of size and body mass allows inferring factors such as paleoecology, paleophysiology, and the study of evolutionary patterns within the group (Aureliano et al., 2015; Godoy et al., 2019; Godoy & Turner, 2020; Iijima & Kubo, 2020; Stockdale & Benton, 2021), as well as creating new hypotheses regarding the biology of these animals.

The study of body dimensions has been largely debated within crocodyliforms, but little attention has been given to Caimaninae, a group of Crocodylia (crown-group) that includes living caimans (*Caiman*, *Melanosuchus*, and *Paleosuchus*) and their relatives; however, Caimaninae fossil record was taxonomically and morphologically diverse during the Neogene, especially the Miocene, when they dominated the tetrapod fauna of South America (Brochu, 2003; Bona et al., 2012; Cidade et al., 2019). They show a great cranial disparity, different body sizes, ranging from small to large dimensions, which are reflected by their different lifestyles, diets, and habitats (Aguilera et al., 2006; Riff et al., 2009; Cidade et al., 2019; Godoy et al., 2019). Recently, Aureliano et al. (2015) performed estimates of the size and body mass in *Purussaurus brasiliensis* using dorsal cranial measurements, inferring to have reached 12.5 m and 8 tons, pointing the species as the largest crocodylian predator that existed. Subsequently, several researchers estimated body size for other crocodilians, such as *Mourasuchus*, obtaining an average of 9 m in total length, and 4 tons of body mass (Cidade et al., 2020b), and in other crocodyliforms (see Solórzano et al., 2019; 2020).

It is known that size and body mass show good correlations with ecology and physiology (Grigg et al., 1998; Seebacher et al., 1999; Hurlburt et al., 2003; Seymour et al., 2012; 2013; Godoy et al., 2019). Regarding caimanines from the Miocene of South America, few paleoecological studies have been carried out that include estimates of body dimensions, and their relationship with biology, the group's evolution, as well as ecological and physiological aspects. Herein, body dimensions of living crocodilians were obtained from the literature to estimate the size and mass of three very peculiar fossil

caimanines (*Acresuchus*, *Mourasuchus*, and *Purussaurus*), representing the great diversity and morphological disparity within Miocene Caimaninae. Three different methods were employed to obtain body dimensions, and to be able to compare new data with previous studies, discussing their ecological and physiological implications of the body size estimates.

Materials and Methods

PROVENANCE AND GEOLOGICAL CONTEXT

The Acre Basin is a region that shows fine fluvial-lacustrine sediments and is attributed to the Solimões Formation (Hoorn et al., 2010b). This unit is located in the northwestern region of South America (Hsiou, 2010), extending from the Acre to the Amazonas states (Brazil), and also in eastern Peru and northern Bolivia (Cozzuol, 2006). It is deposited in horizontal and sub-horizontal layers, with an estimated thickness of 2200 m (Cunha, 2007), consisting of clays, sandstones, siltstones, carbonate concretions with lignite intercalations (Hoorn, 1993; Latrubesse et al., 2010), and mostly clayey rocks (Cunha, 2007; Cidade, 2015). Recently, Bissaro-Júnior et al. (2019) dated two transitional localities from the Solimões Formation, Niterói and Talismã, from 8.5 ± 0.5 Ma and 10.89 ± 0.13 Ma, respectively, confirming a late Miocene age for these fossil levels of the Acre Basin. Overall, the paleoenvironment is characterized by the Pebas and Acre System influence (Figure 5), interpreted as a complex depositional system (Sá et al., 2020), with a large fluvial system of extensive wetlands and flooding by mega lakes and swamps (Cozzuol, 2006; Hoorn et al., 2010a; 2010b; Latrubesse et al., 2010; Leite et al., 2017; Bissaro-Júnior et al., 2019), a lentic environment similar to Venezuela.

The Urumaco Formation (Figure 5), Venezuela, is also from the late Miocene (Díaz de Gamero & Linares, 1989 *apud* Sanchez-Villagra & Aguilera, 2006) and it has a thickness of approximately 2000 m (Aguilera, 2004; Linares, 2004), with several layers of sandstones, clays, limestones interspersed and siltites (Linares, 2004) that were probably deposited in a complex deltaic system (Cidade et al., 2017). This formation is divided into three members: lower, middle, and upper members (Linares, 2004; Hsiou, 2010). In general, the paleoenvironment is interpreted as fluvial channels with flood basins, with some marine influence (Linares, 2004), so it had several associations such as freshwater, savanna, estuarine

and marine incursions (Sanchez-Villagra & Aguilera, 2006). Despite this megadiverse scenario, there was recorded great biodiversity of vertebrates, among them the crocodyliforms (Riff & Aguilera, 2008), whose fauna is considered very similar to Solimões Formation (Cozzuol, 2006; Sanchez-Villagra & Aguilera, 2006).

Another northern Miocene geological unit is the Honda Group (Figure 5), but unlike the two previous formations, belongs to the middle Miocene age (Langston & Gasparini, 1997), located in the Neiva Basin in southern Colombia. It is formed, in part, by the uppermost unit, Villavieja Formation, and by the lowermost unit, La Victoria Formation, both forming part of the Honda Group (Langston & Gasparini, 1997) displaying the intercalation of clays and alternating large cycles-decrescent of lithoarenitic pebbles, sandstone grains (Guerrero, 1997 *apud* Cozzuol, 2006) and mudstones, whose the rocks contain a wide variety of terrestrial and aquatic records (Hsiou, 2010), arboreal vertebrates, among others, indicating a megadiverse paleoenvironment, from forests to aquatic environments in the fluvial-dominated system (Salas-Gismondi et al., 2015).

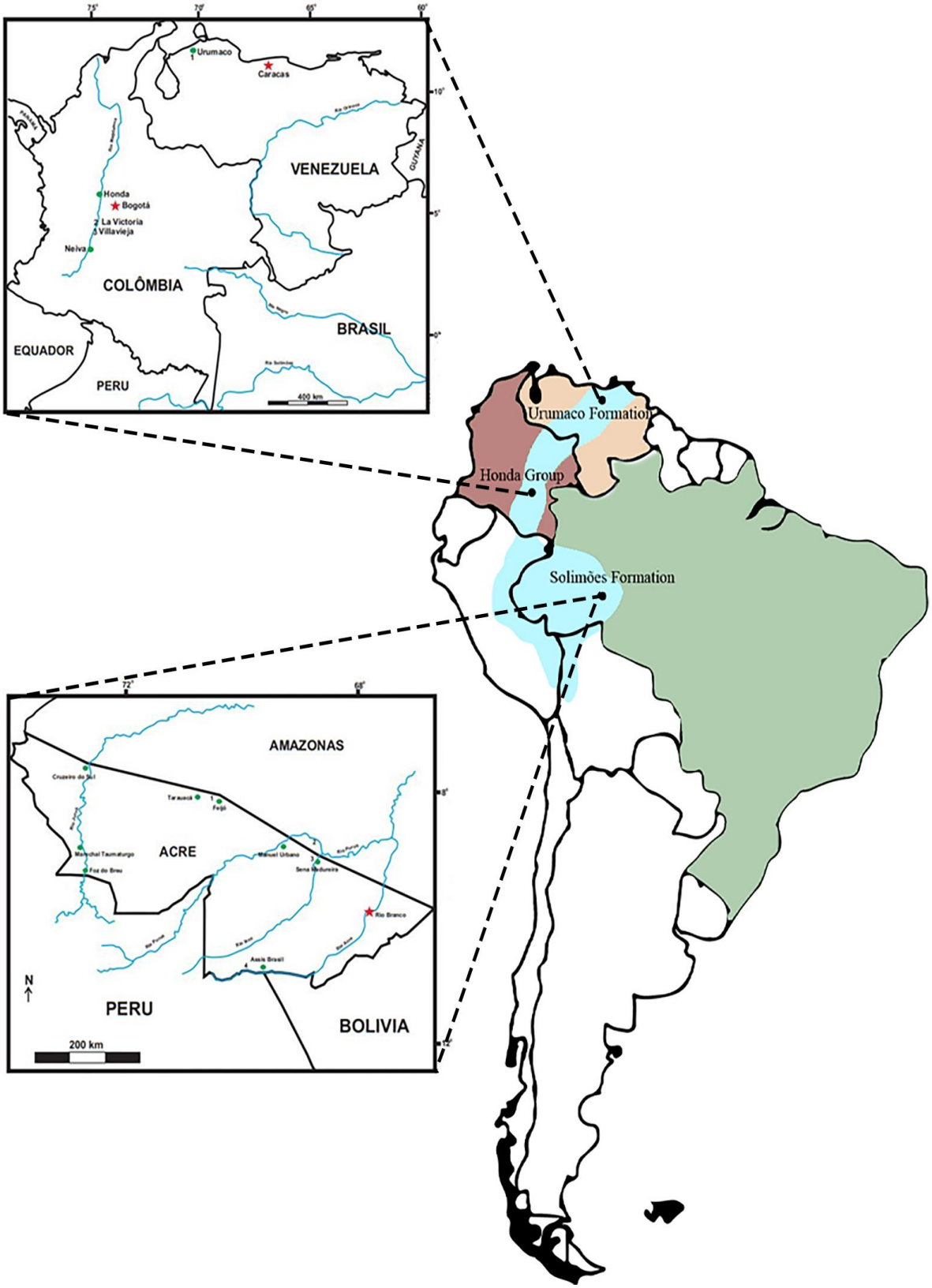

Figure 5 Schematic image from the localities of the provenance of the fossil specimens in Solimões Formation, Brazil (green); Honda Group, Colombia (red); and Urumaco Formation, Venezuela (orange). The blue color represents the Pebas Lake, which extends in this three localities. Taken and modified from Hsiou (2010).

MORPHOLOGICAL DATA FROM LIVING AND EXTINCT CROCODILIANS

To estimate the body size or mass of fossil caimanines, or other vertebrates, it is often necessary to have body size data from extant crocodilians (Sereno et al., 2001; Farlow et al., 2005; Erickson et al., 2012). As a basis for estimating body size and mass, morphometric measurements of living crocodilians were collected from the literature, including males and females, juveniles and adults (e. g. Woodward et al., 1995; Grigg et al., 1998; Verdade, 2000; Seymour et al., 2012; Godoy et al., 2019; Mannion et al., 2019; O'Brien et al., 2019). In total, measurements from 352 specimens were collected, representing 25 of 26 recognized species (Stubbs et al., 2021). The African slender-snouted crocodile was previously described as *Crocodylus cataphractus*, now updated as *Mecistops cataphractus* (McAliley et al., 2006), but in this work, our database contain both names. Within this large number of samples, measurements from 10 *Caiman yacare* specimens from the "Caimasul breeding site" (Mato Grosso do Sul, Brazil) were collected by Dr. Mario Bronzati (FFCLRP/USP) during his research in the location. He used a tape measure for length and a scale for weight in kilograms and provided skull and body measures for our database.

The following measurements were used (Figures 6 and 7): head width (HW - measured from the extremes of quadratojugals), dorsal cranial length (DCL - extending from the tip of the snout to the base of the skull), snout-vent length (SVL - extending from the tip of the snout to the cloaca), total length (TL – from the tip of the snout to tip of the tail), and body mass (BM). The dataset collected from the literature of living crocodilians is available in Table S1 in Supplementary Material I.

As previously mentioned, *Acresuchus*, *Mourasuchus*, and *Purussaurus* demonstrate that Caimaninae were morphologically diverse and represent one of the most peculiar crocodyliforms from the Neogene of the Neotropics. Most of the peculiarities are especially observed in the cranial shape, that fortunately, most specimens have preserved skull, thereby the measurements of DCL and HW were

done using the ImageJ program, version 1.53c, and the pictures of the fossil specimens were taken by Cidade (2019) during his Ph.D. thesis, and were made available for this work (Supplementary Material I).

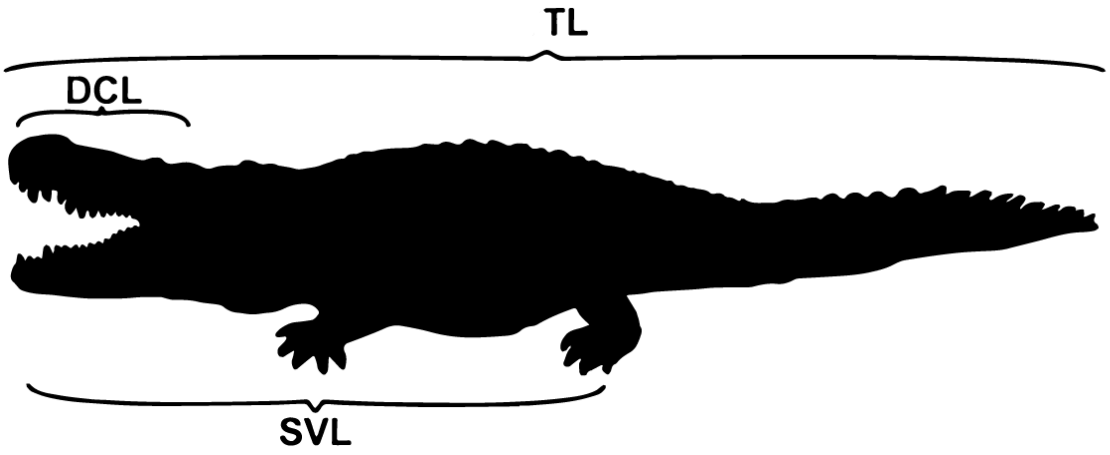

Figure 6 Illustrative image representing the measurements taken from living crocodilians. Dorsal cranial length (DCL); snout-vent length (SVL); and total length (TL). Taken and modified from Aureliano et al. (2015).

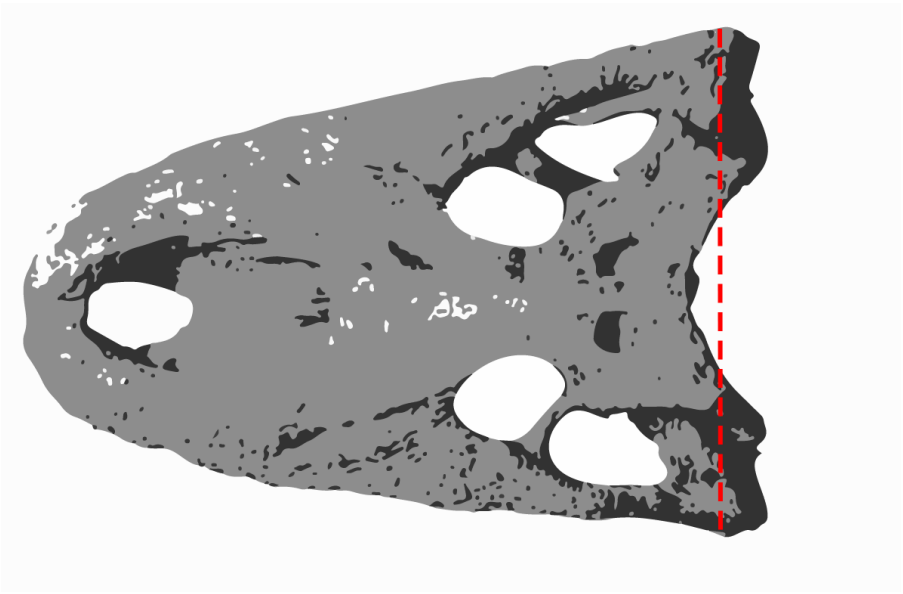

Figure 7 Measurement of the skull width that extends from the extremes of quadratojugals, indicated by dashed red lines.

The following specimens were measured for the present study:

Acresuchus pachytemporalis (UFAC-2507 - holotype); late Miocene, Solimões Formation, Brazil.

Mourasuchus amazonensis (DGM-526-R - holotype); late Miocene, Solimões Formation, Brazil.

Mourasuchus arendsi (CIAAP-1297 - holotype); late Miocene, Urumaco Formation, Venezuela.

Mourasuchus atopus (UCMP-38012 - holotype); middle Miocene, Honda Group, Colombia.

Mourasuchus pattersoni (MCNC-PAL-110-72V - holotype); late Miocene, Urumaco Formation, Venezuela.

Purussaurus brasiliensis (UFAC-1403 - holotype); late Miocene, Solimões Formation, Brazil.

Purussaurus mirandai (CIAAP-1369 - holotype); late Miocene, Urumaco Formation, Venezuela.

Purussaurus neivensis (UCMP-39704 - holotype); middle Miocene, Honda Group, Colombia.

Purussaurus sp. (MCNC-PAL-112-72V); late Miocene, Urumaco Formation, Venezuela.

Institutional abbreviations: Centro de Investigaciónes Antropológicas, Arqueológicas y Paleontológicas, Coro, Venezuela (CIAAP); Museu de Ciências da Terra, Rio de janeiro, Brasil (DGM); Museo de Ciéncias Naturales de Caracas, Caracas, Venezuela (MCNC); University of California Museum of Paleontology, Berkeley, Estados Unidos (UCMP); Universidade Federal do Acre, Acre, Brasil (UFAC).

ESTIMATING SIZE AND BODY MASS

Different methodologies were applied to estimate the total length (TL) and body mass (BM) of fossil Caimaninae. First, the equations from Aureliano et al. (2015) were employed, which used body size data from living *Caiman latirostris* specimens (data collected by Verdade, 2000) to estimate SVL, TL, and BM of *Purussaurus brasiliensis* with confidence intervals obtained via bootstrapping. These equations were constructed using ordinary least squares regressions (OLS) and the same regression equations (presented below) were used by Solórzano et al. (2019; 2020) and Cidade et al. (2020b):

$$Log_{10}(SVL) = a + b * Log_{10}(DCL) \quad (1)$$

$$Log_{10}(TL) = a + b * Log_{10}(SVL) \quad (2)$$

$$Log_{10}(BM) = a + b * Log_{10}(TL) \quad (3)$$

Where *a* is the intercept and *b* is the slope.

A possible issue with these equations is that the number of specimens of *Caiman latirostris* was small and mostly being juveniles, which can add cumulative errors to the estimates. To avoid this, the measurements collected for the database of the present study, containing a larger sample of juvenile and adult specimens of living crocodilians (including gharials, crocodiles, alligators, and caimans) were also used to generate updated regression equations.

Alternatively, other methods have been applied in this study to estimate SVL, TL, and BM. The second methodology was proposed by O'Brien et al. (2019) who employed head width measurements from adult living crocodilians to generate regression equations (equations below) using phylogenetic generalized least square (PGLS) regression. The authors also used a Bayesian framework to create posterior probability distributions of phylogenetic predictions of body size with confidence intervals.

This analysis was applied here due to the phylogenetic non-independence of all variables (O'Brien et al., 2019), but not applied in *Purussaurus neivensis* because of the absence of an HW measure.

$$Log(TL) = 3.05 + 0.80235 * Log(HW); r^2 = 0.92 \quad (4)$$

$$Log(SVL) = 2.525 + 0.768 * Log(HW); r^2 = 0.85 \quad (5)$$

$$Log(BM) = -4.785 + 2.953 * Log(HW); r^2 = 0.93 \quad (6)$$

$$Log(BM) = -11.68 + 3.26 * Log(SVL); r^2 = 0.92 \quad (7)$$

The third methodology was an analysis based on the body proportions of living crocodilians of our dataset, and a regression analysis was performed. In this method, we inferred body mass as an independent variable (x-axis), and the other ones as dependent variables (y-axis), to verify the influence that the mass has on each variable. SVL and TL were based on the measures and proportions of HW and DCL:

$$HW/DCL * 100 / HW/DCL\ proportion. \quad (8)$$

Additionally, we created a hypothetical crocodilian in different mass to compare if the estimations approached balance with the living forms. The dependent variables were based on power regressions of the intercept of the regression of the third methodology *vs.* the increasing mass, under the slope, as demonstrated in the equations below:

$$HW = 47.068 * mass\ (x)\ ^\wedge\ 0.323 \quad (9)$$

$$DCL = 84.035 * mass\ (x)\ ^\wedge\ 0.2901 \quad (10)$$

$$SVL = 343.51 * mass\ (x)\ ^\wedge\ 0.3075 \quad (11)$$

$$TL = 687.28 * mass\ (x)\ ^\wedge\ 0.2977 \quad (12)$$

Posteriorly, we excluded the juveniles' specimens from the dataset to verify their effect on the regressions, and repeated the calculations, compared the regressions with and without the juveniles using a t-test. Lastly, we also separated and analyzed the dataset for each taxonomic group (Alligatoroidea, Crocodyloidea, and Gavialoidea), to observe if the group influences regression equations.

The measures were log-transformed to standardize the variation, and ordinary least squares regression (OLS) was used, as well as confidence intervals were obtained through *Bootstrap*, based on the script by Aureliano et al. (2015) that was modified in this work (R script I in Supplementary Material I). The aforementioned analyzes were conducted in the R language program Core Team, 2020) version 4.1.1, using the following packages: readxl (Wickham & Bryan, 2019) to read excel files; car (Fox & Weisberg, 2019) to apply the regressions; simpleboot (Peng, 2019) to run the *Bootstrap*; esquisse (Meyer & Perrier, 2020) and ggplot2 (Wickham, 2016) to construct a dynamic graphic; broom (Robinson et al., 2021) to organize the tables; viridis (Garnier, 2021) to color the graphs; and plotly (Sievert et al., 2021) to create interactive graphs. The t-test was also executed in R (R script II), and the power regressions were conducted in the Microsoft Excel program (2019).

Results

The first applied methodology generated regressions (Figure 8) between the variables SVL *vs.* DCL (119 tested individuals), TL *vs.* SVL (192 tested individuals), and BM *vs.* TL (244 tested individuals). The slope and intercept values were obtained through regressions and confidence intervals with more than 95%, as given in Table 1 together with the coefficient of determination (R^2) explaining positive results of the generated data. The p-value was significant for all correlations, so the estimates for each individual were calculated. In general, *Acresuchus pachytemporalis* was estimated at 4.67 m in TL and with a mass of 601 kg, whereas *Mourasuchus* had averages of 8.89 m in TL and a weight of 5.6 tons. Regarding *Purussaurus*, showed averages of 9.83 m in TL and BM of 8.2 tons (Table 2).

The second methodology based on regressions by O'Brien et al. (2019) was performed as well (Table 3). *Acresuchus pachytemporalis* reaching 3.57 m in TL and weigh between 217 - 279 kg. The average for *Mourasuchus* was 4.53 m in TL and 666 kg in body mass; whereas the analysis reinforces *Purussaurus* as the largest and heaviest crocodilian with an average total body length of 6.43 m and 2.3 tons in mass.

Table 1 Regression values obtained in the analyzes of snout-vent length (equation 1), total length (equation 2), and body mass (equation 3) based on dorsal cranial length measurements. Confidence intervals (CI) with 95% of reliability were demonstrated along with intercept, slope, and coefficient of determination (R^2).

Equation	Intercept (CI)	Slope (CI)	R^2	P-value
1	0.560 (0.504; 0.615)	1.041 (1.013; 1.069)	0.97	<0.000001
2	0.364 (0.337; 0.390)	0.972 (0.963; 0.981)	0.99	<0.000001
3	-9.427 (-9.558; -9.295)	3.326 (3.284; 3.368)	0.99	<0.000001

Table 2 Dorsal cranial length (DCL) measurements and estimates made in snout-vent length (SVL), total length (TL), and body mass (BM) for each fossil specimen. Body measures in millimeters (mm) and mass in kilograms (kg).

Species	DCL (mm)	SVL (mm)	TL (mm)	BM (kg)
A. pachytemporalis	532	2505	4675	601
M. amazonensis	1135	5514	10069	7712
M. arendsi	1085	5265	9625	6639
M. atopus	712	3396	6284	1607
M. pattersoni	1081	5244	9587	6552
P. brasiliensis	1406	6892	12507	15863
P. mirandai	1228	5989	10910	10071
P. neivensis	910	4384	8056	3673
***Purussaurus* sp.**	888	4272	7854	3376

Table 3 Estimates based on head width (HW) measures with regressions by O'Brien et al. (2019) of snout-vent length (SVL), total length (TL), and body mass (BM). Body measures in centimeters (mm) and mass in kilograms (kg).

Species	HW (mm)	SVL (mm) from HW	TL (mm) from HW	BM (kg) from HW	BM (kg) from SVL
Acresuchus	340	1876	3579	279	217
M. amazonensis	590	2863	5569	1421	865
M. arendsi	452	2333	4495	646	443
M. atopus	270	1572	2977	141	122
M. pattersoni	529	2634	5104	1030	659
P. brasiliensis	980	4226	8363	6344	3076
P. mirandai	-	-	-	-	-
P. neivensis	501	2526	4886	877	575
***Purussaurus* sp.**	657	3109	6068	1948	1131

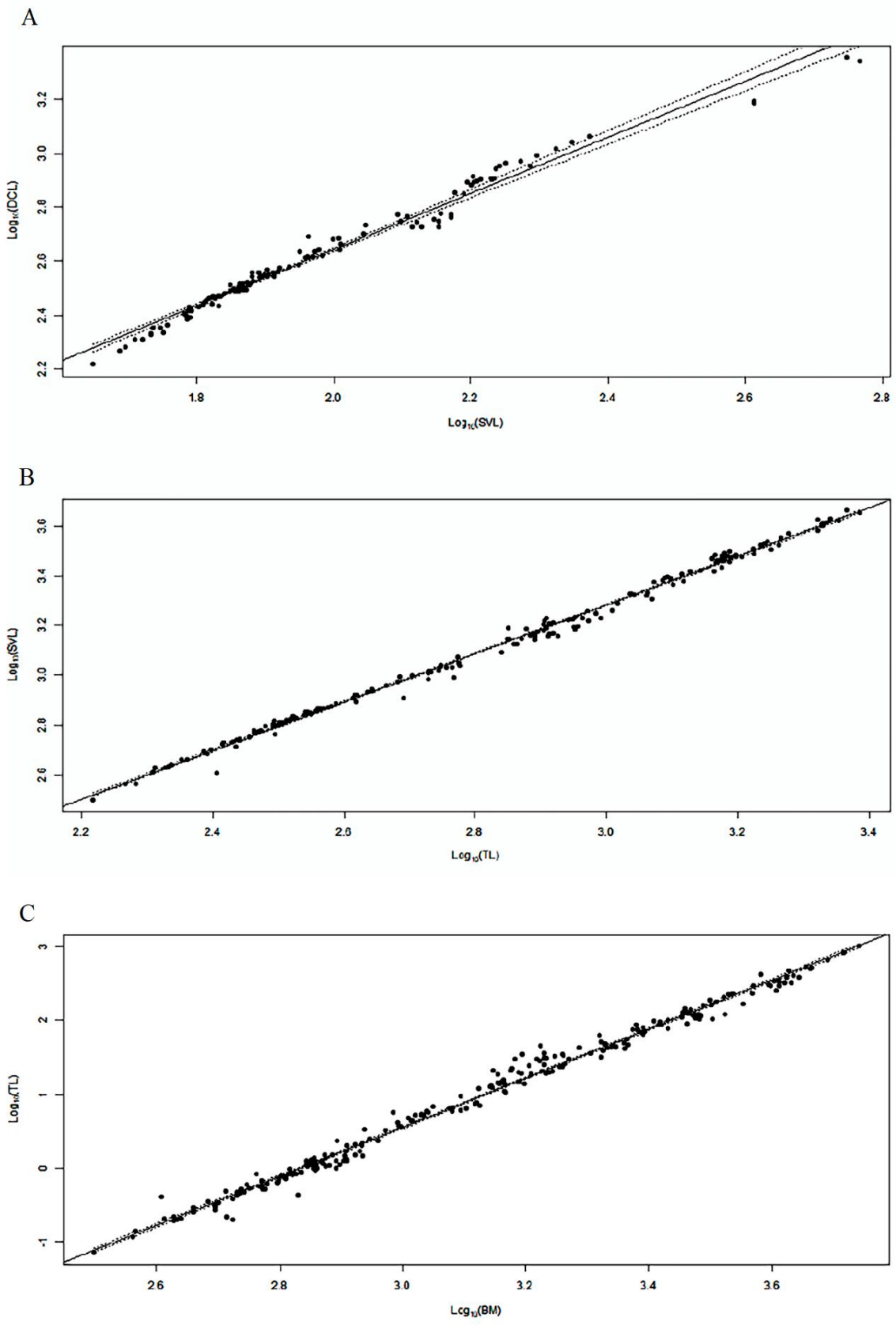

Figure 8 Regression analysis with a confidence interval of 95% (dotted lines) for log-transformed data. A – DCL (dorsal cranial length) x SVL (snout-vent length); B – SVL x TL (total length); C – TL x BM (body mass).

Exploring the database, a very interesting proportion was observed between the variables, with SVL representing 52% of the total body length of a crocodilian, with a standard deviation (SD) of 3%. Such proportions were also made with the other parameters, HW representing 15% of the SVL (SD of 4%) and 8% of the TL (SD of 2%), DCL corresponding to 23% of the SVL (SD of 2%), and 12% of the TL (SD of 2%) (Table S2 in Supplementary Material I). Furthermore, the influence of body mass on other parameters was observed through power regressions, and a positive correlation was observed between all the variables (Figure 9), with the coefficient of determination more than 0.94.

Based on the previous analysis between mass and the other parameters, which demonstrated a positive correlation in living crocodilians, the SVL and TL were estimated based on proportions of DCL and HW obtained from Table S2 (Supplementary Material I). The body mass estimates of the extinct caimanines were calculated from the power regression values presented in Figure 9. Thus, *Acresuchus* reaches an average of 4.59 m and 604 kg, *Mourasuchus* with an average of 7 m and 3.2 tons, and *Purussaurus* with an average of 9 m and 7.1 tons (Table 4).

To further analyze our data, we created a hypothetical crocodilian by simulating body dimensions of HW, DCL, SVL, and TL on different increasing body masses, evaluating and correlating whether the previously estimated data were consistent with such body dimensions. The hypothetical measures are given in Table S4 in Supplementary Material I.

Table 4 Estimates of the extinct caimanines based on body proportions and power regressions in living crocodilians. Head width (HW) corresponding to 15% of the snout-vent length (SVL) and 8% of total length (TL); dorsal cranial length (DCL) corresponding to 23% of the SVL and 12% of the TL. Body mass (BM) is based on the power regressions of Figure 9. Measures in millimeters (mm) and mass in kilograms (kg).

Species	**SVL (mm) from HW**	**TL (mm) from HW**	**BM (kg) from TL**	**SVL (mm) from DCL**	**TL (mm) from DCL**	**BM (kg) from TL**
A. pachytemporalis	2269	4255	457	2574	4934	751

M. amazonensis	3937	7382	2907	4936	9461	6689
M. arendsi	3015	5653	1186	4721	9049	5760
M. atopus	1806	3387	212	3099	5940	1400
M. pattersoni	3532	6622	2018	4703	9014	5685
P. brasiliensis	6535	12254	15948	6114	11720	13731
P. mirandai	-	-	-	5343	10241	8729
P. neivensis	3345	6271	1681	3960	7591	3192
Purussaurus sp.	4382	8216	4164	3862	7403	2935

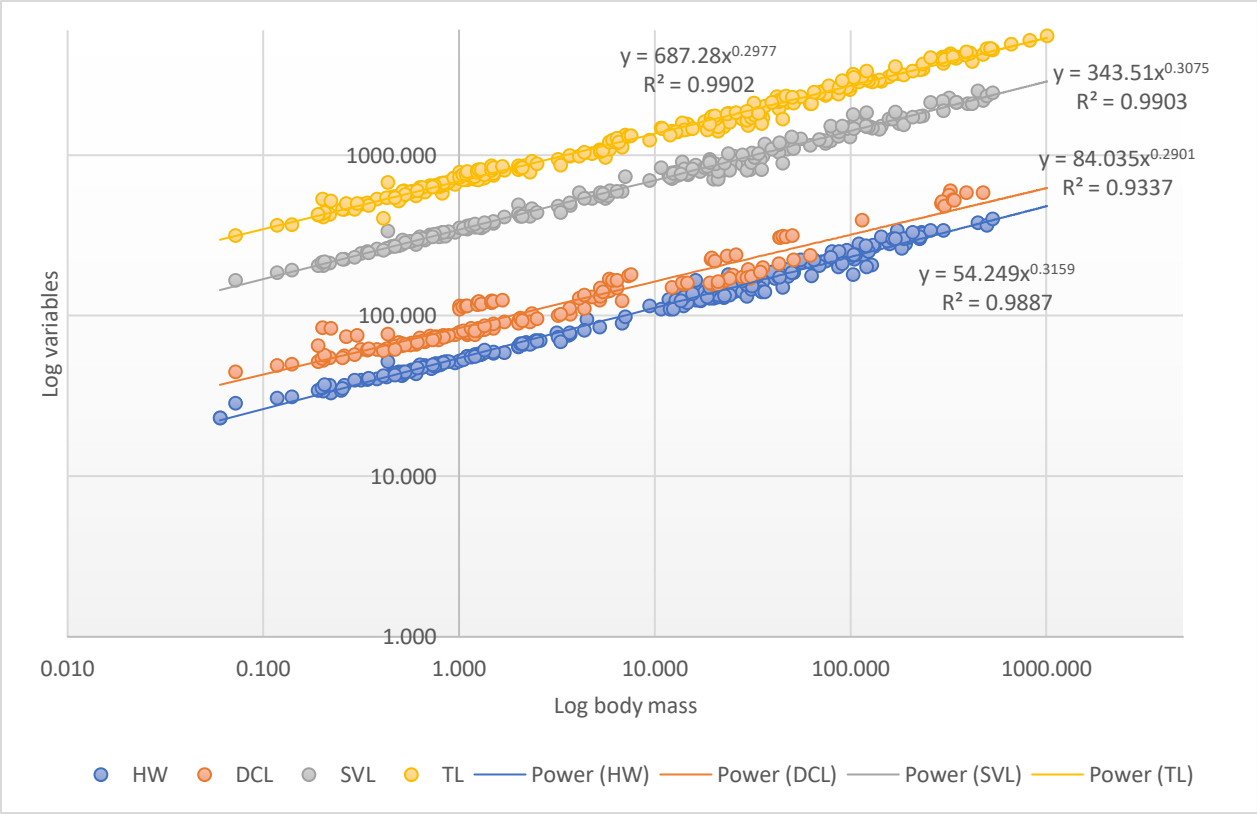

Figure 9 Power regressions in the logarithmic scale. Body mass (BM) as the x-axis against the other variables in the y-axis. Each color represents the body region measured, and the lines represent the power with its respective equation. Blue: head width (HW); orange: dorsal cranial length (DCL); gray: snout-vent length (SVL); and yellow: total length (TL).

Moreover, excluding the juveniles created power regressions different from the dataset containing all the crocodilians (Table 5). We compared statistically both datasets, the one presented in Table S1 (Supplementary Material I) containing all the juveniles and adult crocodilian specimens, and the other one excluding the juveniles (totalizing 219 specimens) according to the literature we took the data, generating regressions (Figure 10) that returned p-values. Although the figure below demonstrates that the regressions of both datasets are very similar, some variables demonstrated a slight difference. The intercept was demonstrated to be significant. On the other hand, the slopes did not demonstrate significance for all the variables against the body mass, being HW and SVL showing that the juveniles do not bias the estimates, but an alteration can be observed in DCL and TL (statistical values presented in Tables S3 and S5 in Supplementary Material I).

Table 5 Power regression values of each body parameter regarding just the adult specimens: head width (HW), dorsal-cranial length (DCL), snout-vent length (SVL), and total length (TL), with their respective intercepts, slopes, and coefficient of determination (R^2).

	Intercept	**Slope**	**R^2**
HW =	69.204	0.341	0.93
DCL =	11.072	0.6815	0.94
SVL =	353.89	0.295	0.95
TL =	611.12	0.3238	0.97

A

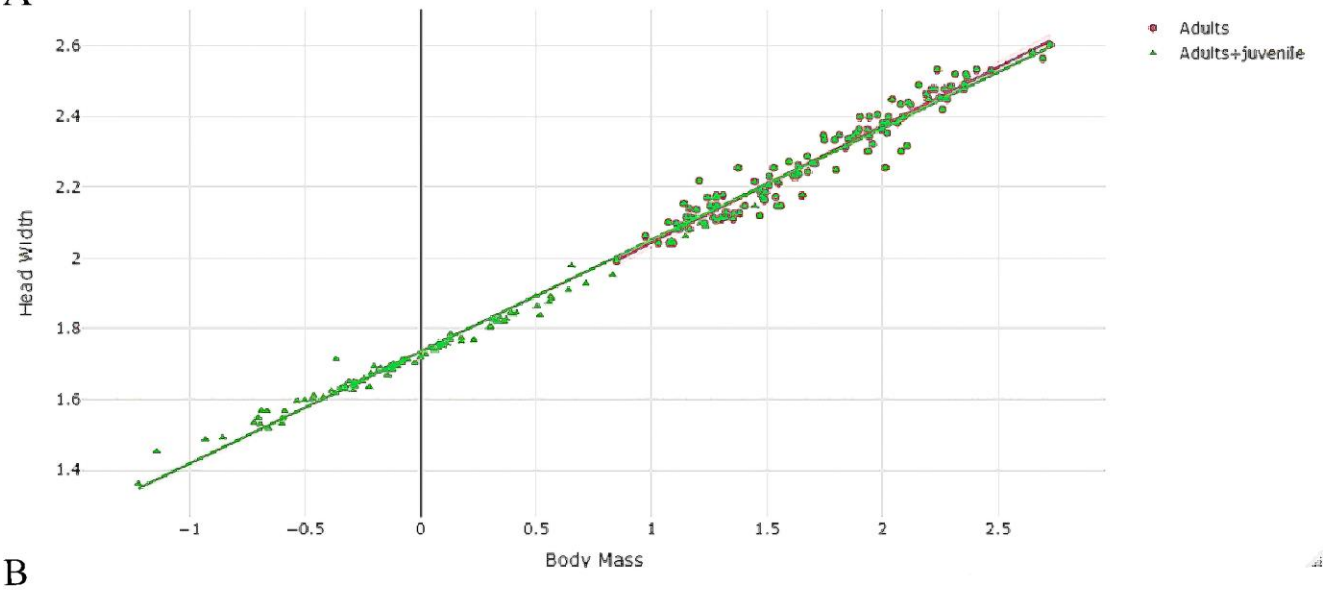
Head Width
Body Mass
Adults
Adults+juvenile

B

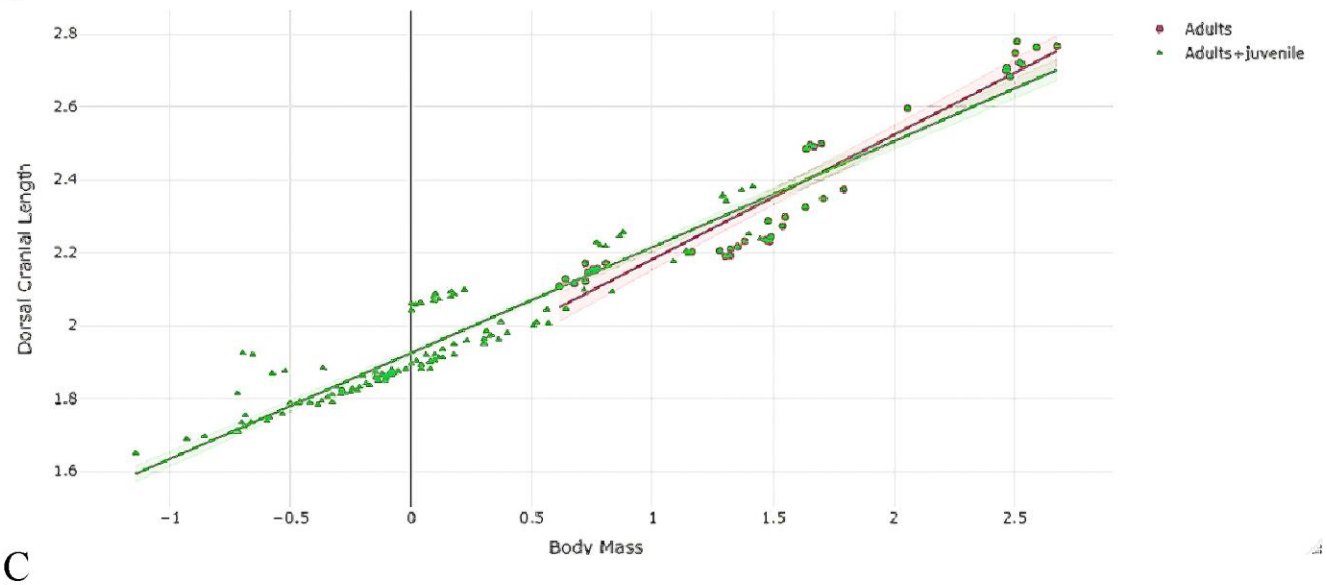
Dorsal Cranial Length
Body Mass
Adults
Adults+juvenile

C

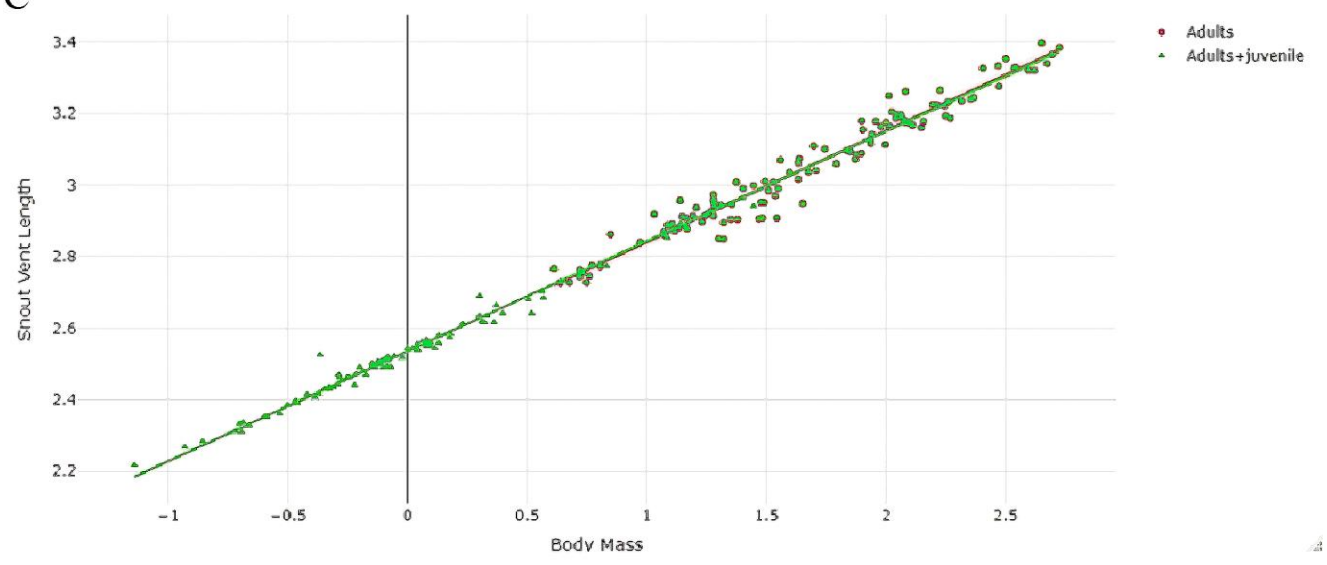
Snout Vent Length
Body Mass
Adults
Adults+juvenile

D

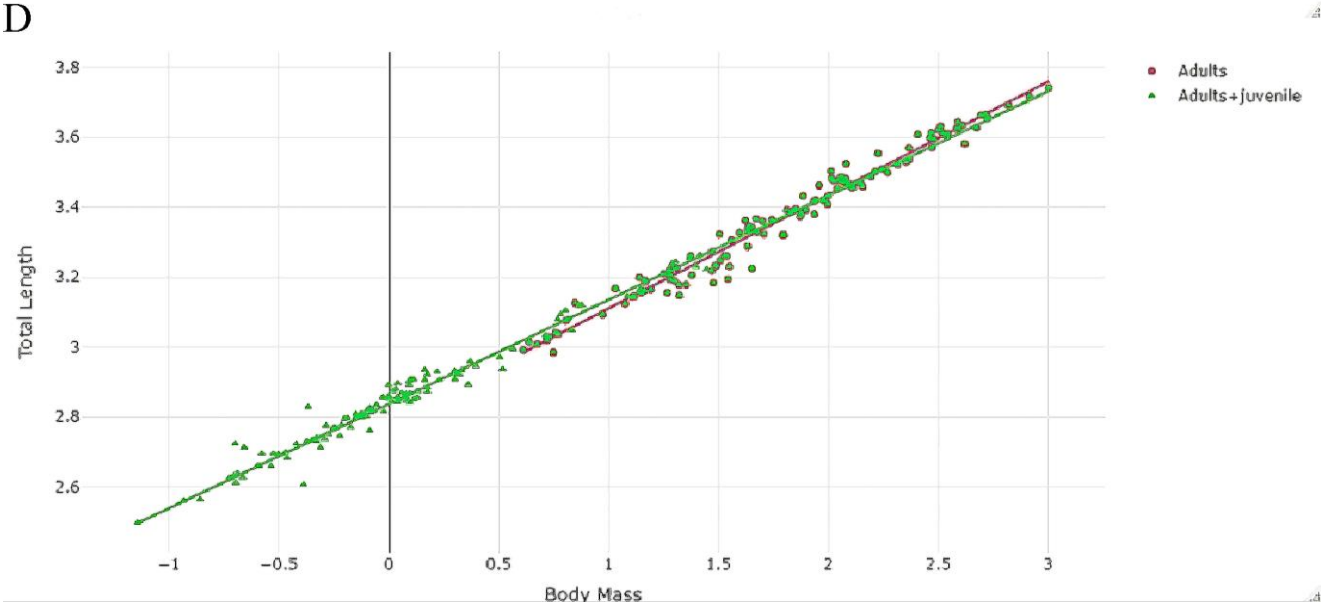

Figure 10 Regression difference between the datasets with and without the juveniles from Table S1, comparing the intercept and slope of the body mass and the variables: head width (A), dorsal-cranial length (B), snout-vent length (C), and total length (D), all log-transformed. Red circle and line represented by the dataset containing only the adult living crocodilian specimens, and green triangle and line represented by the complete dataset.

Regarding the taxonomic group separately (Figure 11), according to Table 6 and comparing with the results of Table 4, we can observe that using HW as a reference, the dataset containing only the adult specimens did not demonstrate a difference in total length relative to the dataset containing the juveniles, decrease using the regression made for Crocodyloidea, and demonstrated difference using the regressions for Alligatoroidea and Gavialoidea. The BM for adults and Gavialoidea did not have significant differences, but using the regression for Alligatoroidea increased significantly the mass, and decrease significantly using the Crocodyloidea's regression. Concerning the DCL, total length was demonstrated to have significantly different values, as well as using the regression for Crocodyloidea and Gavialoidea. The BM decreased significantly in all the comparisons. Finally, the estimates were done following the third methodology without juveniles' specimens, and for each taxonomic group.

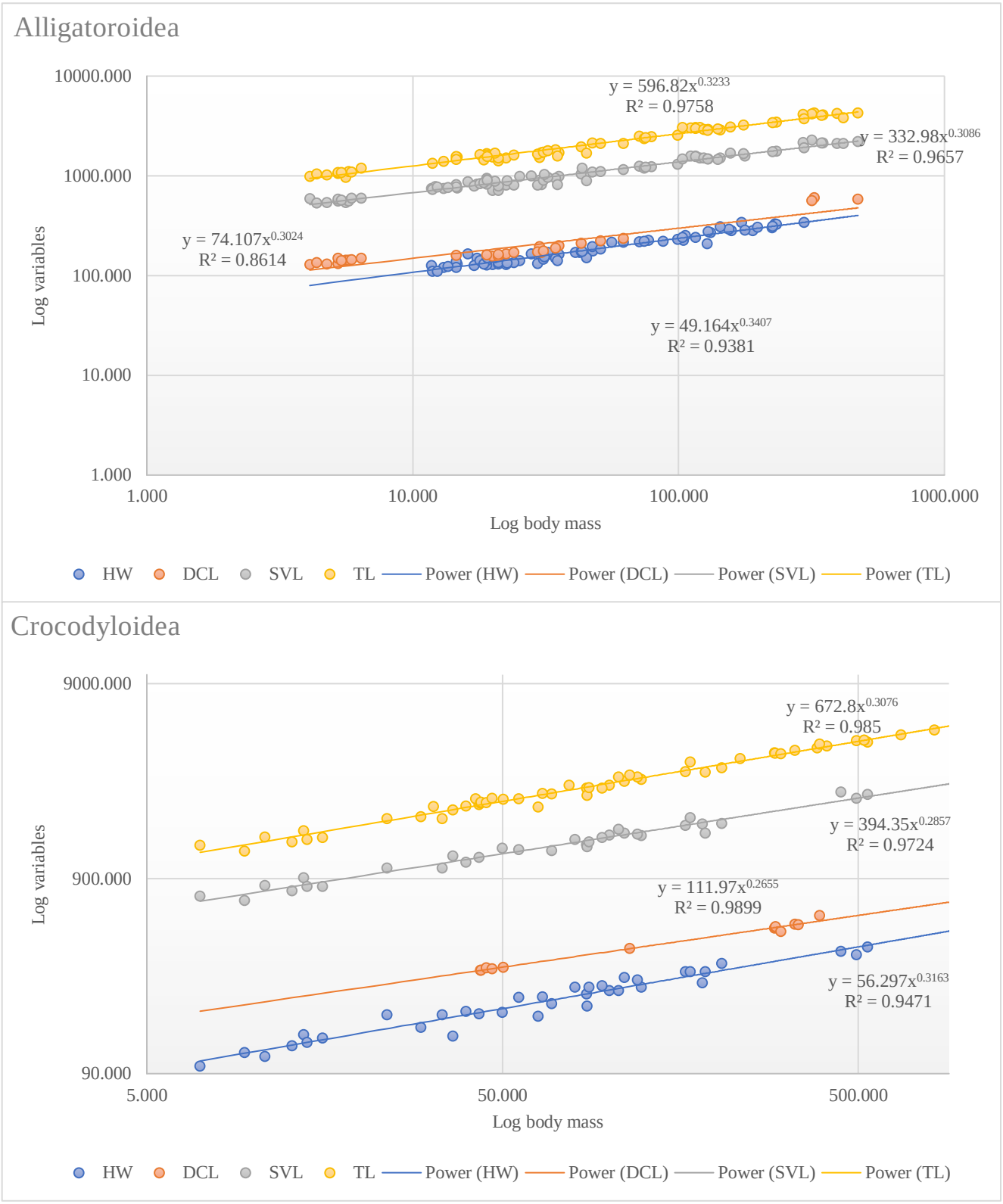
Alligatoroidea
10000.000
1000.000
100.000
10.000
1.000
Log variables
y = 596.82x^0.3233
R² = 0.9758
y = 332.98x^0.3086
R² = 0.9657
y = 74.107x^0.3024
R² = 0.8614
y = 49.164x^0.3407
R² = 0.9381
1.000
10.000
100.000
1000.000
Log body mass
HW
DCL
SVL
TL
Power (HW)
Power (DCL)
Power (SVL)
Power (TL)
Crocodyloidea
9000.000
900.000
90.000
Log variables
y = 672.8x^0.3076
R² = 0.985
y = 394.35x^0.2857
R² = 0.9724
y = 111.97x^0.2655
R² = 0.9899
y = 56.297x^0.3163
R² = 0.9471
5.000
50.000
500.000
Log body mass
HW
DCL
SVL
TL
Power (HW)
Power (DCL)
Power (SVL)
Power (TL)

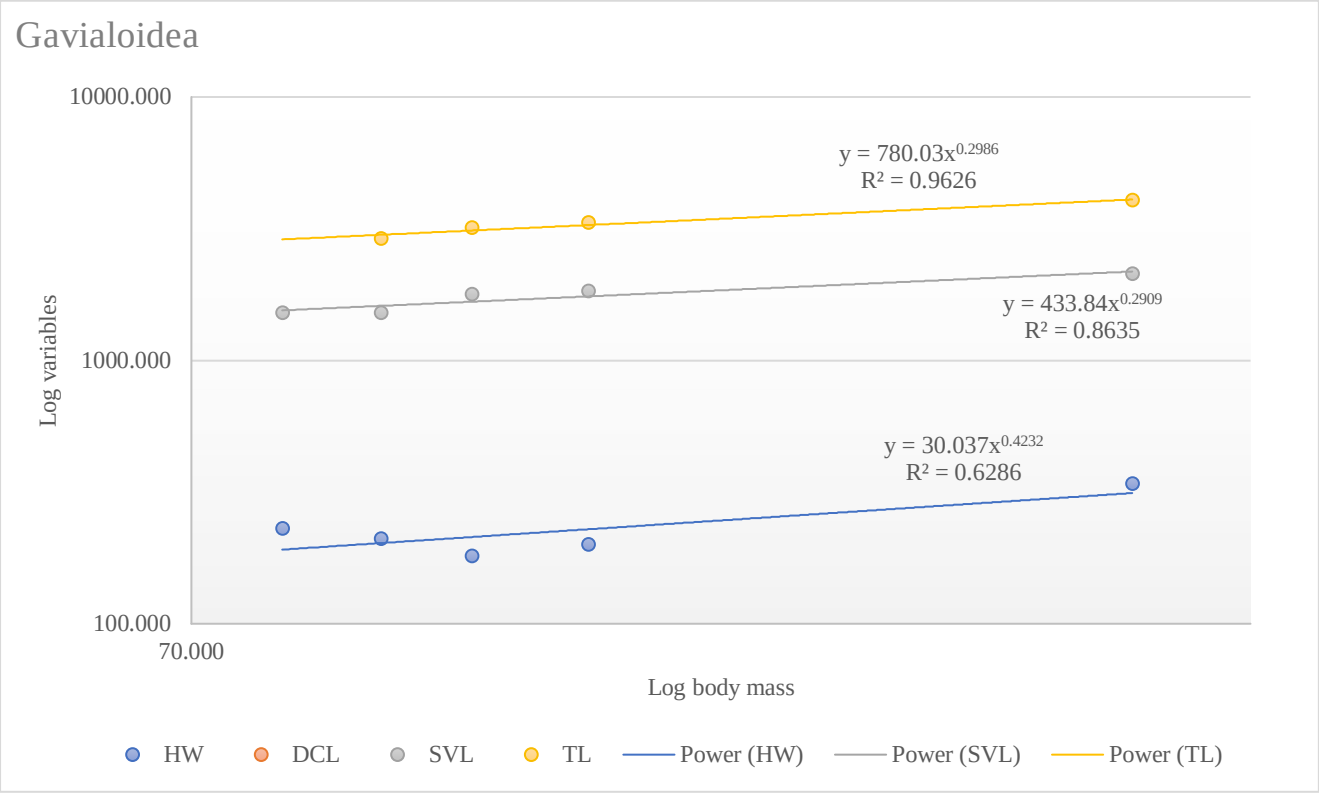

Figure 11 Power regressions in the logarithmic scale between the body mass against the other variables (head width – HW (blue); dorsal-cranial length – DCL (orange); snout-vent length – SVL (gray); and total length – TL (yellow)) for each adult taxonomic group separately: Alligatoroidea (top), Crocodyloidea (middle), and Gavialoidea (bottom).

Table 6 Four different estimates of the extinct caimanines, one based only on adult specimens of crocodilians of our dataset, and the other three based on each taxonomic group of Crocodylia. Total length (TL) based on body proportions of head width (HW), dorsal-cranial length (DCL) measured in millimeters, and body mass (BM) in kilograms based on the regressions of the TL.

Acresuchus pachytemporalis				
	Adults	**Adults taxonomic groups**		
		Alligatoroidea	**Crocodyloidea**	**Gavialoidea**
TL from HW	4255	4863	3783	4863
BM	400	658	274	459
TL from DCL	4554	4934	4554	4554
BM	494	687	501	368
Mourasuchus amazonensis				
	Adults	**Adults taxonomic groups**		
		Alligatoroidea	**Crocodyloidea**	**Gavialoidea**
TL from HW	7382	8437	6562	8437
BM	2197	3616	1643	2905
TL from DCL	8733	9461	8733	8733
BM	3691	5152	4161	3260

Mourasuchus arendsi				
	Adults	**Adults taxonomic groups**		
		Alligatoroidea	**Crocodyloidea**	**Gavialoidea**
TL from HW	5653	6461	5025	6461
BM	963	1583	690	1188
TL from DCL	8353	9049	8353	8353
BM	3217	4490	3601	2809

Mourasuchus atopus				
	Adults	**Adults taxonomic groups**		
		Alligatoroidea	**Crocodyloidea**	**Gavialoidea**
TL from HW	3375	3857	3000	3857
BM	195	321	129	211
TL from DCL	5483	5940	5483	5483
BM	876	1221	916	685

Mourasuchus pattersoni				
	Adults	**Adults taxonomic groups**		
		Alligatoroidea	**Crocodyloidea**	**Gavialoidea**
TL from HW	6622	7568	5886	7568
BM	1570	2583	1154	2018
TL from DCL	8320	9014	8320	8320
BM	3179	4436	3556	2772

Purussaurus brasiliensis				
	Adults	**Adults taxonomic groups**		
		Alligatoroidea	**Crocodyloidea**	**Gavialoidea**
TL from HW	12254	14004	10892	14004
BM	10507	17333	8535	15854
TL from DCL	10818	11720	10818	10818
BM	7150	9992	8348	6679

Purussaurus mirandai				
	Adults	**Adults taxonomic groups**		
		Alligatoroidea	**Crocodyloidea**	**Gavialoidea**
TL from DCL	9453	10241	9453	9453
BM	4715	6584	5385	4251

Purussaurus neivensis				
	Adults	**Adults taxonomic groups**		
		Alligatoroidea	**Crocodyloidea**	**Gavialoidea**
TL from HW	6271	7167	5575	7167
BM	1327	2183	967	1682
TL from DCL	7007	7591	7007	7007
BM	1869	2607	2034	1559

Purussaurus sp.				
	Adults	**Adults taxonomic groups**		
		Alligatoroidea	**Crocodyloidea**	**Gavialoidea**
TL from HW	8216	9390	7303	9390
BM	3057	5034	2327	4157
TL from DCL	6834	7403	6834	6834
BM	1730	2413	1875	1434

Discussion

Analysis of the measurements

In all the regressions, body size and mass showed positive correlations, supporting that mass estimation based on TL is effective. Such correlation can be better visualized in Figure 12, where it is possible to observe different species in our database growing allometrically in size and mass. Some of the species are present in a large number of samples, such as *Crocodylus porosus* and *Alligator mississippiensis*, which are the largest living crocodilians, but smaller than some of the giant extinct crocodilians that existed in the middle and late Miocene.

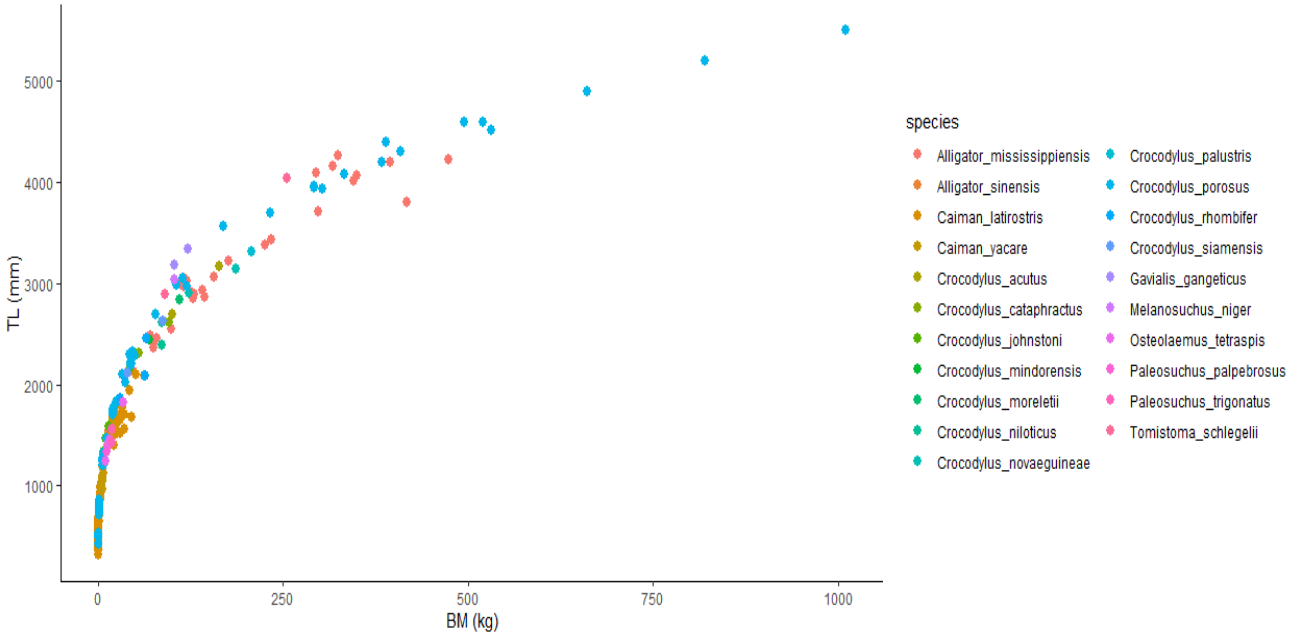

Figure 12 Correlation between total length (TL) and body mass (BM) on the x-axis and y-axis, respectively, of crocodilians in our database, each color representing a species of living Crocodylia. Measurements in millimeters (mm) and mass in kilograms (kg).

The largest living caiman, *Melanosuchus niger*, has an average DCL of 31.5 cm, according to Foth et al. (2015), being smaller than *Acresuchus pachytemporalis* (53.2 cm), considered a medium-sized Caimaninae. The skull measurement of *A. pachytemporalis* differs slightly in centimeters from that recorded by Souza-Filho et al. (2018), that it was 51.5 cm, probably because our measurement was made digitally. In addition, males of *M. niger* have an average of 4-5 m of total length (Thorbjarnarson, 2010), similar to that estimated for the studied fossil. Recently, Deem et al. (2021) recorded large females of *Alligator mississippiensis* reaching a total size of 3.2 m, with DCL at 43.5 cm, and a mass of 170 kg. Other studies have shown an average of the mass estimate for crocodilians using several regression equations. The average mass for *A. pachytemporalis* was 242.71 kg in a study by Solórzano et al. (2020), being very close to our estimated value based on HW; however, the authors registered a skull length measurement of 47 cm, using several different approaches to estimate body mass. In our analysis, based on DCL measurements in adult living crocodilians, *A. pachytemporalis* reached 4.5 m and weight of approximately 500kg.

Focusing on large extinct caimanines, *Mourasuchus* and *Purussaurus* have shown cranial measurement, total length, and body mass greater than that of any living crocodylian. On the other hand, the extant saltwater crocodile, *Crocodylus porosus*, displays between 6 to 7 m in length and weighs more than one ton (Grigg et al., 1998; Britton et al., 2012; Grigg & Kirshner, 2015). In our database, this species represents the largest specimen with 5.5 m and 1 ton. This result is interesting, as it can be noted that the largest extant crocodile is comparable to the smallest species of *Mourasuchus* (*M. atopus*), also reaching a size of approximately 5.4 m and 870 kg without the juveniles, showing that not all species of the genus reached extreme sizes in the Miocene. Estimates for the genus *Mourasuchus* have already been published by Solórzano et al. (2020) and Cidade et al. (2020b), both studies being based on the analysis of Aureliano et al. (2015). They also used a restricted database (i.e., extant juvenile specimens to estimate SVL and TL, in addition to estimating mass based on crocodilian's mass average). Moreover,

Solórzano et al. (2020) estimated the smallest species of *Mourasuchus* at 1 ton and the largest (*M. amazonensis*) at 3.7 tons. According to Cidade et al. (2020b), the smallest species of *Mourasuchus* shows 6.30 m in length and 1.1 tons, and the largest member at 9.47 m and 4.3 tons. Another large and extinct crocodyliform with similar morphology to *Mourasuchus* is *Aegisuchus* (Aegyptosuchidae) from the Cretaceous of North Africa that would exceed 15 m in total length; however, the authors themselves mention that it is an overestimated value, but the notoriety of being a large crocodyliform remains (Holliday & Gardner, 2012).

Our data confirm that the largest caimanine of the Neogene of South America was *Purussaurus*. *P. brasiliensis* is considered the biggest species, reaching 12.5 m in total size and a mass of approximately 15 tons (based on the first methodology), differing from the weight registered by Aureliano et al. (2015) and Solórzano et al. (2020) of 8 tons. In general, we observed that the results of our analysis using the DCL parameter almost doubled the group's mass concerning the previous estimates. Associating the DCL and HW methodologies, the first one demonstrates greater values. Thinking about a crocodile that reaches 6 m and 1 ton, this methodology seems to be exaggerated. *P. brasiliensis* is a perfect example of this exaggeration, weighing ten times more than a living crocodilian. But taking into account the DCL measurement with no extant juveniles, *Purussaurus* could reach an average of 8.5 m in total length and 3,800 kg in mass, wich is reasonable. The second methodology resembles the living crocodilians, but doubt remains if this is the best way to estimate extinct organisms. The skull of *Mourasuchus* is longer than in *Acresuchus pachytemporalis*, resulting in a greater size estimate. When taking HW into account, *A. pachytemporalis* has a wider skull than *Mourasuchus*, causing an increase in its size and mass estimates. Thus, these proportions bias the size estimates of the organisms, and a study concerning the skull proportions in different species and their relation to body mass seems promising.

Head width measurement has been used in several studies, showing a strong correlation with the mass and size of extinct animals (Gignac & O'Brien, 2016; O'Brien et al., 2019). Moreover, as most fossil skulls are quite fragmented and the morphotypes of the rostra are diverse, the HW allows another approach to improve such estimates (Gignac & O'Brien, 2016). O'Brien et al. (2019) adopted this methodology to integrate the data with the phylogeny of crocodilians and estimated the mass and body size of some crocodyliforms, including *Sarcosuchus*, who has demonstrated a similar size to *Purussaurus brasiliensis*. *S. imperator* was estimated between 7.36 m to 8.97 m in total length and mass around 1.9 ton to 3.4 tons. An apparent discrepancy with the previously published estimate by Sereno et al. (2001), who estimated the size and mass of *Sarcosuchus* at 11.5 m and 8 tons, respectively. This difference can also be observed in our data, where the estimated values based on HW were smaller than the size and mass of the extinct crocodilians compared to the first and third methodologies. *P. brasiliensis* was estimated at 8.3 m and 3 to 6.3 tons, smaller than the values calculated based on the first and third methodologies, and those published by Aureliano et al. (2015) and Solórzano et al. (2020). *Mourasuchus* also showed a smaller size and mass, the largest species in the group reaching 5.5 m and about 1.4 tons, consistent with the dimensions of *Crocodylus porosus*. *M. atopus*, the smallest one, obtained values close to *Alligator mississippiensis*, but its DCL is bigger.

Our database contained 352 specimens taken from previous studies with analyzes of body dimensions among living crocodilians. The data applied by Aureliano et al. (2015) contain less than half of the individuals presented here. The author's data, based on TL measurements of *Caiman latirostris*, totalize 29 specimens, in which the DCL average of these animals is 7 cm and a total length of 59 cm. The total length for this species in the adult phase may reach 2.5 m (Verdade, 1995; Verdade & Piña, 2006). Therefore, we observed two issues that can skew the estimates: a small number of samples and the presence of juveniles. In addition, the data used to estimate the mass is an average of each current

crocodilian species, which can once again interfere with the analysis, demonstrating the importance of obtaining morphometric data of the specimens uniquely.

Although our database contained more data points, juveniles might show different body proportions or relationships between body mass and body measurements, since juveniles may show greater growth rates than adults. Consequently, investigating the effect of juveniles on allometric relations is necessary to improve the quality of regression analysis. Therefore, we calculated regressions excluding the juveniles from the database. For HW, the juveniles did not demonstrate any influence on the regression. For DCL, the exclusion of the juveniles decreases the regression, and in consequence, the body size estimates, suggesting that not all head measurements provide equally good estimates of crocodilian body size and body mass.

BODY PROPORTIONS

According to Cooper et al. (2020), body dimensions based on the proportion of size from living vertebrates are an excellent predictor for such estimates. The authors analyzed the body dimensions of living sharks resulting in positive regressions with their total size, managing to reconstruct these dimensions for the largest fossil known shark *Otodus megalodon* (Cooper et al., 2020). Here, we adopted the same approach analyzing body dimensions of living crocodilians to estimate extinct taxa, emphasizing the influence of such measurements on the body mass of these animals.

As demonstrated previously, in our database the width of the skull represents 8% of the total size of an extant crocodilian. DCL represents 23% and 12% of the SVL and TL, respectively. These proportions in living crocodilians allow making more concrete calculations of extinct body dimensions since it is necessary to use them to determine measurements of fossil animals (Sereno et al., 2001; Farlow et al., 2005; Aureliano et al., 2015, Cooper et al., 2020). Body mass seems to correlate with all body

parameters, this can also be corroborated in several previous studies (Erickson et al., 2012; Aureliano et al., 2015; O'Brien et al., 2019). This factor is related to the animal's lifestyle, not only in ecological but also it has physiological importance (Grigg et al., 1998; Lyons & Smith, 2010; Grigg & Kirshner, 2015).

Accordingly, the estimates based on DCL by Aureliano et al. (2015), and also approached by Cidade et al. (2020b) and Solórzano et al. (2020), are consistent with a hypothetical living crocodilian, because all of the specimens had close values, possibly due to a similarity in the database used. Stockdale & Benton (2021) criticizes the use of DCL to estimate size and mass due to the great cranial disparity present in crocodyliforms, as the result would be higher for those with elongated snout skulls and lower for those skulls whose face is short. In contrast, HW did not fit with the hypothetical measurements, because another type of regression and equations were used. In contrast to the first and second methodologies, the third can be observed that most of the specimens were similar to living crocodylians when using HW proportions, as well as the regressions using only adult living specimens. When we look at the second methodology, which O' Brien et al. (2019) based on adult specimens, and the regressions and estimations made by us excluding juveniles, the values estimated show a decrease, suggesting that the elevated slope was influenced by the juveniles, thereby biasing the values estimated, being overestimated. Regarding the body mass and size estimates based on body proportions, the juveniles did not influence the estimates, as demonstrated in Tables 4 and 6, but the DCL proportions just using adult living crocodilians decreased estimates.

The regression and estimation for different taxonomic groups are relevant because they differ in body proportions and may influence the estimated values. Alligatoroidea presented greater or similar values as the dataset containing the juveniles' specimens. We have to take into account that in this group, a lot of small specimens were included in the dataset, possibly introducing a bias into the regression. Regarding Crocodyloidea, the group presented lower values, considering that this group showed proportions similar to the adult's dataset. We could not evaluate Gavialoidea due to the low number of

samples. Therefore, using juveniles in a database can increase the slope and introduce bias into body size and body mass estimates of extinct crocodilians. Especially HW resulted in greater estimates, while DCL resulted in lower estimates when compared to the complete dataset. Crocodyloidea's regression presented values close to the adult's dataset using DCL as reference. Additionally, the result illustrated in Figure 10 confirms that DCL and TL against BM indicate a small alteration for both datasets. For that reason, DCL is a good proxy to estimate size and mass, using a database containing only adult specimens showing estimations close to a body length and body mass of a living crocodilian.

All different methods estimating the body size and mass of the crocodyliforms proposed by previous and our studies try to reach their real sizes. Some body regions serve as a proxy to represent size and mass, and based on the regressions performed, such proxies are analyzed (Godoy & Turner, 2020). The absence of complete skulls in some crocodyliforms enabled the search for other proxies to estimate size and mass, such as the femur (Farlow et al., 2005; Young et al., 2016), morphological character scores (Stockdale & Benton, 2021), and vertebrae of mature individuals (Iijima & Kubo, 2020). The individuals in the present study contained relatively complete skulls, while post-cranium is almost always absent or only fragmented, not allowing to be used as a proxy. For those skulls whose rostrum was fragmented, Hurlburt et al. (2003) proposed the use of the orbital-cranial length, which had been applied in later studies showing a total positive correlation with size and mass (Scheyer et al., 2013; Godoy et al., 2019; Mannion et al., 2019). Recently, O'Brien et al. (2019) proposed the use of head width as a proxy to estimate size and mass for those individuals with incomplete rostra. Meanwhile, as we agree with Stockdale & Benton (2021), such analysis shows lower predicted values in crocodyliforms. The use of HW measures can be a problem for those small or medium sized crocodilians that have large skulls, or also for longirostrine taxa.

Dorsal cranial measurements, in turn, are commonly used (Godoy et al., 2019; Godoy & Turner, 2020) and have shown highly positive correlations. Previous studies used this cranial measurement to

estimate the size and mass in other crocodyliforms, e.g., *Sarcosuchus imperator*, from the Cretaceous of North Africa (Sereno et al., 2001), *Gryposuchus croizati*, the large gavialoid from the Miocene of South America (Riff & Aguilera, 2008), and *Purussaurus brasiliensis*, the largest caimanine also from the Miocene of South America (Aureliano et al., 2015). Figure 13 demonstrates the compilation of body size and mass in different approached analyses. The evaluation of body proportions and the hypothetical measurements for living crocodilians were important parameters to compare whether the other methodologies were applicable. Besides, to refine such measures, it was evident that the exclusion of the juveniles made the estimates more plausible, as well as the comparison of both regressions with and without juveniles, presenting the best proxy for body mass and body size estimates. Future studies with analysis of the morphometric correlation between DCL and HW may be carried out among extinct and living Caimaninae, to observe if these measurements bias the dimensions of body proportions.

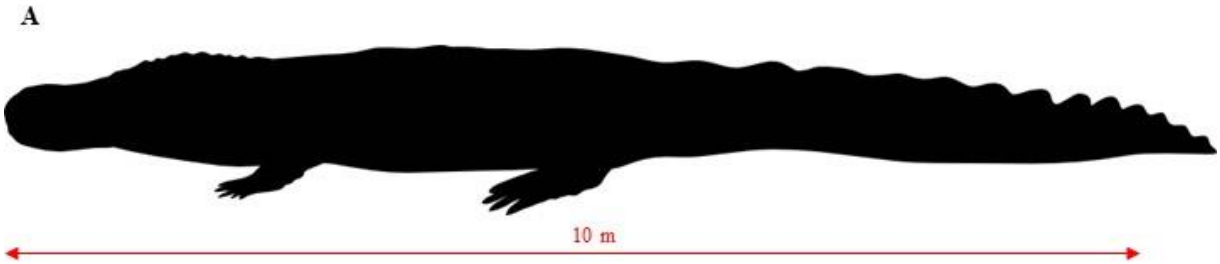

Purussaurus

Based DCL: 9.8 m; 8.2 tons – Based HW: 6.4 m; 2.3 tons – Body proportions: 9 m; 7.1 tons – Adult (DCL): 8.5 m; 3.8 tons – Solórzano et al. (2020): 4.8 tons – Aureliano et al. (2015): 12.5 m; 8.4 tons (*P. brasiliensis*)

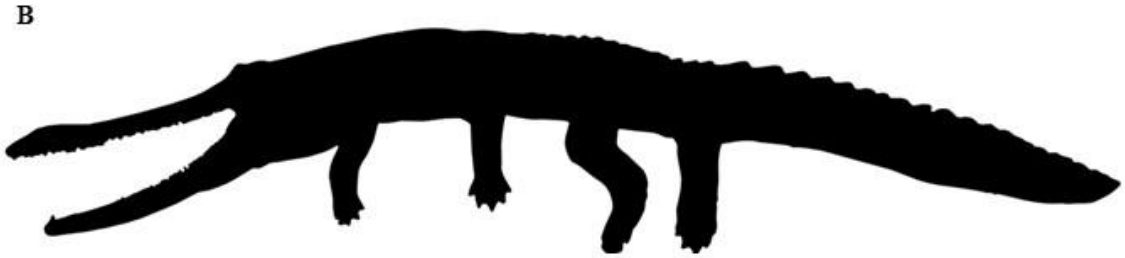

Mourasuchus

Based DCL: 8.8 m; 5.6 tons – Based HW: 4.5 m; 666 kg – Body proportions: 7 m; 3.2 tons – Adult (DCL): 7.7 m; 2.7 tons – Solórzano et al. (2020): 2.3 tons – Cidade et al. (2020b): 9 m; 4 tons

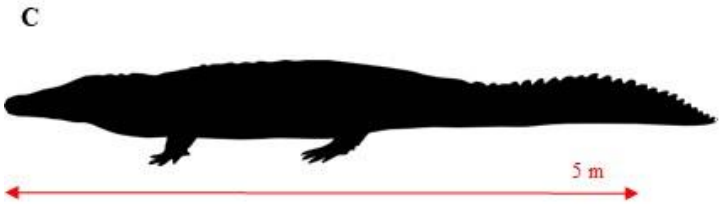

Crocodylus porosus

5.5 m; 1 ton

Acresuchus pachytemporalis

Based DCL: 4.6 m; 601 kg – Based HW: 3.5 m; 217 – 279 kg – Body proportions: 4.5 m; 604 kg – Adult (DCL): 4.5 m; 494 kg – Solórzano et al. (2020): 242 kg

Figure 13 Comparing results based on different previous studies and our research, such as DCL measurement (first methodology), HW measurement (second methodology), body proportions (third methodology), and also the estimation containing only adult living crocodilians, taking as reference DCL. The body mass and body length of *Purussaurus* and *Mourasuchus* are demonstrated as average sizes. A – estimates of *Purussaurus*; B – estimates of *Mourasuchus*; C – body length and body mass of the largest crocodile of our database, *Crocodylus porosus*; and D – estimates of the *Acresuchus pachytemporalis*. Silhouettes taken from philopic.org, by Smokeybjb, Nicholas J. Czaplewski, and Zimices.

ECOLOGICAL AND PHYSIOLOGICAL IMPLICATIONS

The ecology and physiology of crocodilians are important factors directly related to their body size and mass. Size is linked to several aspects of the animal's life, such as specialization in diet, habitat, physiology (Seymour et al., 2013; Godoy et al., 2019; Godoy & Turner, 2020), or thermal relations (Godoy et al., 2019; Stockdale & Benton, 2021). The diversity of caimanines in cranial shapes, body dimensions, and ecological habits are evident from the Miocene age (Riff et al., 2009; Scheyer et al., 2013; Cidade et al., 2019), with small durophagous taxa, e.g., *Caiman wannlangstoni*, *C. brevirostris*, *Kuttanacaiman*, *Globidentosuchus,* and *Gnatusuchus* (Riff et al., 2009; Scheyer et al., 2013; Fortier et al., 2014; Salas-Gismondi et al., 2015), generalist medium sizes, e.g., *Acresuchus*, *Caiman*, *Melanosuchus,* and *Paleosuchus* (Riff et al., 2009; Souza-Filho et al., 2018), the giant predator *Purussaurus* (Riff & Aguilera, 2008; Aureliano et al., 2015), and the gulp-feeder *Mourasuchus* (Cidade et al., 2017; 2019; 2020b).

The present study agrees with Aureliano et al. (2015) that *Purussaurus brasiliensis* was the largest crocodyliform that has ever existed, surpassing the dimensions of *Sarcosuchus* (Sereno et al., 2001; O'Brien et al., 2019) and *Deinosuchus* (Erickson & Brochu, 1999; Schwimmer, 2002; Farlow et al., 2005), which could feed on large prey. *Mourasuchus* was also a large crocodyliform, but on the other hand, it fed on much smaller organisms collected in large quantities (Cidade et al., 2017). *Acresuchus*, a generalist predator of medium size, together with the other species of the middle and late Miocene of South America, form a fauna with a very peculiar diversity, which shared similar habitats, the Pebas and Acre Systems, except for *M. arendsi* also found in Argentina, which form regions with high humidity with an equatorial climate (Cidade et al., 2019).

The Pebas System formed a cluster of lakes, rivers, and swamps with a certain marine influence, which extended from the Acre region, part of the Amazon, Peru, Venezuela and Bolivia, and which has expanded extensively in the middle Miocene (Wesselingh & Salo, 2006; Hoorn et al., 2010a; 2010b;

Alvim et al., 2021). This mega-wetland system originated about 23 Ma (Hoorn et al., 2010a; Wesselingh et al., 2006) as a result of the Andean uplift, making all hydrodynamics flowing from the mountains to the central portion of northwestern South America, providing diversification of invertebrate and vertebrate faunas (Wesselingh & Salo, 2006), and high availability of resources (Hoorn et al., 2010a; 2010b). According to Hoorn (2006), such uplift created a barrier in the atmospheric circulation capable of drastically changing climate. The middle Miocene was known as the *Miocene Climatic Optimum*, due to its significantly increasing temperature in the epoch (Buchardt, 1978; Böhme, 2003; Kaandorp et al., 2005; Super et al., 2018; Methner et al., 2020; Steinthorsdottir et al., 2020). In the early late Miocene, approximately 10 Ma, the huge lake went from a lacustrine system to a fluvial system, denominated as Acre System (Hoorn et al., 2010a; Latrubesse et al., 2010), in which the vertebrate fauna, especially the crocodilians, reached its peak body size. These simultaneous factors allowed for the evolution and diversification of these large and peculiar crocodilians who shared this fauna.

The Pebas and Acre Systems were full of diversified crocodilians, showing differences in diet, that may be directly linked to the size of the animal. In living crocodilians, the diet varies according to the size of the individual (Aureliano et al., 2015). The specialization of the diet is also manifested by its cranial shape. Notosuchia (mostly terrestrial forms) is the group with the largest cranial disparity that can be reflected in dietary strategies (Godoy et al., 2020; Godoy & Turner, 2020), from herbivory to hypercarnivory. Caimaninae is also a group with high cranial disparity due to its diet, which the broader skulls, the increased the amount of food, with short rostra caimanines feeding on terrestrial mammals and reptiles, and those with long snouts, as *Mourasuchus*, have a more piscivorous (Webb et al., 1978) or invertebrate diet. This fauna of the Pebas and Acre Systems was home to large predators, such as *Purussaurus*, with the shore laded in generalist and durophagous predators and its calm waters being propitious to the survival of *Mourasuchus* (Cidade et al., 2020b). Beyond the quiet water, it is already well established that *Mourasuchus* was not an active predator. Its delicate jaws, small teeth, and long,

flat dorsoventrally face indicate a diet of small organisms that could collect with the ventral portion of the rostrum (Cidade et al., 2017). In addition, its cervical vertebrae were short and flat, indicating little mobility, being a lentic animal unable of doing "death-roll" (Cidade et al., 2020b), a feeding strategy that living crocodilians adopt to acquire large preys; however, until now, there is no biomechanical evidence has yet been made for the genus that supports it. *Mourasuchus* can be considered one of the largest crocodyliforms that have ever existed, showing that large caimans are not limited to a lifestyle as active predators. Likewise, Blanco et al. (2015) analyzed that *Purussaurus* did not exert the "death-roll" strategy. Taking this into account, it can be concluded that animals with large body sizes are slower than the smaller ones, not so active, and the huge mass for itself is advantageous in terms of metabolism. Subsequently, they did not need to embrace such a tactic, as they already had the advantage of being large and strong, and maybe their preys were not as big as those crocodilians (e.g., turtles, sloths, mollusks). Outside caimanines, other crocodilians could inhabit the same paleoenvironment, e.g., the large gavialoids *Gryposuchus*, *Hesperogavialis*, and *Ikanogavialis* (Cidade et al., 2020a), and the crocodyloids *Charactosuchus* and *Brasilosuchus* (Cidade et al., 2019).

Another hypothesis is that evolution itself could have played a role in gigantism, i.e., at a certain point in the lineage of the evolutionary history of organisms, they will reach extreme sizes in deep time, denominated as Cope's rule (Stanley, 1973; Hone & Benton, 2005). Notwithstanding, Godoy et al. (2019) and Stockdale & Benton (2021) found little support for this hypothesis, so this evidence is still questionable, and we agree that the habitat dynamic was vital for gigantism.

Blanckenhorn (2000) mentioned some aspects that affect the life of large animals, such as long growth and development, late sexual maturity, time and energy spent on mating, predation, metabolic demand, less agility, visibility, and need more resources to maintain themselves. However, for an animal to grow it needs to be in good conditions (Blanckenhorn, 2000), and together with the typical and favorable environment where these large crocodilians lived, it would have provided them with all

available resources, being present in the fossil record for some 8 million years. Another point to be mentioned is that large body masses hinder the locomotion in a terrestrial environment (Blanckenhorn, 2000) and this factor is linked to more aquatic animals (Godoy et al., 2019), and the Pebas System provided a good place to live. The caimanines are semi-aquatic, but thinking about the large and heavy ones, they probably only went out to lay their eggs, basking in shallow water, and would have spent more time in it, as this would represent lower energetic costs associated with locomotion. Seymour et al. (2004) and Gearty & Payne (2020) analyzed that the ability of crocodyliforms to remain submerged is linked to body mass, increasing dive duration with increasing mass.

Large organisms may find it difficult to dissipate heat at high temperatures due to their relative small surface area. Smith (1976) and Seebacher et al. (1999) analyzed the thermoregulation in *Crocodylus porosus* and *Alligator mississippiensis*, concluding that in winter the heat loss was slower than in summer when heat gain was faster. Similar relations might have applied to extinct large caimans, seasonal changes during the Miocene, however, are currently unknown. Even without large seasonal temperature fluctuation in the Pebas system, the large caimans might have stayed longer in the water than on land to avoid overheating. Since moving around on land at tropical temperatures would have increased body temperature, heat loss might have been increased through direct contact with water. A detailed discussion regarding thermal physiology and climatic conditions will be given in the next chapter.

Possibly all of these ecological and physiological factors might have influenced the body size and diversity of crocodilians during the Miocene. What remains unknown, however, are the main factors that contributed to the extinction of these giant crocodilians. Probably more than one factor did result in the disappearance of giant caimanines from the Pebas system. We can suggest that the abiotic and biotic conditions that favored the evolution of gigantism, possibly caused the disappearance of these huge and diverse crocodilian species, once those conditions were reverted. The Pebas and Acre Systems were

factors that influenced both cases, the diversification, and extinction of the group. While in the middle Miocene happened intense building of the Andean Uplift, developing the large Pebas System (Hoorn et al., 2010a) and coinciding with the global warming (Zachos et al., 2008), at the end of the Miocene, this mountain established a direct connection with the Atlantic (Hoorn, 2006; Hoorn et al., 2010a) causing a change in the system. The Acre System was established, being similar to current Amazon (Latrubesse et al., 2010), and coinciding with global cooling (Zachos et al., 2008), sediments were dumped (Hoorn, 2006) and the lack of resources was increasing, as well as niche reduction, food availability (Cidade et al., 2019; Godoy et al., 2019), essential for large individuals, decreasing the diversity. In addition, the Andes Cordillera were no longer at their highest altitude, unblocking the atmospheric circulation (Hoorn et al., 2010a) that, concomitantly with global cooling, extinguished those large and peculiar crocodilians that survived for 8 million years.

Supplementary Material I

1.1 LIST OF TABLES

Table S1 Complete data of living crocodilians measures, taken from previous literature (Woodward et al, 1995; Grigg et al, 1998; Verdade, 2000; Seymour et al, 2013; Godoy et al, 2019; Mannion et al, 2019; O'Brien et al, 2019). HW = head width; DCL = dorsal cranial length; SVL = snout-vent length; TL = total length; BM = body mass. All the measurements are in millimeters and mass in kilos.

Species	HW	DCL	SVL	TL	BM
Alligator_mississippiensis	23.000				0.060
Alligator_mississippiensis	23.000				0.060
Alligator_mississippiensis	33.000				0.220
Alligator_mississippiensis	34.000				0.250
Alligator_mississippiensis	68.000				2.200
Alligator_mississippiensis	70.000				2.450
Alligator_mississippiensis	70.000				2.600
Alligator_mississippiensis	75.000				3.600
Alligator_mississippiensis	78.000				3.150
Alligator_mississippiensis	95.000				4.500
Alligator_mississippiensis	123.000				17.200
Alligator_mississippiensis	125.000				16.300
Alligator_mississippiensis	130.000				15.500
Alligator_mississippiensis	130.000				20.000
Alligator_mississippiensis	140.000				18.000
Alligator_mississippiensis	160.000				32.100
Alligator_mississippiensis	170.000				42.600
Alligator_mississippiensis	170.000				41.000
Alligator_mississippiensis	175.000				47.600
Alligator_mississippiensis	207.000				128.000
Alligator_mississippiensis	215.000				56.000
Alligator_mississippiensis	220.000				87.500
Alligator_mississippiensis	225.000				77.100
Alligator_mississippiensis	225.000				104.500
Alligator_mississippiensis	240.000				116.000
Alligator_mississippiensis	250.000				106.200

Alligator_mississippiensis	270.000				132.000
Alligator_mississippiensis	275.000				129.500
Alligator_mississippiensis	280.000				158.000
Alligator_mississippiensis	280.000				190.500
Alligator_mississippiensis	290.000				155.000
Alligator_mississippiensis	300.000				225.000
Alligator_mississippiensis	305.000				198.000
Alligator_mississippiensis	330.000				230.200
Alligator_mississippiensis	340.000				173.000
Alligator_mississippiensis		600.000		4269.000	324.100
Alligator_mississippiensis		584.000	2189.000	4229.000	473.100
Alligator_mississippiensis			2096.000	4197.000	394.600
Alligator_mississippiensis		559.000	2260.000	4166.000	317.500
Alligator_mississippiensis			2159.000	4089.000	294.800
Alligator_mississippiensis			2134.000	4064.000	349.300
Alligator_mississippiensis			2134.000	4013.000	344.700
Alligator_mississippiensis			2096.000	3810.000	417.300
Alligator_mississippiensis			1515.000	3099.000	
Alligator_mississippiensis			1575.000	3048.000	115.700
Alligator_mississippiensis			1499.000	3023.000	120.200
Alligator_mississippiensis		410.000	1530.000	3000.000	
Alligator_mississippiensis			1575.000	2997.000	111.100
Alligator_mississippiensis			1500.000	2990.000	
Alligator_mississippiensis		410.000	1555.000	2980.000	
Alligator_mississippiensis			1549.000	2972.000	115.700
Alligator_mississippiensis			1499.000	2921.000	124.700
Alligator_mississippiensis			1473.000	2896.000	129.300
Alligator_mississippiensis	193.600		1090.000	2130.000	47.400
Alligator_mississippiensis	216.800		1240.000	2480.000	71.100
Alligator_mississippiensis	219.000		1182.000	2361.000	74.400
Alligator_mississippiensis	230.000		1300.000	2555.000	99.400
Alligator_mississippiensis	323.100		1760.000	3430.000	233.600
Alligator_mississippiensis	308.000		1508.000	2870.000	143.600
Alligator_mississippiensis	283.900		1565.000		177.600
Alligator_mississippiensis	309.700		1740.000	3380.000	225.900
Alligator_mississippiensis	338.000		1890.000	3715.000	296.700
Alligator_mississippiensis			1670.000	3225.000	175.700
Alligator_mississippiensis			1680.000	3070.000	156.800

Alligator_mississippiensis			1230.000	2460.000	79.000
Alligator_mississippiensis			1450.000	2935.000	140.600
Alligator_mississippiensis			1470.000	2850.000	128.600
Alligator_mississippiensis			1220.000	2405.000	75.200
Alligator_sinensis	126.000		740.000		11.800
Alligator_sinensis	120.000		743.000	1395.000	13.100
Alligator_sinensis	130.000		755.000	1540.000	14.730
Alligator_sinensis	138.000		810.000	1550.000	14.600
Alligator_sinensis		198.700		1524.937	
Alligator_sinensis				2225.784	
Caiman_crocodilus		260.500		1983.049	
Caiman_crocodilus				2288.879	
Caiman_crocodilus	148.000		820.000		17.500
Caiman_crocodilus	148.000		940.000	1660.000	19.000
Caiman_crocodilus	140.000		875.000		19.200
Caiman_crocodilus	140.000		980.000		25.270
Caiman_crocodilus		260.500		1983.049	
Caiman_crocodilus				2288.879	
Caiman_latirostris	81.000	111.000	540.000	1030.000	4.370
Caiman_latirostris	149.800	178.100	920.000	1700.000	25.000
Caiman_latirostris	112.200	149.800	713.000	1400.000	12.200
Caiman_latirostris	115.000	157.000	780.000	1465.000	14.000
Caiman_latirostris	124.400	160.200	780.000	1440.000	13.800
Caiman_latirostris	140.000	172.900	875.000	1670.000	28.000
Caiman_latirostris	120.400	159.100	765.000	1450.000	14.600
Caiman_latirostris	173.600	211.000	1040.000	1940.000	43.000
Caiman_latirostris	215.000	236.000	1150.000	2090.000	62.000
Caiman_latirostris	149.400	193.500	895.000	1525.000	30.000
Caiman_latirostris	162.500	198.100	980.000	1700.000	35.500
Caiman_latirostris	145.900	170.100	809.500	1700.500	30.500
Caiman_latirostris	128.700	164.200	803.500	1505.800	22.500
Caiman_latirostris	128.500	154.800	709.000	1545.000	20.000
Caiman_latirostris	131.600	171.500	806.200	1650.000	29.500
Caiman_latirostris	127.600	160.100	820.000	1615.000	19.000
Caiman_latirostris	145.500	175.100	895.000	1710.000	31.000
Caiman_latirostris	184.400	223.000	1101.500	2100.000	51.000
Caiman_latirostris	148.800	187.400	935.000	1820.000	34.500
Caiman_latirostris	133.600	170.200	803.500	1605.000	24.000

Caiman_latirostris	130.100	155.100	707.600	1403.900	21.000
Caiman_latirostris	134.600	162.000	786.000	1503.000	21.000
Caiman_latirostris	63.600	91.700	490.000	810.000	2.000
Caiman_latirostris	58.000	83.300	376.000	746.000	1.500
Caiman_latirostris	66.200	93.900	432.000	856.000	2.150
Caiman_latirostris	58.600	90.900	410.000	806.000	1.700
Caiman_latirostris	57.100	81.700	350.000	710.000	1.300
Caiman_latirostris	56.700	79.200	354.000	706.000	1.200
Caiman_latirostris	64.200	89.300	432.000	856.000	2.000
Caiman_latirostris	43.200	66.400	276.000	558.000	0.600
Caiman_latirostris	67.000	96.400	416.000	836.000	2.050
Caiman_latirostris	55.600	78.000	346.000	698.000	1.100
Caiman_latirostris	67.300	102.300	462.000	911.000	2.350
Caiman_latirostris	42.200	64.700	277.000	547.000	0.510
Caiman_latirostris	55.800	76.100	348.000	711.000	1.100
Caiman_latirostris	58.700	81.500	362.000	718.000	1.350
Caiman_latirostris	50.600	75.900	329.000	655.000	0.950
Caiman_latirostris	57.500	83.000	363.000	738.000	1.250
Caiman_latirostris	73.000	99.800	480.000	936.000	3.200
Caiman_latirostris	76.600	101.500	484.000	985.000	3.700
Caiman_latirostris	66.100	91.600	414.000	783.000	2.300
Caiman_latirostris	77.700	110.600	505.000	993.000	3.650
Caiman_latirostris	68.800	101.900	439.000	866.000	3.300
Caiman_latirostris	44.700	67.900	272.000	517.000	0.490
Caiman_latirostris	59.300	89.000	386.000	768.000	1.500
Caiman_latirostris	50.500	74.500	312.000	578.000	0.820
Caiman_latirostris	89.600	123.900	594.000	1118.500	6.800
Caiman_latirostris	69.500	95.100	439.000	882.000	2.500
Caiman_latirostris	84.500	125.100	558.000	1081.000	5.200
Caiman_latirostris	66.500	93.200	413.000	836.000	2.100
Caiman_latirostris	48.400	73.700	318.000	640.000	0.760
Caiman_latirostris	36.900	54.300	213.000	425.000	0.217
Caiman_latirostris	31.100	49.700	192.000	368.000	0.139
Caiman_latirostris	33.900	52.700	204.000	410.000	0.202
Caiman_latirostris	36.900	56.000	225.000	458.000	0.258
Caiman_latirostris	39.600	61.200	243.000	495.000	0.315
Caiman_latirostris	30.700	48.800	185.000	365.000	0.117
Caiman_latirostris	34.200	51.400	205.000	424.000	0.190

Caiman_latirostris	28.400	44.600	165.000	315.000	0.072
Caiman_latirostris	39.400	57.200	230.000	457.000	0.292
Caiman_latirostris	35.400	54.200	215.000	430.000	0.198
Caiman_latirostris	37.000	56.600	217.000	437.000	0.205
Caiman_latirostris	55.500	77.800	360.000	722.000	1.100
Caiman_latirostris	50.300	72.700	320.000	646.000	0.760
Caiman_latirostris	39.900	61.100	250.000	501.000	0.340
Caiman_latirostris	40.400	61.400	260.000	529.000	0.380
Caiman_latirostris	57.300	76.100	360.000	720.000	1.200
Caiman_latirostris	42.900	63.500	270.000	544.000	0.450
Caiman_latirostris	51.700	76.400	336.000	675.000	0.430
Caiman_latirostris	35.200	54.600	225.000	457.000	0.252
Caiman_latirostris	49.700	72.900	316.000	631.000	0.750
Caiman_latirostris	51.100	75.400	325.000	652.000	0.830
Caiman_latirostris	56.400	80.300	355.000	697.000	1.250
Caiman_latirostris	48.200	72.200	310.000	630.000	0.710
Caiman_latirostris	43.600	64.500	273.000	552.000	0.470
Caiman_latirostris	40.700	61.800	246.000	483.000	0.345
Caiman_latirostris	43.400	65.800	290.000	597.000	0.520
Caiman_latirostris	49.300	73.100	325.000	661.000	0.800
Caiman_latirostris	41.500	62.000	261.000	539.000	0.425
Caiman_latirostris	44.700	66.700	295.000	593.000	0.515
Caiman_latirostris	42.000	60.600	255.000	405.000	0.410
Caiman_latirostris	49.800	71.800	310.000	635.000	0.790
Caiman_latirostris	45.700	67.200	290.000	591.000	0.570
Caiman_latirostris	50.900	73.800	330.000	670.000	0.820
Caiman_latirostris	49.000	68.500	295.000	590.000	0.670
Caiman_latirostris	44.800	65.800	290.000	587.000	0.560
Caiman_latirostris	52.300	78.500	350.000	716.000	1.000
Caiman_latirostris	44.400	65.300	285.000	565.000	0.530
Caiman_latirostris	49.300	72.700	310.000	625.000	0.630
Caiman_latirostris	51.700	74.000	311.000	658.000	0.850
Caiman_latirostris	51.500	74.900	333.000	684.000	0.880
Caiman_latirostris	53.300	80.100	349.000	701.000	1.050
Caiman_latirostris	48.600	74.400	318.000	645.000	0.710
Caiman_latirostris	55.000	83.000	365.000	740.000	1.150
Caiman_latirostris	46.600	71.600	315.000	630.000	0.720
Caiman_latirostris	47.700	69.400	302.000	627.000	0.650

Caiman_latirostris	49.600	70.700	324.000	645.000	0.780
Caiman_latirostris	55.500	80.000	370.000	735.000	1.200
Caiman_latirostris	50.800	73.000	330.000	667.000	0.830
Caiman_latirostris	48.200	73.200	321.000	646.000	0.750
Caiman_latirostris	42.500	61.600	269.000	539.000	0.470
Caiman_latirostris	49.300	70.600	310.000	630.000	0.730
Caiman_latirostris	47.200	67.900	297.000	601.000	0.610
Caiman_latirostris	60.800	86.000	380.000	750.000	1.350
Caiman_latirostris		237.700		1814.464	
Caiman_latirostris				2442.833	
Caiman_latirostris	165.000		865.000		16.100
Caiman_latirostris	169.800		965.000	1768.000	32.300
Caiman_latirostris	150.000		890.000	1675.000	45.000
Caiman_latirostris	150.000		880.000	1680.000	20.400
Caiman_latirostris	140.000		810.000	1565.000	35.000
Caiman_yacare	125.000		790.000		17.000
Caiman_yacare	140.000		830.000	1620.000	17.900
Caiman_yacare	140.000		910.000		19.000
Caiman_yacare			774.000		12.200
Caiman_yacare	133.000		885.000		22.700
Caiman_yacare		322.700		2440.816	
Caiman_yacare				3061.384	
Caiman_yacare		142.000	535.000	965.000	5.600
Caiman_yacare		130.000	535.000	1020.000	4.750
Caiman_yacare		142.000	558.000	1100.000	5.750
Caiman_yacare		132.000	555.000	1045.000	5.250
Caiman_yacare		128.000	585.000	980.000	4.100
Caiman_yacare		134.000	534.000	1035.000	4.350
Caiman_yacare		143.000	597.000	1090.000	5.900
Caiman_yacare		148.000	593.000	1190.000	6.400
Caiman_yacare		148.000	580.000	1070.000	5.250
Caiman_yacare		140.000	570.000	1070.000	5.400
Crocodylus_acutus	240.000		1500.000	2700.000	100.000
Crocodylus_acutus	300.000		1680.000	3175.000	163.640
Crocodylus_acutus				3389.504	
Crocodylus_cataphractus	221.700		1263.700	2311.000	55.500
Crocodylus_cataphractus	254.000		1460.000	2620.000	95.300
Crocodylus_cataphractus	185.000		1290.000		49.900

Crocodylus_intermedius	262.400		1710.000		182.200
Crocodylus_intermedius				4000.000	
Crocodylus_johnstoni	98.000		730.000	1335.000	7.060
Crocodylus_johnstoni	110.000		830.000	1470.000	10.730
Crocodylus_johnstoni	142.500		906.000	1580.000	13.800
Crocodylus_johnstoni	179.900		1020.000	1820.000	23.700
Crocodylus_johnstoni	182.400		1155.000	2150.000	43.000
Crocodylus_johnstoni				2000.000	
Crocodylus_mindorensis	205.000		1250.000	2444.000	68.820
Crocodylus_mindorensis				2500.000	
Crocodylus_moreletii				3000.000	
Crocodylus_moreletii	280.000		1540.000	2840.000	110.000
Crocodylus_niloticus	230.000		1340.000	2610.000	86.090
Crocodylus_niloticus	200.000		1310.000	2395.000	86.500
Crocodylus_niloticus		493.400		3684.709	
Crocodylus_niloticus				3657.478	
Crocodylus_niloticus		560.700		4171.273	
Crocodylus_niloticus				5396.066	
Crocodylus_novaeguineae				3000.000	
Crocodylus_novaeguineae	250.000		1495.000	2905.000	123.000
Crocodylus_novaeguineae	300.000		1540.000	3150.000	185.950
Crocodylus_palustris	330.000		1720.000	3320.000	206.900
Crocodylus_palustris				4500.000	
Crocodylus_porosus		424.600		3185.228	
Crocodylus_porosus				3698.172	
Crocodylus_porosus	140.000		1175.000	2020.000	36.270
Crocodylus_porosus	240.000		1605.000	2990.000	106.000
Crocodylus_porosus	300.000		1845.000	3570.000	168.500
Crocodylus_porosus	380.000		2500.000		447.000
Crocodylus_porosus	365.000		2320.000	4590.000	495.000
Crocodylus_porosus	400.000		2430.000	4510.000	531.000
Crocodylus_porosus	271.400		1520.000	2975.000	119.900
Crocodylus_porosus				2100.000	32.000
Crocodylus_porosus				2300.000	42.000
Crocodylus_porosus				2700.000	77.000
Crocodylus_porosus				3700.000	233.000
Crocodylus_porosus				4200.000	383.000
Crocodylus_porosus				4300.000	408.000

Crocodylus_porosus				4600.000	520.000
Crocodylus_porosus				4600.000	520.000
Crocodylus_porosus				4900.000	660.000
Crocodylus_porosus				5200.000	820.000
Crocodylus_porosus				5500.000	1010.000
Crocodylus_porosus		65.000		425.000	0.190
Crocodylus_porosus		84.000		530.000	0.200
Crocodylus_porosus		83.000		518.000	0.220
Crocodylus_porosus		74.000		497.000	0.265
Crocodylus_porosus		75.000		497.000	0.300
Crocodylus_porosus				720.000	0.940
Crocodylus_porosus		115.000		780.000	1.000
Crocodylus_porosus		110.000		725.000	1.000
Crocodylus_porosus		114.000		750.000	1.040
Crocodylus_porosus		115.000		760.000	1.080
Crocodylus_porosus		115.000		790.000	1.100
Crocodylus_porosus		120.000		800.000	1.240
Crocodylus_porosus		117.000		780.000	1.240
Crocodylus_porosus		122.000		810.000	1.260
Crocodylus_porosus		118.000		810.000	1.300
Crocodylus_porosus		120.000		805.000	1.460
Crocodylus_porosus		124.000		860.000	1.460
Crocodylus_porosus		122.000		836.000	1.500
Crocodylus_porosus		125.000		850.000	1.660
Crocodylus_porosus		169.000		1202.000	5.860
Crocodylus_porosus		166.000		1240.000	6.060
Crocodylus_porosus		165.000		1272.000	6.380
Crocodylus_porosus				1206.000	6.560
Crocodylus_porosus		176.000		1310.000	7.320
Crocodylus_porosus		180.000		1320.000	7.550
Crocodylus_porosus				1463.000	10.900
Crocodylus_porosus		225.000		1710.000	19.400
Crocodylus_porosus		228.000		1733.000	19.500
Crocodylus_porosus		219.000		1754.000	20.200
Crocodylus_porosus		235.000		1797.000	23.400
Crocodylus_porosus		240.000		1835.000	26.000
Crocodylus_porosus		305.000		2189.000	43.400
Crocodylus_porosus		305.000		2215.000	43.500

Crocodylus_porosus		313.000		2200.000	45.000
Crocodylus_porosus		309.000		2325.000	46.800
Crocodylus_porosus		315.000		2291.000	50.200
Crocodylus_porosus		393.000		3057.000	114.000
Crocodylus_porosus		500.000		3960.000	291.000
Crocodylus_porosus		505.000		3953.000	292.000
Crocodylus_porosus		510.000			293.000
Crocodylus_porosus		481.000		3930.000	303.000
Crocodylus_porosus		525.000		4077.000	332.000
Crocodylus_porosus		520.000			339.000
Crocodylus_porosus		580.000		4394.000	389.000
Crocodylus_rhombifer	155.000			1865.000	29.500
Crocodylus_rhombifer	177.000			2090.000	63.000
Crocodylus_rhombifer	222.000			2462.000	64.820
Crocodylus_rhombifer		294.300		2232.166	
Crocodylus_rhombifer				2663.928	
Crocodylus_siamensis				3000.000	
Crocodylus_siamensis	187.000		1088.000	2120.000	39.500
Crocodylus_siamensis	250.000		1430.000		80.000
Crocodylus_siamensis	250.000		1390.000	2630.000	87.450
Crocodylus_suchus				2000.000	
Gavialis_gangeticus	180.000		1780.000	3180.000	102.900
Gavialis_gangeticus	200.000		1830.000	3335.000	120.730
Gavialis_gangeticus		598.300		4442.336	
Gavialis_gangeticus				3005.509	
Gavialis_gangeticus		621.300		4607.892	
Gavialis_gangeticus				3008.298	
Mecistops_cataphractus		519.500		3873.629	
Mecistops_cataphractus				3233.095	
Mecistops_cataphractus		459.900		3441.783	
Mecistops_cataphractus				3066.983	
Melanosuchus_niger	153.000		1025.000		31.250
Melanosuchus_niger	173.000		1187.000		43.400
Melanosuchus_niger	240.000		1465.000	3035.000	103.450
Melanosuchus_niger		524.000		3906.172	
Melanosuchus_niger				5402.357	
Melanosuchus_niger		669.400		4953.534	
Melanosuchus_niger				8535.117	

Osteolaemus_tetraspis		246.900		1882.545	
Osteolaemus_tetraspis				2899.935	
Osteolaemus_tetraspis	115.000		693.000	1240.000	9.400
Osteolaemus_tetraspis	130.000		817.000	1430.000	14.100
Osteolaemus_tetraspis	137.000		820.000	1460.000	15.600
Osteolaemus_tetraspis	125.000		780.000	1390.000	12.800
Osteolaemus_tetraspis	180.000		1020.000	1825.000	33.800
Paleosuchus_palpebrosus	110.000		725.000	1330.000	11.900
Paleosuchus_palpebrosus	110.000		770.000		12.410
Paleosuchus_palpebrosus	123.000		760.000		13.600
Paleosuchus_palpebrosus		196.700		1510.046	
Paleosuchus_palpebrosus				2204.833	
Paleosuchus_trigonatus		227.700		1740.372	
Paleosuchus_trigonatus				2531.336	
Paleosuchus_trigonatus	130.000		845.000	1430.000	18.540
Paleosuchus_trigonatus	150.000		894.000	1560.000	19.100
Paleosuchus_trigonatus	164.000		999.000		28.000
Tomistoma_schlegelii	230.000		1515.000		79.300
Tomistoma_schlegelii	210.000		1510.000	2895.000	90.800
Tomistoma_schlegelii	340.000		2125.000	4045.000	255.000
Tomistoma_schlegelii		588.000		4368.135	
Tomistoma_schlegelii				3469.770	

Table S2 Mean and standard deviation of body dimensions in living crocodilians calculated from values given in Table S1. HW: head width; DCL: dorsal cranial length; SVL: snout-vent length; and TL: total length.

	HW/SVL	**HW/TL**	**DCL/SVL**	**DCL/TL**	**SVL/TL**
Mean	15%	8%	23%	12%	52%
Standard Deviation	4%	2%	2%	2%	3%

Table S3 Mean and standard deviation of body dimensions only in adult living crocodilians calculated from values given in Table S1. HW: head width; DCL: dorsal cranial length; SVL: snout-vent length; and TL: total length.

	HW/SVL	HW/TL	DCL/SVL	DCL/TL	SVL/TL
Mean	15%	8%	23%	13%	53%
Standard Deviation	5%	3%	2%	1%	3%

Table S4 Estimates of HW, DCL, SVL, and TL for different body masses for a hypothetical crocodilian, based on power regressions. BM: body mass in kilos; HW: head width in millimeters; DCL: dorsal cranial length in millimeters; SVL: snout-vent length in millimeters; and TL: total length in millimeters.

BM (kg)	HW (mm)	DCL (mm)	SVL (mm)	TL (mm)
1	47.07	84.04	343.51	687.28
10	99.78	163.89	697.33	1364.06
20	125.10	200.40	862.99	1676.68
30	142.79	225.41	977.58	1891.79
40	156.85	245.03	1068.00	2060.95
50	168.69	261.42	1143.86	2202.51
100	211.51	319.64	1415.60	2707.28
200	265.19	390.83	1751.89	3327.75
300	302.70	439.62	1984.51	3754.68
400	332.49	477.88	2168.07	4090.41
500	357.60	509.84	2322.06	4371.37
600	379.52	537.53	2455.96	4615.19
700	399.10	562.11	2575.18	4831.92
800	416.87	584.31	2683.12	5027.86
900	433.21	604.62	2782.08	5207.29
1000	448.36	623.39	2873.69	5373.21
2000	562.15	762.24	3556.36	6604.66
3000	641.67	857.38	4028.60	7452.00
4000	704.82	932.00	4401.22	8118.33
5000	758.05	994.33	4713.82	8675.95
6000	804.52	1048.34	4985.64	9159.87
7000	846.02	1096.28	5227.66	9590.02
8000	883.70	1139.58	5446.78	9978.92
9000	918.32	1179.20	5647.67	10335.03
10000	950.44	1215.79	5833.64	10664.33

11000	980.47	1249.88	6007.14	10971.25
12000	1008.70	1281.83	6170.03	11259.16
13000	1035.39	1311.94	6323.78	11530.67
14000	1060.74	1340.45	6469.55	11787.89
15000	1084.89	1367.55	6608.26	12032.51
16000	1107.98	1393.40	6740.72	12265.92
17000	1130.11	1418.12	6867.56	12489.31
18000	1151.39	1441.83	6989.33	12703.64
19000	1171.88	1464.63	7106.51	12909.77
20000	1191.66	1486.58	7219.48	13108.42
30000	1360.22	1672.14	8178.13	14790.15
40000	1494.09	1817.68	8934.55	16112.65
50000	1606.94	1939.24	17219.36	17219.36

Table S5 Ordinary least squares regressions for the complete dataset of Table S1 (OLS1), and the dataset containing only adult specimens (OLS2), with their respective confidence intervals (CI). The regressions returned values of the intercept and slopes for head width (HW), dorsal-cranial length (DCL), snout-vent length (SVL), and total length (TL). T-test returned the p-value showing the difference and the significance of both datasets used.

	Intercept	**HW**	**DCL**	**SVL**	**TL**
OLS1	-8.53	0.12	1.96	0.66	1.03
CI	-8.90; -8.15	0.07; 0.17	1.29; 2.63	-0.12; 1.45	0.43; 1.63
OLS2	-5.62	0.28	1.96	-0.43	1.03
CI	-7.16; -4.08	0.19; 0.37	0.85; 3.06	-1.55; 0.67	0.14; 1.92
p-value	5.50E-29	1.76E-09	0.996601	6.62E-03	0.999493

1.2 R SCRIPT I

Script for R, based on Aureliano et al. (2015), estimating total length and body mass of the caimanine fossils (*Acresuchus*, *Mourasuchus*, and *Purussaurus*) with an updated database of extant crocodilians. In "separated_measures" contains the database available in Table S1 of Appendix A, but it was separated for each measure used.

#==#

```
# Set working directory
setwd("C:/Users/anapa/OneDrive/Desktop/estimates")


# Load libraries
library(car)
library(boot)
library(simpleboot)
library(esquisse)
library(ggplot2)
library(readxl)

# Generic function to obtain regression coefficients (required by boot function)
regr <- function(formula, data, indices) {
  d <- data[indices,] # allows boot to select sample
  fit <- lm(formula, data=d)
  return(coef(fit))
}

########################################################################
# FIRST PART: Regression analysis - SVL~DCL
########################################################################

# Here we will use just the data that have both DCL and SVL measures
simultaneously


# Load database
crocsdata1 <- read_excel("separated_measures.xlsx", sheet = 1)

# Transform data to logarithms
logcrocsdata1 <- data.frame(crocsdata1$species, log10(crocsdata1$DCL_mm),
log10(crocsdata1$SVL_mm))

# Rename columns of the logged dataframes
names(logcrocsdata1)[1] <- "species"
names(logcrocsdata1)[2] <- "LOGDCL"
names(logcrocsdata1)[3] <- "LOGSVL"

# Make all variables available by name
attach(logcrocsdata1)

# Perform OLS (ordinary least squares)
print("Regression Analysis SVL~DCL")
ols1 <- lm(LOGSVL ~ LOGDCL, data=logcrocsdata1)
print(summary(ols1))

# Confidence intervals for the regression
print("Confidence Intervals SVL~DCL:")
ci1 <- confint(ols1)
print(ci1)


# Bootstrap 95% CI for regression coefficients
```

```
# Bootstrapping with 1000 replications
results1      <-      boot(data=logcrocsdata1,      statistic=regr,      R=1000,
formula=LOGSVL~LOGDCL)
print("Boostrap Results:")
print(results1)
plot(results1, index=1) # intercept
plot(results1, index=2) # variable

# Get bootstrapped regression coefficients
coef1 <- apply(results1$t, 2, mean)
print("Bootstrapped regression coefficients:")
print(coef1)

# Bootstrap again with simpleboot to get confidence bands
lboot1 <- lm.boot(ols1, R=1000)

# Plot data and regression line with confidence bands
png(file="SVLxDCL.png", height = 480, width = (2*480), bg = "transparent")
plot(lboot1,                                  xlab=expression('Log'[10]*'(DCL)'),
ylab=expression('Log'[10]*'(SVL)'), pch=16)
dev.off()

# Estimate values for Acresuchus
print("Estimates for Acresuchus:")
dcl <- 592.111
newdata1 <- data.frame(LOGDCL = log10(dcl))
predsvl <- predict(ols1, newdata1, interval="predict")
svl <- 10 ^ predsvl[1]
minsvl <- 10 ^ predsvl[2]
maxsvl <- 10 ^ predsvl[3]

print("SVL=")
print(svl)
print("min. SVL=")
print(minsvl)
print("max. SVL=")
print(maxsvl)

detach(logcrocsdata1)

# Dynamic plot
ggplot(crocsdata1) +
  aes(x = DCL_mm, y = SVL_mm, colour = species) +
  geom_point(size = 2.08) +
  scale_color_hue() +
  theme_classic()


#####################################################################
#-------- SECOND PART: Regression analysis - TL~SVL
#####################################################################

# Here we will use just the data that have both SVL and TL measures simultaneously


crocsdata2 <- read_excel("separated_measures.xlsx", sheet = 2)
```

```
logcrocsdata2 <- data.frame(crocsdata2$species, log10(crocsdata2$SVL_mm),
log10(crocsdata2$TL_mm))

names(logcrocsdata2)[1] <- "species"
names(logcrocsdata2)[2] <- "LOGSVL"
names(logcrocsdata2)[3] <- "LOGTL"

attach(logcrocsdata2)

print("Regression Analysis TL~SVL")
ols2 <- lm(LOGTL ~ LOGSVL, data=logcrocsdata2)
print(summary(ols2))

# Confidence intervals for the regression
print("Confidence Intervals TL~SVL:")
ci2 <- confint(ols2)
print(ci2)


# Bootstrap 95% CI for regression coefficients

results2 <- boot(data=logcrocsdata2, statistic=regr, R=1000,
formula=LOGTL~LOGSVL)
print("Boostrap Results:")
print(results2)
plot(results2, index=1)
plot(results2, index=2)

coef2 <- apply(results2$t, 2, mean)
print("Bootstrapped regression coefficients:")
print(coef2)

lboot2 <- lm.boot(ols2, R=1000)

# Plot data and regression line with confidence bands
png(file="TLxSVL.png", height = 480, width = (2*480), bg = "transparent")
plot(lboot2, xlab=expression('Log'[10]*'(SVL)'),
ylab=expression('Log'[10]*'(TL)'), pch=16)
dev.off()

# Estimate values for Acresuchus
print("Estimates for Acresuchus:")
newdata2 <- data.frame(LOGSVL = predsvl[1])
predtl <- predict(ols2, newdata2, interval="predict")
tl <- 10 ^ predtl[1]
mintl <- 10 ^ predtl[2]
maxtl <- 10 ^predtl[3]

print("TL=")
print(tl)
print("min. TL=")
print(mintl)
print("max. TL=")
print(maxtl)
```

```
detach(logcrocsdata2)

ggplot(crocsdata2) +
  aes(x = SVL_mm, y = TL_mm, colour = species) +
  geom_point(size = 2.08) +
  scale_color_hue() +
  theme_classic()


##########################################################################
# THIRD PART: Regression Analysis BM~TL
##########################################################################

# Here we will use just the data that have both TL and BM measures simultaneously

crocsdata3 <- read_excel("separated_measures.xlsx", sheet = 3)

logcrocsdata3   <-   data.frame(crocsdata3$species,   log10(crocsdata3$TL_mm),
log10(crocsdata3$BM_kg))

names(logcrocsdata3)[1] <- "species"
names(logcrocsdata3)[2] <- "LOGTL"
names(logcrocsdata3)[3] <- "LOGBM"

attach(logcrocsdata3)

print("Regression Analysis BM~TL")
ols3 <- lm(LOGBM ~ LOGTL, data=logcrocsdata3)
print(summary(ols3))

print("Confidence Intervals BM~TL")
ci3 <- confint(ols3)
print(ci3)

# Bootstrap 95% CI for regression coefficients

results3     <-     boot(data=logcrocsdata3,     statistic=regr,     R=1000,
formula=LOGBM~LOGTL)
print(results3)
plot(results3, index=1)
plot(results3, index=2)

coef3 <- apply(results3$t, 2, mean)
print("Bootstrapped regression coefficients:")
print(coef3)

lboot3 <- lm.boot(ols3, R=1000)

png(file="BMxTL.png", height=480, width=(2*480))
plot(lboot3,                                xlab=expression('Log'[10]*'(TL)'),
ylab=expression('Log'[10]*'(BM)'), pch=16)
dev.off()

# Estimate values for Acresuchus
print("Estimates for Acresuchus:")
logbm <- ols3$coef[1] + ols3$coef[2] * log10(tl)
```

```
n <- length(logcrocsdata3$LOGBM)
xbar <- mean(logcrocsdata3$LOGBM)
sdev <- sd(logcrocsdata3$LOGBM)
sum <- sum(logcrocsdata3$LOGBM)
sumsq <- sum(logcrocsdata3$BM ^ 2)
serr <- summary(ols3)$sigma
alpha <- 0.05
tval <- qt(alpha / 2, n - 2)
num <- (logbm[[1]] - xbar) ^ 2
dem <- sumsq - 1 / n * (sum ^ 2)
pint <- tval * serr * sqrt(1 + 1 / n + num / dem)

bm <- 10 ^ logbm[[1]]
minbm <- 10 ^ (logbm[[1]] + pint)
maxbm <- 10 ^ (logbm[[1]] - pint)

print("BM=")
print(bm[[1]])
print("min. BM=")
print(minbm)
print("max. BM=")
print(maxbm)

detach(logcrocsdata3)

ggplot(crocsdata3) +
  aes(x = TL_mm, y = BM_kg, colour = species) +
  geom_point(size = 2.08) +
  scale_color_hue() +
  theme_classic()

##############################################################################
# Mourasuchus amazonensis
##############################################################################


# Estimate SVL
print("Estimates for M. amazonensis:")
dcl <- 1135.338
newdata1 <- data.frame(LOGDCL = log10(dcl))
predsvl <- predict(ols1, newdata1, interval="predict")
svl <- 10 ^ predsvl[1]
minsvl <- 10 ^ predsvl[2]
maxsvl <- 10 ^ predsvl[3]

print("SVL=")
print(svl)
print("min. SVL=")
print(minsvl)
print("max. SVL=")
print(maxsvl)

# Estimate TL
print("Estimates for M. amazonensis:")
newdata2 <- data.frame(LOGSVL = predsvl[1])
```

```
predtl <- predict(ols2, newdata2, interval="predict")
tl <- 10 ^ predtl[1]
mintl <- 10 ^ predtl[2]
maxtl <- 10 ^predtl[3]

print("TL=")
print(tl)
print("min. TL=")
print(mintl)
print("max. TL=")
print(maxtl)

# Estimate BM
print("Estimates for M. amazonensis:")
logbm <- ols3$coef[1] + ols3$coef[2] * log10(tl)

n <- length(logcrocsdata3$LOGBM)
xbar <- mean(logcrocsdata3$LOGBM)
sdev <- sd(logcrocsdata3$LOGBM)
sum <- sum(logcrocsdata3$LOGBM)
sumsq <- sum(logcrocsdata3$BM ^ 2)
serr <- summary(ols3)$sigma
alpha <- 0.05
tval <- qt(alpha / 2, n - 2)
num <- (logbm[[1]] - xbar) ^ 2
dem <- sumsq - 1 / n * (sum ^ 2)
pint <- tval * serr * sqrt(1 + 1 / n + num / dem)

bm <- 10 ^ logbm[[1]]
minbm <- 10 ^ (logbm[[1]] + pint)
maxbm <- 10 ^ (logbm[[1]] - pint)

print("BM=")
print(bm[[1]])
print("min. BM=")
print(minbm)
print("max. BM=")
print(maxbm)

##############################################################################
# Mourasuchus arendsi
##############################################################################


# Estimate SVL
print("Estimates for M. arendsi:")
dcl <- 1085.962
newdata1 <- data.frame(LOGDCL = log10(dcl))
predsvl <- predict(ols1, newdata1, interval="predict")
svl <- 10 ^ predsvl[1]
minsvl <- 10 ^ predsvl[2]
maxsvl <- 10 ^ predsvl[3]

print("SVL=")
print(svl)
print("min. SVL=")
```

```
print(minsvl)
print("max. SVL=")
print(maxsvl)

# Estimate TL
print("Estimates for M. arendsi:")
newdata2 <- data.frame(LOGSVL = predsvl[1])
predtl <- predict(ols2, newdata2, interval="predict")
tl <- 10 ^ predtl[1]
mintl <- 10 ^ predtl[2]
maxtl <- 10 ^predtl[3]

print("TL=")
print(tl)
print("min. TL=")
print(mintl)
print("max. TL=")
print(maxtl)

# Estimate BM
print("Estimates for M. arendsi:")
logbm <- ols3$coef[1] + ols3$coef[2] * log10(tl)

n <- length(logcrocsdata3$LOGBM)
xbar <- mean(logcrocsdata3$LOGBM)
sdev <- sd(logcrocsdata3$LOGBM)
sum <- sum(logcrocsdata3$LOGBM)
sumsq <- sum(logcrocsdata3$BM ^ 2)
serr <- summary(ols3)$sigma
alpha <- 0.05
tval <- qt(alpha / 2, n - 2)
num <- (logbm[[1]] - xbar) ^ 2
dem <- sumsq - 1 / n * (sum ^ 2)
pint <- tval * serr * sqrt(1 + 1 / n + num / dem)

bm <- 10 ^ logbm[[1]]
minbm <- 10 ^ (logbm[[1]] + pint)
maxbm <- 10 ^ (logbm[[1]] - pint)

print("BM=")
print(bm[[1]])
print("min. BM=")
print(minbm)
print("max. BM=")
print(maxbm)

#############################################################################
# Mourasuchus atopus
#############################################################################


# Estimate SVL
print("Estimates for M. atopus:")
dcl <- 712.803
newdata1 <- data.frame(LOGDCL = log10(dcl))
predsvl <- predict(ols1, newdata1, interval="predict")
```

```
svl <- 10 ^ predsvl[1]
minsvl <- 10 ^ predsvl[2]
maxsvl <- 10 ^ predsvl[3]

print("SVL=")
print(svl)
print("min. SVL=")
print(minsvl)
print("max. SVL=")
print(maxsvl)

# Estimate TL
print("Estimates for M. atopus:")
newdata2 <- data.frame(LOGSVL = predsvl[1])
predtl <- predict(ols2, newdata2, interval="predict")
tl <- 10 ^ predtl[1]
mintl <- 10 ^ predtl[2]
maxtl <- 10 ^predtl[3]

print("TL=")
print(tl)
print("min. TL=")
print(mintl)
print("max. TL=")
print(maxtl)

# Estimate BM
print("Estimates for M. atopus:")
logbm <- ols3$coef[1] + ols3$coef[2] * log10(tl)

n <- length(logcrocsdata3$LOGBM)
xbar <- mean(logcrocsdata3$LOGBM)
sdev <- sd(logcrocsdata3$LOGBM)
sum <- sum(logcrocsdata3$LOGBM)
sumsq <- sum(logcrocsdata3$BM ^ 2)
serr <- summary(ols3)$sigma
alpha <- 0.05
tval <- qt(alpha / 2, n - 2)
num <- (logbm[[1]] - xbar) ^ 2
dem <- sumsq - 1 / n * (sum ^ 2)
pint <- tval * serr * sqrt(1 + 1 / n + num / dem)

bm <- 10 ^ logbm[[1]]
minbm <- 10 ^ (logbm[[1]] + pint)
maxbm <- 10 ^ (logbm[[1]] - pint)

print("BM=")
print(bm[[1]])
print("min. BM=")
print(minbm)
print("max. BM=")
print(maxbm)

#############################################################################
# Mourasuchus pattersoni
#############################################################################
```

```
# Estimate SVL
print("Estimates for M. pattersoni:")
dcl <- 1081.717
newdata1 <- data.frame(LOGDCL = log10(dcl))
predsvl <- predict(ols1, newdata1, interval="predict")
svl <- 10 ^ predsvl[1]
minsvl <- 10 ^ predsvl[2]
maxsvl <- 10 ^ predsvl[3]

print("SVL=")
print(svl)
print("min. SVL=")
print(minsvl)
print("max. SVL=")
print(maxsvl)

# Estimate TL
print("Estimates for M. pattersoni:")
newdata2 <- data.frame(LOGSVL = predsvl[1])
predtl <- predict(ols2, newdata2, interval="predict")
tl <- 10 ^ predtl[1]
mintl <- 10 ^ predtl[2]
maxtl <- 10 ^predtl[3]

print("TL=")
print(tl)
print("min. TL=")
print(mintl)
print("max. TL=")
print(maxtl)

# Estimate BM
print("Estimates for M. pattersoni:")
logbm <- ols3$coef[1] + ols3$coef[2] * log10(tl)

n <- length(logcrocsdata3$LOGBM)
xbar <- mean(logcrocsdata3$LOGBM)
sdev <- sd(logcrocsdata3$LOGBM)
sum <- sum(logcrocsdata3$LOGBM)
sumsq <- sum(logcrocsdata3$BM ^ 2)
serr <- summary(ols3)$sigma
alpha <- 0.05
tval <- qt(alpha / 2, n - 2)
num <- (logbm[[1]] - xbar) ^ 2
dem <- sumsq - 1 / n * (sum ^ 2)
pint <- tval * serr * sqrt(1 + 1 / n + num / dem)

bm <- 10 ^ logbm[[1]]
minbm <- 10 ^ (logbm[[1]] + pint)
maxbm <- 10 ^ (logbm[[1]] - pint)

print("BM=")
print(bm[[1]])
print("min. BM=")
```

```
print(minbm)
print("max. BM=")
print(maxbm)

#############################################################################
# Purussaurus brasiliensis
#############################################################################


# Estimate SVL
print("Estimates for P. brasiliensis:")
dcl <- 1406.416
newdata1 <- data.frame(LOGDCL = log10(dcl))
predsvl <- predict(ols1, newdata1, interval="predict")
svl <- 10 ^ predsvl[1]
minsvl <- 10 ^ predsvl[2]
maxsvl <- 10 ^ predsvl[3]

print("SVL=")
print(svl)
print("min. SVL=")
print(minsvl)
print("max. SVL=")
print(maxsvl)

# Estimate TL
print("Estimates for P. brasiliensis:")
newdata2 <- data.frame(LOGSVL = predsvl[1])
predtl <- predict(ols2, newdata2, interval="predict")
tl <- 10 ^ predtl[1]
mintl <- 10 ^ predtl[2]
maxtl <- 10 ^predtl[3]

print("TL=")
print(tl)
print("min. TL=")
print(mintl)
print("max. TL=")
print(maxtl)

# Estimate BM
print("Estimates for P. brasiliensis:")
logbm <- ols3$coef[1] + ols3$coef[2] * log10(tl)

n <- length(logcrocsdata3$LOGBM)
xbar <- mean(logcrocsdata3$LOGBM)
sdev <- sd(logcrocsdata3$LOGBM)
sum <- sum(logcrocsdata3$LOGBM)
sumsq <- sum(logcrocsdata3$BM ^ 2)
serr <- summary(ols3)$sigma
alpha <- 0.05
tval <- qt(alpha / 2, n - 2)
num <- (logbm[[1]] - xbar) ^ 2
dem <- sumsq - 1 / n * (sum ^ 2)
pint <- tval * serr * sqrt(1 + 1 / n + num / dem)
```

```
bm <- 10 ^ logbm[[1]]
minbm <- 10 ^ (logbm[[1]] + pint)
maxbm <- 10 ^ (logbm[[1]] - pint)

print("BM=")
print(bm[[1]])
print("min. BM=")
print(minbm)
print("max. BM=")
print(maxbm)

##############################################################################
# Purussaurus mirandai
##############################################################################


# Estimate SVL
print("Estimates for P. mirandai:")
dcl <- 1228.976
newdata1 <- data.frame(LOGDCL = log10(dcl))
predsvl <- predict(ols1, newdata1, interval="predict")
svl <- 10 ^ predsvl[1]
minsvl <- 10 ^ predsvl[2]
maxsvl <- 10 ^ predsvl[3]

print("SVL=")
print(svl)
print("min. SVL=")
print(minsvl)
print("max. SVL=")
print(maxsvl)

# Estimate TL
print("Estimates for P. mirandai:")
newdata2 <- data.frame(LOGSVL = predsvl[1])
predtl <- predict(ols2, newdata2, interval="predict")
tl <- 10 ^ predtl[1]
mintl <- 10 ^ predtl[2]
maxtl <- 10 ^predtl[3]

print("TL=")
print(tl)
print("min. TL=")
print(mintl)
print("max. TL=")
print(maxtl)

# Estimate BM
print("Estimates for P. mirandai:")
logbm <- ols3$coef[1] + ols3$coef[2] * log10(tl)

n <- length(logcrocsdata3$LOGBM)
xbar <- mean(logcrocsdata3$LOGBM)
sdev <- sd(logcrocsdata3$LOGBM)
sum <- sum(logcrocsdata3$LOGBM)
sumsq <- sum(logcrocsdata3$BM ^ 2)
```

```
serr <- summary(ols3)$sigma
alpha <- 0.05
tval <- qt(alpha / 2, n - 2)
num <- (logbm[[1]] - xbar) ^ 2
dem <- sumsq - 1 / n * (sum ^ 2)
pint <- tval * serr * sqrt(1 + 1 / n + num / dem)

bm <- 10 ^ logbm[[1]]
minbm <- 10 ^ (logbm[[1]] + pint)
maxbm <- 10 ^ (logbm[[1]] - pint)

print("BM=")
print(bm[[1]])
print("min. BM=")
print(minbm)
print("max. BM=")
print(maxbm)

##############################################################################
# Purussaurus neivensis
##############################################################################


# Estimate SVL
print("Estimates for P. neivensis:")
dcl <- 910.939
newdata1 <- data.frame(LOGDCL = log10(dcl))
predsvl <- predict(ols1, newdata1, interval="predict")
svl <- 10 ^ predsvl[1]
minsvl <- 10 ^ predsvl[2]
maxsvl <- 10 ^ predsvl[3]

print("SVL=")
print(svl)
print("min. SVL=")
print(minsvl)
print("max. SVL=")
print(maxsvl)

# Estimate TL
print("Estimates for P. neivensis:")
newdata2 <- data.frame(LOGSVL = predsvl[1])
predtl <- predict(ols2, newdata2, interval="predict")
tl <- 10 ^ predtl[1]
mintl <- 10 ^ predtl[2]
maxtl <- 10 ^predtl[3]

print("TL=")
print(tl)
print("min. TL=")
print(mintl)
print("max. TL=")
print(maxtl)

# Estimate BM
print("Estimates for P. neivensis:")
```

```
logbm <- ols3$coef[1] + ols3$coef[2] * log10(tl)

n <- length(logcrocsdata3$LOGBM)
xbar <- mean(logcrocsdata3$LOGBM)
sdev <- sd(logcrocsdata3$LOGBM)
sum <- sum(logcrocsdata3$LOGBM)
sumsq <- sum(logcrocsdata3$BM ^ 2)
serr <- summary(ols3)$sigma
alpha <- 0.05
tval <- qt(alpha / 2, n - 2)
num <- (logbm[[1]] - xbar) ^ 2
dem <- sumsq - 1 / n * (sum ^ 2)
pint <- tval * serr * sqrt(1 + 1 / n + num / dem)

bm <- 10 ^ logbm[[1]]
minbm <- 10 ^ (logbm[[1]] + pint)
maxbm <- 10 ^ (logbm[[1]] - pint)

print("BM=")
print(bm[[1]])
print("min. BM=")
print(minbm)
print("max. BM=")
print(maxbm)

#############################################################################
# Purussaurus sp
#############################################################################


# Estimate SVL
print("Estimates for Purussaurus sp:")
dcl <- 888.44
newdata1 <- data.frame(LOGDCL = log10(dcl))
predsvl <- predict(ols1, newdata1, interval="predict")
svl <- 10 ^ predsvl[1]
minsvl <- 10 ^ predsvl[2]
maxsvl <- 10 ^ predsvl[3]

print("SVL=")
print(svl)
print("min. SVL=")
print(minsvl)
print("max. SVL=")
print(maxsvl)

# Estimate TL
print("Estimates for Purussaurus sp:")
newdata2 <- data.frame(LOGSVL = predsvl[1])
predtl <- predict(ols2, newdata2, interval="predict")
tl <- 10 ^ predtl[1]
mintl <- 10 ^ predtl[2]
maxtl <- 10 ^predtl[3]

print("TL=")
print(tl)
```

```
print("min. TL=")
print(mintl)
print("max. TL=")
print(maxtl)

# Estimate BM
print("Estimates for Purussaurus sp:")
logbm <- ols3$coef[1] + ols3$coef[2] * log10(tl)

n <- length(logcrocsdata3$LOGBM)
xbar <- mean(logcrocsdata3$LOGBM)
sdev <- sd(logcrocsdata3$LOGBM)
sum <- sum(logcrocsdata3$LOGBM)
sumsq <- sum(logcrocsdata3$BM ^ 2)
serr <- summary(ols3)$sigma
alpha <- 0.05
tval <- qt(alpha / 2, n - 2)
num <- (logbm[[1]] - xbar) ^ 2
dem <- sumsq - 1 / n * (sum ^ 2)
pint <- tval * serr * sqrt(1 + 1 / n + num / dem)

bm <- 10 ^ logbm[[1]]
minbm <- 10 ^ (logbm[[1]] + pint)
maxbm <- 10 ^ (logbm[[1]] - pint)

print("BM=")
print(bm[[1]])
print("min. BM=")
print(minbm)
print("max. BM=")
print(maxbm)
```

1.3 R SCRIPT II

R script containing the regressions made for two datasets, one with adult and juvenile specimens (ols1), and the other with only adult specimens (ols2). The table used is the same as Table S1. Additionally, this script uses a t-test to compare the intercept and slopes between both datasets, and plot the differences in each variable.

```
setwd("C:/Users/anapa/OneDrive/Desktop/Test")

library(broom)
library(viridis)
```

```
library(plotly)
library(car)
library(boot)
library(simpleboot)
library(esquisse)
library(readxl)

# Generic function to obtain regression coefficients (required by boot
function)
regr <- function(formula, data, indices) {
  d <- data[indices,] # allows boot to select sample
  fit <- lm(formula, data=d)
  return(coef(fit))
}

crocs <- read_excel("datasets.xlsx")

# Filtering the dataset containing adults and juveniles for the regression
(ols1)
allcrocs <- filter(crocs, Phase == "Adults+juvenile")

# Log data
logallcrocs <- data.frame(allcrocs$Species, log10(allcrocs$HW_mm),
log10(allcrocs$DCL_mm), log10(allcrocs$SVL_mm), log10(allcrocs$TL_mm),
log10(allcrocs$BM_kg))

names(logallcrocs)[1] <- "species"
names(logallcrocs)[2] <- "LOGHW"
names(logallcrocs)[3] <- "LOGDCL"
names(logallcrocs)[4] <- "LOGSVL"
names(logallcrocs)[5] <- "LOGTL"
names(logallcrocs)[6] <- "LOGBM"

attach(logallcrocs)

print("Regression Analysis")
ols1 <- lm(LOGBM ~ LOGHW+LOGDCL+LOGSVL+LOGTL, data=logallcrocs)
print(ols1)

print("Confidence Intervals")
ci1 <- confint(ols1)
print(ci1)

results1 <- boot(data=logallcrocs, statistic=regr, R=1000, formula=LOGBM ~
LOGHW+LOGDCL+LOGSVL+LOGTL)
print("Boostrap Results:")
print(results1)
plot(results1, index=1) # intercept
plot(results1, index=2) #variable

coef1 <- apply(results1$t, 2, mean)
print("Bootstrapped regression coefficients:")
print(coef1)

lboot1 <- lm.boot(ols1, R=1000)
```

```
##############################################################################
####################################

# Filtering the dataset containing only the adults (ols2)
adultcrocs <- filter(crocs, Phase == "Adults")

logadults <- data.frame(adultcrocs$Species, log10(adultcrocs$HW_mm),
log10(adultcrocs$DCL_mm), log10(adultcrocs$SVL_mm), log10(adultcrocs$TL_mm),
log10(adultcrocs$BM_kg))

names(logadults)[1] <- "species"
names(logadults)[2] <- "LOGHW"
names(logadults)[3] <- "LOGDCL"
names(logadults)[4] <- "LOGSVL"
names(logadults)[5] <- "LOGTL"
names(logadults)[6] <- "LOGBM"

attach(logadults)

print("Regression Analysis")
ols2 <- lm(LOGBM ~ LOGHW+LOGDCL+LOGSVL+LOGTL, data=logadults)
print(ols2)

print("Confidence Intervals")
ci2 <- confint(ols2)
print(ci2)

results2 <- boot(data=logadults, statistic=regr, R=1000, formula=LOGBM ~
LOGHW+LOGDCL+LOGSVL+LOGTL)
print("Boostrap Results:")
print(results2)
plot(results2, index=1) # intercept
plot(results2, index=2) #variable

coef2 <- apply(results2$t, 2, mean)
print("Bootstrapped regression coefficients:")
print(coef2)

lboot2 <- lm.boot(ols2, R=1000)

##############################################################################
################################
# Statistic difference between slopes and intercepts
##############################################################################
################################

ttest <- function(reg1, coefnun, reg2){
  co1 <- coef(summary(reg1))
  co2 <- coef(summary(reg2))
  tstat <- (co1[coefnun,1] - co2[coefnun,1])/co1[coefnun,2]
  2 * pt(abs(tstat), reg1$df.residual, lower.tail = F)
}

################# FIRST: INTERCEPT ####################################
```

```
compinter <- ttest(ols1, 1, ols2)
co1 <- coef(summary(ols1))
co2 <- coef(summary(ols2))
co1
tstat <- (co1[1,1] - co2[1,1])/co1[1,2]
2 * pt(abs(tstat), ols1$df.residual, lower.tail = F)


################## FIRST: SLOPES ########################################

# HW
compslope <- ttest(ols1, 2, ols2)
tstat <- (co1[2, 1] - co2[2, 1])/co1[2, 2]
2 * pt(abs(tstat), ols1$df.residual, lower.tail = F)

# DCL
compslope2 <- ttest(ols1, 3, ols2)
tstat <- (co1[3, 1] - co2[3, 1])/co1[3, 2]
2 * pt(abs(tstat), ols1$df.residual, lower.tail = F)

# SVL
compslope3 <- ttest(ols1, 4, ols2)
tstat <- (co1[4, 1] - co2[4, 1])/co1[4, 2]
2 * pt(abs(tstat), ols1$df.residual, lower.tail = F)

# TL
compslope4 <- ttest(ols1, 5, ols2)
tstat <- (co1[5, 1] - co2[5, 1])/co1[5, 1]
2 * pt(abs(tstat), ols1$df.residual, lower.tail = F)


#####################################################################
# Plotting
#####################################################################

# HW ~ BM

data_crocs <- read_excel("datasets.xlsx", sheet = 1)

# Removing the columns that will not use (keeping HW and BM)
groupDatahwbm <- data_crocs[,-c(4,5,6)]
# Revoming missing values
groupDatahwbm  <- na.omit(groupDatahwbm)

log_crocs_hwbm <- data.frame(groupDatahwbm$Phase, groupDatahwbm$Species,
log10(groupDatahwbm[,c(3,4)]))
names(log_crocs_hwbm)[1] <- "Phase"
names(log_crocs_hwbm)[2] <- "Species"

# Sequencing the table
length(log_crocs_hwbm$Phase)
rownames(log_crocs_hwbm) <- seq(1, 348)

# Removing the crocs that are too small
log_crocs_hwbm2 <- log_crocs_hwbm[-c(64:73, 289:298),]
```

```
# Sequencing the table again
length(log_crocs_hwbm2$Phase)
rownames(log_crocs_hwbm2) <- seq(1, 328)

# Function
plotly_interaction <- function(data, x, y, category, ...) {
  # Create Plotly scatter plot of x vs y, with separate lines for each level
of the categorical variable.
  # In other words, create an interaction scatter plot.
  # The "colors" must be supplied in a RGB triplet, as produced by col2rgb().

  groups <- unique(data[[category]])

  p <- plot_ly(...)

  colors <- col2rgb(2:3)

  for (i in 1:length(groups)) {
    groupData = data[which(data[[category]]==groups[[i]]), ]

    p <- add_lines(p, data = groupData,
                   y = fitted(lm(data = groupData, groupData[[y]] ~
groupData[[x]])),
                   x = groupData[[x]],
                   line = list(color = paste('rgb', '(', paste(colors[, i],
collapse = ", "), ')')),
                   name = groups[[i]],
                   showlegend = FALSE)

    reg_aug<-augment(lm(data = groupData, groupData[[y]] ~ groupData[[x]]),
se_fit = T)
    .fitted<-reg_aug$.fitted
    .se.fit<-reg_aug$.fitted
    p <- add_ribbons(p, data = reg_aug,
                     y = groupData[[y]],
                     x = groupData[[x]],
                     ymin = ~.fitted - 1.96 * .se.fit,
                     ymax = ~.fitted + 1.96 * .se.fit,
                     line = list(color = paste('rgba','(', paste(colors[, i],
collapse = ", "), ', 0.05)')),
                     fillcolor = paste('rgba', '(', paste(colors[, i],
collapse = ", "), ', 0.1)'),
                     showlegend = FALSE)

    p <- add_markers(p, data = groupData,
                     x = groupData[[x]],
                     y = groupData[[y]],
                     symbol = groupData[[category]],
                     marker = list(color=paste('rgb','(', paste(colors[, i],
collapse = ", "))))
  }
  p <- layout(p, xaxis = list(title = "Body Mass"), yaxis = list(title = "Head
Width"))
  p
}
```

```
plotly_interaction(log_crocs_hwbm, "BM_kg", "HW_mm", "Phase")
plotly_interaction(log_crocs_hwbm2, "BM_kg", "HW_mm", "Phase")


#####################################################################

# DCL ~ BM

groupDatadclbm <- data_crocs[,-c(3,5,6)]

groupDatadclbm  <- na.omit(groupDatadclbm)

log_crocs_dclbm <- data.frame(groupDatadclbm$Phase, groupDatadclbm$Species,
log10(groupDatadclbm[,c(3,4)]))
names(log_crocs_dclbm)[1] <- "Phase"
names(log_crocs_dclbm)[2] <- "Species"

length(log_crocs_dclbm$Phase)
rownames(log_crocs_dclbm) <- seq(1, 200)

plotly_interaction <- function(data, x, y, category, ...) {

  groups <- unique(data[[category]])

  p <- plot_ly(...)

  colors <- col2rgb(2:3)

  for (i in 1:length(groups)) {
    groupData = data[which(data[[category]]==groups[[i]]), ]

    p <- add_lines(p, data = groupData,
                   y = fitted(lm(data = groupData, groupData[[y]] ~
groupData[[x]])),
                   x = groupData[[x]],
                   line = list(color = paste('rgb', '(', paste(colors[, i],
collapse = ", "), ')')),
                   name = groups[[i]],
                   showlegend = FALSE)

    reg_aug<-augment(lm(data = groupData, groupData[[y]] ~ groupData[[x]]),
se_fit = T)
    .fitted<-reg_aug$.fitted
    .se.fit<-reg_aug$.fitted
    p <- add_ribbons(p, data = reg_aug,
                     y = groupData[[y]],
                     x = groupData[[x]],
                     ymin = ~.fitted - 1.96 * .se.fit,
                     ymax = ~.fitted + 1.96 * .se.fit,
                     line = list(color = paste('rgba','(', paste(colors[, i],
collapse = ", "), ', 0.05)')),
                     fillcolor = paste('rgba', '(', paste(colors[, i],
collapse = ", "), ', 0.1)'),
                     showlegend = FALSE)

    p <- add_markers(p, data = groupData,
```

```
                    x = groupData[[x]],
                    y = groupData[[y]],
                    symbol = groupData[[category]],
                    marker = list(color=paste('rgb','(', paste(colors[, i],
collapse = ", "))))
  }
  p <- layout(p, xaxis = list(title = "Body Mass"), yaxis = list(title =
"Dorsal Cranial Length"))
  p
}

plotly_interaction(log_crocs_dclbm, "BM_kg", "DCL_mm", "Phase")


#################################################################

# SVL ~ BM

groupDatasvlbm <- data_crocs[,-c(3,4,6)]

groupDatasvlbm  <- na.omit(groupDatasvlbm)

log_crocs_svlbm <- data.frame(groupDatasvlbm$Phase,
groupDatasvlbm$Species,log10(groupDatasvlbm[,c(3, 4)]))
names(log_crocs_svlbm)[1] <- "Phase"
names(log_crocs_svlbm)[2] <- "Species"

length(log_crocs_svlbm$Phase)
rownames(log_crocs_svlbm) <- seq(1, 326)

plotly_interaction <- function(data, x, y, category, ...) {

  groups <- unique(data[[category]])

  p <- plot_ly(...)

  colors <- col2rgb(2:3)

  for (i in 1:length(groups)) {
    groupData = data[which(data[[category]]==groups[[i]]), ]

    p <- add_lines(p, data = groupData,
                   y = fitted(lm(data = groupData, groupData[[y]] ~
groupData[[x]])),
                   x = groupData[[x]],
                   line = list(color = paste('rgb', '(', paste(colors[, i],
collapse = ", "), ')')),
                   name = groups[[i]],
                   showlegend = FALSE)

    reg_aug<-augment(lm(data = groupData, groupData[[y]] ~ groupData[[x]]),
se_fit = T)
    .fitted<-reg_aug$.fitted
    .se.fit<-reg_aug$.fitted
    p <- add_ribbons(p, data = reg_aug,
                     y = groupData[[y]],
```

```
                    x = groupData[[x]],
                    ymin = ~.fitted - 1.96 * .se.fit,
                    ymax = ~.fitted + 1.96 * .se.fit,
                    line = list(color = paste('rgba','(', paste(colors[, i],
collapse = ", "), ', 0.05)')),
                    fillcolor = paste('rgba', '(', paste(colors[, i],
collapse = ", "), ', 0.1)'),
                    showlegend = FALSE)

    p <- add_markers(p, data = groupData,
                    x = groupData[[x]],
                    y = groupData[[y]],
                    symbol = groupData[[category]],
                    marker = list(color=paste('rgb','(', paste(colors[, i],
collapse = ", "))))
  }
  p <- layout(p, xaxis = list(title = "Body Mass"), yaxis = list(title =
"Snout Vent Length"))
  p
}

plotly_interaction(log_crocs_svlbm, "BM_kg", "SVL_mm", "Phase")



#####################################################################

# TL ~ BM

groupDatatlbm <- data_crocs[,-c(3,4,5)]

groupDatatlbm  <- na.omit(groupDatatlbm)

log_crocs_tlbm <- data.frame(groupDatatlbm$Phase,
groupDatatlbm$Species,log10(groupDatatlbm[,c(3, 4)]))
names(log_crocs_tlbm)[1] <- "Phase"
names(log_crocs_tlbm)[2] <- "Species"

length(log_crocs_tlbm$Phase)
rownames(log_crocs_tlbm) <- seq(1, 369)

plotly_interaction <- function(data, x, y, category, ...) {

  groups <- unique(data[[category]])

  p <- plot_ly(...)

  colors <- col2rgb(2:3)

  for (i in 1:length(groups)) {
    groupData = data[which(data[[category]]==groups[[i]]), ]

    p <- add_lines(p, data = groupData,
                   y = fitted(lm(data = groupData, groupData[[y]] ~
groupData[[x]])),
                   x = groupData[[x]],
```

```
                    line = list(color = paste('rgb', '(', paste(colors[, i],
collapse = ", "), ')')),
                    name = groups[[i]],
                    showlegend = FALSE)

    reg_aug<-augment(lm(data = groupData, groupData[[y]] ~ groupData[[x]]),
se_fit = T)
    .fitted<-reg_aug$.fitted
    .se.fit<-reg_aug$.fitted
    p <- add_ribbons(p, data = reg_aug,
                     y = groupData[[y]],
                     x = groupData[[x]],
                     ymin = ~.fitted - 1.96 * .se.fit,
                     ymax = ~.fitted + 1.96 * .se.fit,
                     line = list(color = paste('rgba','(', paste(colors[, i],
collapse = ", "), ', 0.05)')),
                     fillcolor = paste('rgba', '(', paste(colors[, i],
collapse = ", "), ', 0.1)'),
                     showlegend = FALSE)

    p <- add_markers(p, data = groupData,
                     x = groupData[[x]],
                     y = groupData[[y]],
                     symbol = groupData[[category]],
                     marker = list(color=paste('rgb','(', paste(colors[, i],
collapse = ", "))))
  }
  p <- layout(p, xaxis = list(title = "Body Mass"), yaxis = list(title =
"Total Length"))
  p
}


plotly_interaction(log_crocs_tlbm, "BM_kg", "TL_mm", "Phase")
```

1.4 CRANIAL FIGURES OF THE CAIMANINAE FROM THE MIOCENE

Figures used to measure the head width (HW) and dorsal cranial length (DCL) in ImageJ program, version 1.53c, of the nine specimens from the middle and late Miocene of South America.

Figure S1 Holotype of *Acresuchus pachytemporalis* (UFAC-2507) from the late Miocene of Solimões Formation, Brazil. Taken and modified from Cidade (2019). Scale bar = 50 mm.

Figure S2 Holotype of *Mourasuchus amazonensis* (DGM-526-R) from the late Miocene of Solimões Formation, Brazil. Taken and modified from Cidade (2019). Scale bar = 200 mm.

Figure S3 Holotype of *Mourasuchus arendsi* (CIAAP-129) from the late Miocene of Urumaco Formation, Venezuela. Taken and modified from Cidade (2019). Scale bar = 100 mm.

Figure S4 Holotype of *Mourasuchus atopus* (UCMP-3801) from the middle Miocene of Honda Group, Colombia. Taken and modified from Cidade (2019). Scale bar = 100 mm.

Figure S5 Holotype of *Mourasuchus pattersoni* (MCNC-PAL-110-72) from the late Miocene of Urumaco Formation, Venezuela. Taken and modified from Cidade (2019). Scale bar = 200 mm.

Figure S6 Holotype of *Purussaurus brasiliensis* (UFAC-1403) from the late Miocene of Solimões Formation, Brazil. Taken and modified from Cidade (2019). Scale bar = 200 mm.

Figure S7 Holotype of *Purussaurus mirandai* (CIAAP-1369) from the late Miocene of Urumaco Formation, Venezuela. Taken and modified from Cidade (2019). Scale bar = 100 mm.

Figure S8 Holotype of *Purussaurus neivensis* (UCMP-39704) from the middle Miocene of Honda Group, Colombia. Taken and modified from Cidade (2019). Scale bar = 100 mm.

Figure S9 *Purussaurus* sp. (MCNC-PAL-112-72V) from the late Miocene of Urumaco Formation, Venezuela. Scale bar = 100 mm.

Chapter II

BODY MASS AND TEMPERATURE CORRELATIONS IN CAIMANINAE CROCODILIANS FROM THE MIOCENE OF SOUTH AMERICA

Abstract

Crocodilians are ectothermic animals that rely on environmental temperature to regulate their body temperature. Caimaninae diversified during the middle Miocene when the climate was considered hot. Their habitat was composed of huge lakes and swamps, denominated Pebas System. Body size and body mass are influenced by biotic and abiotic factors, such as diet, habitat, physiology, and temperature. Considering this, we used measures of total length of caimanines from the middle and late Miocene from South America, to correlate with body mass and paleotemperature. Oxygen isotope data were used as a proxy for temperature. Additionally, we extracted data regarding the oxygen isotope of phosphate of some crocodilian teeth from the Solimões Formation (being one of them *Purussaurus*), as a proxy to estimate their body temperature. The diversity of caimanines were great during the middle Miocene when the temperature was high. However, an increase in body mass has been demonstrated to occur during the late Miocene, when the temperature was decreasing. Also, the body temperature of some crocodilians might have varied between 7.9ºC and 44.1ºC, in a water body with low values (-1.0ºC to 30ºC). Body temperature seems to have varied a lot, suggesting an ectothermic metabolism. However, to explain the survival of these huge crocodilians in the Late Miocene, we propose a homeothermic condition, as associated to gigantothermy. With this feature, huge crocodilians showed a lower variation in body temperature and the decrease in global temperature seemed not to have been a limiting factor, providing some advantages for their thermoregulation, avoiding overheating, for example, allowing them to survive during global cooling until the Pebas System disappearance.

Keywords: Paleotemperature; body temperature; crocodilians; thermophysiology; gigantothermy.

Introduction

Crocodilians are ectothermic reptiles that rely on environmental conditions and behavioral strategies to regulate body temperature (Séon et al., 2020), such as shuttling between water and land, for example (Seebacher et al., 1999). Overall environmental conditions are therefore of great importance for crocodilian thermal physiology (Grigg et al., 1998; Markwick, 1998; Seebacher et al., 1999; Seymour et al., 2004; Amiot et al., 2007). During the middle Miocene (16.9 ~ 14.7 Ma, Steinthorsdottir et al., 2021), occurred an increase in global temperature (Methner et al., 2020; Steinthorsdottir et al., 2021) known as the *Miocene Climatic Optimum* (Buchardt, 1978; Böhme, 2003; Steinthorsdottir et al., 2021), which coincided with a significant diversification of many tetrapod taxa, especially crocodilians. Additionally, the extensive landscape known as the Pebas System provided favorable conditions for semi-aquatic neotropical ectotherms (Hoorn et al., 2010a; Latrubesse et al., 2010; Alvim et al., 2021), providing an environment rich in resources, niche partitioning, and food (Böhme, 2003; Riff et al., 2009; Wilberg, 2017; Cidade et al., 2019). On the other hand, the late Miocene was marked by a drop in temperature towards present levels (Zachos et al., 2008). According to Godoy et al. (2019), during the Cenozoic, the body size in Crocodylia showed a correlation with an increase in oxygen isotope ($\delta^{18}O$) values within the fossil remains, being inversely proportional to a temperature decrease, seemingly contradicting conditions favorable for ectotherms.

Body mass is related to many aspects of a crocodilian's lifecycle (Godoy et al., 2019), including body temperature regulation. An increase in body mass has been demonstrated to be advantageous for their metabolism (Paladino et al., 1990; Markwick, 1998) by reducing daily body temperature variations (Grigg et al., 1998; Seebacher et al., 1999). The stabilizing effect of increasing body mass on body temperature is known as gigantothermy (Paladino et al., 1990). Seebacher et al. (1999) have investigated body temperatures in a 1,000 kg crocodile and extrapolated their findings to a "crocodile-like dinosaur"

with 10,000 kg, demonstrating very low variation in body temperature. As body mass increases, mean body temperature rises, exposing the animal to the risk of overheating since large animals have a proportionally smaller surface area to dissipate heat (Grigg et al., 1998; Seebacher et al., 1999; 2003).

Taking the importance of environmental temperatures for ectothermic thermoregulation into account, $\delta^{18}O$ has been used as a proxy to reconstruct paleoclimates, paleoenvironments, and body temperature (Amiot et al., 2007; Prokoph et al., 2008; Zachos et al., 2008; Godoy et al., 2019). This isotope is found in skeletal tissues such as carbonates and phosphates (Amiot et al., 2007), the latter being found in tooth enamel (Amiot et al., 2007). $\delta^{18}O$ has also been associated with body water or drinking water (Longinelly & Nuti, 1973; Amiot et al., 2007), thereby inferring body temperature (Lécuyer et al., 2013; Amiot et al., 2017; Séon et al., 2020).

Living crocodilians show body temperatures ranging from 26ºC to 36ºC (Markwick, 1998). However, the body temperature of fossil vertebrates is poorly known as it depends on $\delta^{18}O$ values directly recovered from the fossils. Recently, the thermophysiology of Thalattosuchia (marine crocodylomorphs) was reconstructed and the body temperature was found to range between 29ºC to 37ºC (Séon et al., 2020). To investigate the thermophysiology of large fossil crocodilians, we analyzed the influence of paleotemperature on the body mass of the crocodilians from the middle and late Miocene of South America, specifically the Caimaninae. We asked if changes in paleotemperature may be correlated with changes in body size over time. Additionally, we estimated the body temperature of some fossil crocodilians from Brazil to discuss aspects in the thermophysiology of large Miocene crocodilians.

Materials and Methods

SPECIMENS AND PALEOTEMPERATURE CORRELATION

The data of the Caimaninae fossils were collected according to skull pictures from the literature. They came from four different localities of northern South America, which represent the most incredible biodiversity of the middle and late Miocene:

a) Three (03) specimens from the Pebas Formation, middle Miocene of Peru (Salas-Gismondi et al., 2015; Cidade, 2019);
b) Four (04) species from the Honda Group, middle Miocene of Colombia (Langston, 1965; Langston & Gasparini, 1997; Aguilera et al., 2006; Cidade, 2019; Cidade et al., 2019);
c) Six (06) specimens from the Solimões Formation, late Miocene of Brazil (Aguilera et al., 2006; Fortier et al., 2014; Cidade, 2019; Cidade et al., 2019; Souza-Filho et al., 2018);
d) 12 specimens from the Urumaco Formation, late Miocene of Venezuela (Aguilera et al., 2006; Souza-Filho & Guilherme, 2011; Scheyer & Delfino, 2016; Cidade et al., 2017; Cidade, 2019).

Additionally, measurements were made in their skulls using the ImageJ program, version 1.53c, to estimate body size. We used DCL as a proxy to estimate the body size as detailed in Chapter 1 (by the first methodology) and head width measurements following O'Brien et al. (2019; by the second methodology). The measurement of orbito-dorsal cranial length was made only on one specimen following Aguilera et al. (2006). For incomplete or very fragmented skulls, we used proportional estimates to obtain skull length. The measurements of *Caiman brevirostris* were taken from Fortier et al. (2014). The complete data are given in Tables S6 to S9 (Supplementary Material II).

We extracted information about oxygen isotope ($\delta^{18}O$) values from Zachos et al. (2008), who used isotopic values from benthic foraminifera, and Prokoph et al. (2008), who used sea surface isotopic

values from different organisms. Nonetheless, we used isotopic values from planktic foraminifera in the tropical sea surface region only from the Miocene. For the correlation analysis, an average of these $\delta^{18}O$ data was calculated, according to each of the four geological units that carry Caimanine fossils. We calculated the mean, maximum, and minimum body sizes using the group's average, the largest, and the smallest specimen, respectively, for each unit. The fossils were analyzed through time, specifically middle (~13 Ma; Pebas and Honda formations) and late (~8.3 Ma; Urumaco and Solimões formations) Miocene. The detailed data are given in Table 7. We used two correlation tests: ordinary least squares (OLS), which is a linear regression, and also generalized least squares (GLS) regression that incorporates a first-order autoregressive model to avoid autocorrelation leading with two curves in a time series (Godoy et al., 2019; Mannion et al., 2019). These analyses were performed using the R language program (Core Team, 2020) version 4.1.1. To read files, the package readxl was used (Wickham et al., 2019), for the graphics, we used the packages esquisse (Meyer & Perrier, 2020) and ggplot2 (Wickham, 2016), and nlme (Pinheiro et al., 2021) for the correlation (R script III).

Table 7 Average of the parameters used in the four different units from the middle and late Miocene of South America. The age is in million years (Ma). The oxygen isotopic ($\delta^{18}O$) values are also represented on average. Additionally, three body size parameters were used: minimum, mean, and maximum body size (the smallest, the average, and the largest crocodilian of the Caimaninae group) in millimeters (mm).

Unit	Age (Ma)	$\delta^{18}O$ from Zachos et al. (2001)	$\delta^{18}O$ from Prokoph et al. (2008)	Minimum body size (mm)	Mean body size (mm)	Maximum body size (mm)
Honda Group	12.55	2.36	-0.76	3409	3809	8056
Pebas Formation	13.75	2.16	-0.92	2264	2724	3123
Solimões Formation	8.11	2.87	-0.87	1428	7594	12507
Urumaco Formation	8.48	2.84	-0.79	2150	6130	10910

ESTIMATING BODY TEMPERATURE

To investigate the thermal relations of the fossil crocodilians in correlation with their size/mass, we took oxygen isotopic phosphate ($\delta^{18}O_p$) data available in the literature (Bissaro-Júnior, 2019). Bissaro-Júnior (2019) examined shells of fossilized chelonians, tooth enamel of crocodilians, and mammals in four different localities of the Solimões Formation (Brazil): Niterói, Talismã, and other two unnamed localities – PRJ26 and PRJ20. $\delta^{18}O_p$ depends totally on the oxygen isotope of the body water ($\delta^{18}O_{bw}$) (Longinelli & Nuti, 1973) and they are highly correlated (Longinelli & Nutti, 1973; Amiot et al., 2007; Royer et al., 2013). Bissaro-Júnior (2019) also inferred the $\delta^{18}O_{bw}$ where these animals lived/ingested based on previous literature (Amiot et al., 2007; Royer et al., 2013; Pouech et al., 2014), and are demonstrated as a fractionation equation (Longinelli & Nuti, 1973; Amiot et al., 2007). According to Longinelli & Nuti (1973), the $\delta^{18}O_p$ values extracted from tooth enamel depend not only on the water ingested or where they lived but also on their body temperature (T_b) or air/water temperature; therefore, Lécuyer et al. (2013) used an updated equation to infer temperature:

$$T(^oC) = 117.4 - 4.5\ (\delta^{18}O_p - \delta^{18}O_{bw}), \qquad (13)$$

The constants 117.4 and -4.5 are empirical values measured by biogenic phosphate (see Lécuyer et al., 2013). Therefore, this equation allows inferring both the water and the body temperature from the oxygen isotope. We adopted this method to estimate the body temperature of crocodilians available in the database by Bissaro-Júnior (2019), which contains 52 samples from 22 specimens. However, we used the average of the $\delta^{18}O_p$ values for each specimen. Previous studies demonstrated that the oxygen isotope of the $\delta^{18}O_{bw}$ is roughly equal to environmental water (Lécuyer et al., 2003; Pucéat et al., 2003; Amiot et al., 2007). Amiot et al. (2007) assumed that crocodilians, as large semi-aquatic reptiles, show

2% of oxygen enrichment (O-enrichment), which could be related to their body mass. We thus applied the equation below to estimate body temperature:

$$T_b(^oC) = 117.4 - 4.5 * (\delta^{18}O_p - (\delta^{18}O_{bw} + 2)). \quad (14)$$

Moreover, the $\delta^{18}O_{bw}$ value of a turtle shell collected in the same study was included (Bissaro-Júnior, 2019).

Results

CORRELATION BETWEEN BODY SIZE AND OXYGEN ISOTOPIC ($\Delta^{18}O$) DATA

The maximum, mean and minimum body sizes (largest, average, and smallest crocodilian) of Caimaninae from the Miocene of South America were analyzed. Most of our data demonstrated weak or no correlation, such as the values extracted from Prokoph et al. (2008), which showed a coefficient of determination from 0.06 to 0.32 and p-values greater than 0.25 (Table S10 in Supplementary Material II). The values extracted from Zachos et al. (2008) for maximum and mean body sizes were the most significant ones showing strong correlations, demonstrating that paleotemperature influenced the animal's body size. The maximum size was revealed to be significant for GLS regression, and the mean size was indicated to be effective using both regressions, GLS and OLS. The coefficient of determination (R^2) was about 0.97, and the p-value <0.02 (Table 8). In GLS regression, the use of an autoregressive model returned a phi coefficient ranging from -0.84 to -0.95, indicating a solid negative relationship. The Akaike Information Criterion (AIC) also presented negative values, which indicates a good model of correlation. The minimum size showed no correlation in both datasets and regressions. The positive values of the slope demonstrates the increasing body length as the values of oxygen isotope increases, being inversely proportional to temperature. Thus, the global paleotemperature influenced the maximum and mean body sizes of those Caimaninae. The script used is given in Supplementary Material II.

BODY TEMPERATURE RECONSTRUCTION

The teeth of the crocodilians analyzed by Bissaro-Júnior (2019) showed oxygen isotopic phosphate ($\delta^{18}O_p$) values ranging between 13.71% and 21.76% (Table 9). The sample N118 represents

a *Purussaurus* specimen (the giant Caimaninae), and its $\delta^{18}O_p$ reached an average of 16.48%. The water temperature (T_w) where these animals lived was calculated, according to equation (13), ranging from -1.0ºC to 30.0ºC. As mentioned in Materials and Methods, we inferred the $\delta^{18}O_p$ value of a turtle shell from the J26-13B site, also extracted from Bissaro-Júnior (2019), based on the study of Pouech et al. (2014), at 16.74% and its body water ($\delta^{18}O_{bw}$) -4.55%. Therefore, to estimate the body temperature (T_b), we added 2% of the $\delta^{18}O_{bw}$ value (equation 14) considering working with huge reptiles (Amiot et al., 2007). Their T_b ranged from 7.9ºC to 44.1ºC (Table 9). *Purussaurus* showed an average of 31.7ºC. The absolute values of the 52 samples are available in Table S12 (Supplementary Material II).

Table 8 Regression analysis of maximum (GLS regression) and mean (both GLS and OLS regressions) body sizes of the Caimaninae with paleotemperature ($\delta^{18}O$) data from Zachos et al. (2008), which have shown a correlation. The values include the phi coefficient, intercept, and slope (being part of the curve), Akaike Information Criterion (AIC), and the coefficient of determination (R^2). Complete information in Table S6, Supplementary Material II.

Data	**GLS**				**OLS**			
	Phi	Intercept	Slope	AIC	R^2	Intercept	Slope	AIC
Maximum size	-0.84	2.262	0.641	-2.375				
Mean size	-0.95	2.267	0.547	-15.570	0.97	2.237	0.560	-10.788

Table 9 Oxygen isotopic values extracted from the phosphate ($\delta^{18}O_p$) of the tooth enamel of crocodilians from the late Miocene Solimões Formation (Brazil), taken from the dissertation of Bissaro-Júnior (2019). Based on these values and using oxygen isotopic of body water value of turtle shell as an independent parameter, the water (T_w) and body (T_b) temperatures were estimated according to the equation adapted by Lécuyer et al. (2013). To evaluate the T_b 2% of body water value, large crocodilians have high O-enrichment relative to the body water. N = Niterói site; T = Talismã site; and the other two localities are unnamed. The values are given as average, the complete table with all the number of samples, with their respective $\delta^{18}O_p$ and temperature estimations, are presented in Table S12 (Supplementary Material II).

Sample	$\delta^{18}O_p$ (‰)	T_w (ºC)	T_b (ºC)
N102	18.66	12.9	21.9
N118	16.48	22.7	31.7
N128	17.09	20.0	29.0
N139	17.78	16.8	25.8
N144	13.71	35.1	44.1
N177	16.79	21.3	30.3
N17	15.77	25.9	34.9
N208	18.22	14.8	23.8
N211	18.43	13.9	22.9
N214	19.04	11.1	20.1
N87	16.33	23.3	32.3
NQ2R	17.25	19.2	28.2
T52	18.12	15.3	24.3
TSN3	17.55	17.9	26.9
TSN6	20.03	6.7	15.7
TSN5	19.86	7.5	16.5
TSN	17.09	20.0	29.0
T177	20.20	5.9	14.9
J20-SN2	16.34	23.3	32.3
J20-4C	21.76	-1.0	7.9
J26-10B	17.25	19.2	28.2
J26-23B	14.85	30.0	39.0

Discussion

THE INFLUENCE OF THE TEMPERATURE ON THE BODY SIZE

The oxygen isotope levels were inversely proportional to temperature (Godoy et al., 2019). The more oxygen (positive values), the lower the temperature, and when the temperature was elevated, oxygen isotope values were low. The influence of the paleotemperature on the mean and maximum sizes of those caimanines is quite interesting because the larger ones date from the late Miocene, when the levels of oxygen isotopes were increasing (i.e., temperature declining). Our correlation results are consistent with those pointed by Godoy et al. (2019), which found correlations between the average size in Crocodylia against abiotic factors, such as paleotemperature and paleolatitude, indicating that this group showed an increase in average size during decreasing ambient temperature, and, as consequence, diversified more in tropical regions, as it can be seen in living crocodilians inhabiting warm regions (Markwick, 1998). Our results are not different; Caimaninae fossils from South America showed an increase in size in the late Miocene, coincidental with the advent of global cooling. According to Grigg & Kirshner (2015), crocodilians that inhabit tropical regions tend to grow faster and reach larger sizes. In contrast, the crocodilians from the middle Miocene were smaller, with higher temperatures (Figure 14). The *Miocene Climatic Optimum* (MCO) provided greater availability of resources (Böhme, 2003; Wilberg, 2017), mainly due to the presence of a complex system with huge lakes, swampy areas, warm and humid climate (Pebas System) with all resources available (Hoorn et al., 2010a; 2010b; Jaramillo et al., 2017; Sá et al., 2020). The diversification of species seems to have been favored by the MCO, especially regarding ectothermic ones such as crocodyliforms (Böhme, 2003; Riff et al., 2009; Grigg & Kirshner, 2015).

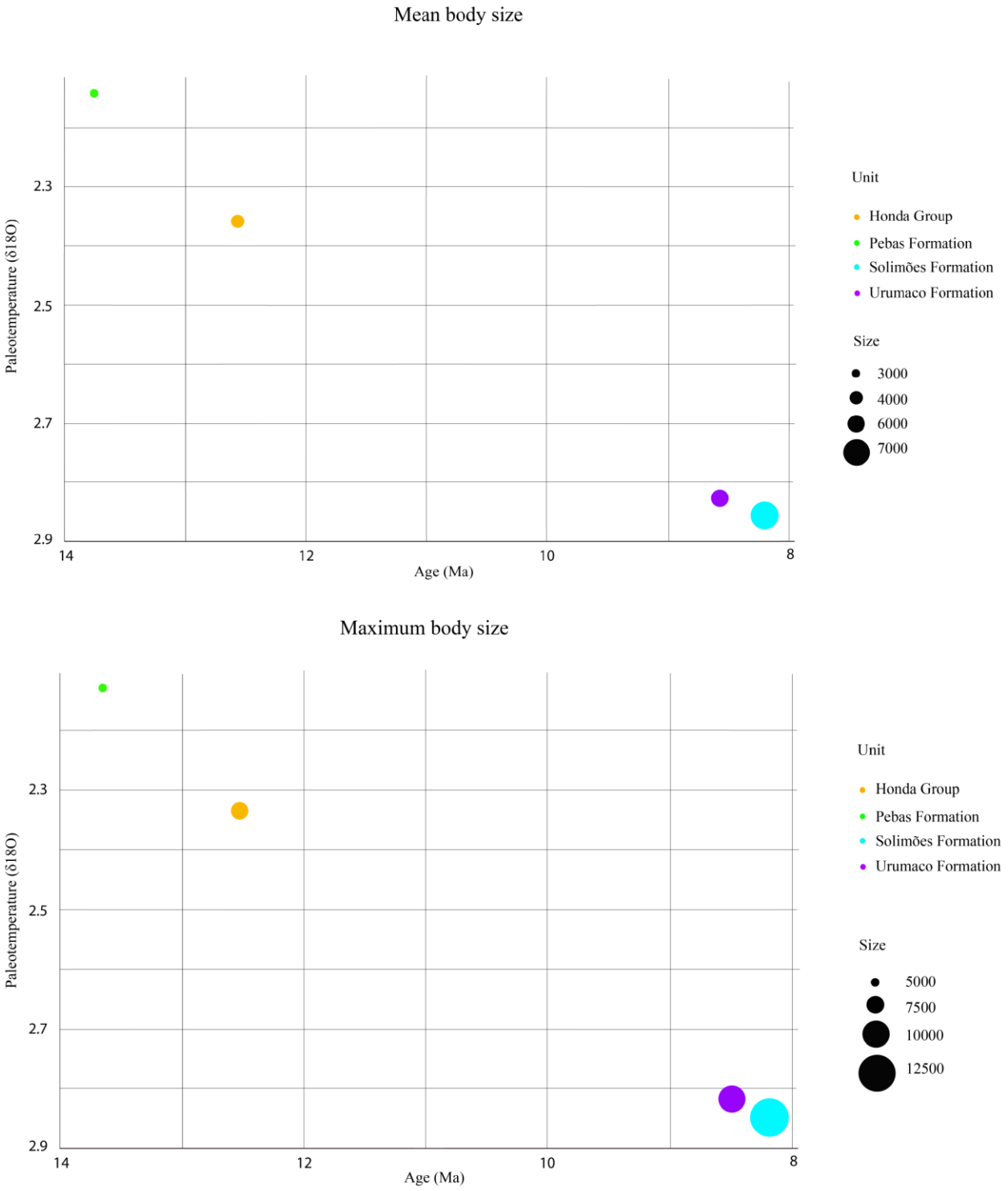

Figure 14 Correlation between body mass and oxygen isotopic values of the middle and late Miocene for four different units of South America: Honda Group (orange), Pebas Formation (green), Urumaco Formation (purple), and Solimões Formation (blue), the last two with the most significant body sizes. The isotopic data for the paleotemperature correlation were taken from Zachos et al. (2008). The top graph indicates the correlation with mean body sizes, and the bottom graph shows the correlation with maximum body sizes, both represented in kilograms.

The Honda Group and the Pebas Formation from Colombia and Peru, respectively (middle Miocene, Langston, 1965; Salas-Gismondi et al., 2015), showed similar paleoenvironments and faunas, dominated by a Pebas mega wetland system (Hoorn et al., 2010a). The presence of some giant caimanines (*Mourasuchus*, *Purussaurus*) and gavialoids (*Gryposuchus*, *Hesperogavialis*) indicates a lentic environment and large flooded areas (Cidade et al., 2017). In the late Miocene, the Amazonia drainage changed its configuration (Hoorn et al., 2010a) to a fluvial-tidal environment (Hoorn et al., 2010b) with freshwater rivers, marine incursions, and a complex depositional system (Sá et al., 2020). The disappearance of the mega wetland due to the Andean uplift coincides with global cooling (Hoorn et al., 2010a), with the main units (Urumaco and Solimões formations) containing a rich diversity of similar faunas, with huge body sizes. But why did not the middle Miocene have more giant crocodilians than the late Miocene, taking into account the differences in the paleotemperature demonstrated by oxygen isotope levels?

The results suggest that the temperature decline was just one more factor for the evolution of gigantism, besides their ecology and physiology. As discussed in Chapter 1, biotic factors influenced larger body sizes, such as specializations in diet, different niches, and their thermoregulation. The declining temperature might have influenced environmental dynamics, such as competition, primary productivity, food/prey availability, territories, habitat preference, and many others, affecting ultimately body size (Grigg & Kirshner, 2015; Cidade et al., 2019). Furthermore, the decline in temperature could have been an advantage for thermoregulation of large crocodilians, because the risk of overheating might have been reduced.

The slight increase in the temperature in the middle Miocene was primordial for the diversification of different ecomorphotypes that caused the species to live sympatrically. According to Grigg & Kirshner (2015), the differences in body sizes in crocodilians imply sympatric species resulting in little competition, such as *Crocodylus acutus* and *Alligator mississippiensis*, occupying the same

habitat. Scheyer et al. (2013) stated that at least seven sympatric species with different ecomorphotypes were inhabiting the same environment during the middle Miocene, suggesting niche partitioning within the Pebas System (Salas-Gismondi et al., 2015).

However, coincidentally with temperature decline through the late Miocene, the Pebas System was losing its support due to the appearance of an actual Amazonian River (Hoorn et al. 2010a). Such a change might have reduced resource availability, as well as niche diversity, food supply (Grigg & Kirshner, 2015), and the similarity in body sizes within such a restricted habitat probably increased the competition between species (Godoy et al., 2019). Also, the significant differences in body size allowed for specializations in diet that could have affected the small caimanines, which probably suffered predatory pressures by larger ones. In living caimanines, *Melanosuchus niger* and *Caiman crocodilus*, the largest and one of the smallest crocodilians, respectively, from the Amazonia ecosystem, compete for territories or prey (Grigg & Kirshner, 2015). The implication for territoriality was a factor that should have guided the evolution of gigantism, favoring their selection and restricting habitat choice (Godoy et al., 2019; Gearty & Payne, 2020). Nonetheless, a drop in temperature following the MCO from ~13 Ma onwards, can be considered as the onset of a period of global cooling (Zachos et al., 2008; Godoy et al., 2019). While different ecomorphotypes evolved in the Pebas System during the MCO, global cooling reduced resource availability and selective pressures on small caimanines; the larger ones have some advantages in the thermal relations that favored their diversification during the global cooling, which will be discussed in the next section.

THERMAL CORRELATIONS

Before discussing the thermal physiology in crocodilians, it is essential to evaluate the oxygen isotope ($\delta^{18}O$) extracted from tooth enamel. In fossils, the extraction of this component is possible in

skeletal tissues containing carbonates and phosphates (Amiot et al., 2007). Several studies have demonstrated that the phosphate, extracted from the tooth enamel of vertebrates, is the best proxy to extract the $\delta^{18}O$ to reconstruct past conditions due to their high preservation (Lécuyer et al., 2003; Pucéat et al., 2003; Amiot et al., 2007; Rey et al., 2013). The most common parameter inferred is paleotemperature.

Amiot et al. (2007) analyzed the $\delta^{18}O_p$ rate in crocodilians to reconstruct body temperature in these animals and demonstrate the importance of $\delta^{18}O$ for reconstructions. Some studies infer that the precipitation of the $\delta^{18}O$ composition in vertebrates is similar to their body water or environmental water (Lécuyer et al., 2003; 2013; Amiot et al., 2007; Royer et al., 2013), and this composition is related to their ecology and physiology (Pouech et al., 2014). These oxygen isotopic rates are demonstrated as a fractionation equation because the $\delta^{18}O_{bw}$ is altered by intake and loss of oxygen isotopes within water (Longinelli & Nuti, 1973; Amiot et al., 2007) by drinking, through food, metabolism, urine, feces, and others (Lécuyer et al., 2003; Amiot et al., 2007; 2017). Besides the temperature, diet and physiology contribute to $\delta^{18}O_p$ values (Amiot et al., 2007), and the values extracted by Bissaro-Júnior (2019), demonstrated in Tables 9 and S12, indicate a $\delta^{18}O_p$ values not differing much from those published by Amiot et al. (2007) in living crocodilians (12.5% - 24.3%).

The $\delta^{18}O_p$ and $\delta^{18}O_{bw}$ compositions depend on the crocodilians' body temperature (Lécuyer et al., 2013), which contributes to the physiology of these large vertebrates, and is influenced by environmental temperature, behavior, and metabolic rates. Previous studies have inferred the body temperature (T_b) in extinct organisms. Bernard et al. (2010) estimated the T_b of giant marine reptiles from the Mesozoic (ichthyosaurs, plesiosaurs, and mosasaurs), which could reach 35ºC to 39ºC, stating that these animals had high metabolic activities and they could regulate their body temperature, possibly possessing some degree of endothermy.

A recent study also has estimated the T_b of marine crocodylomorphs (Thalattosuchia) using the equation adapted by Lécuyer et al. (2013), obtaining temperatures ranging between 29ºC to 37ºC (Séon et al., 2020). In extant vertebrates, T_b in birds was analyzed, showing that *Gallus gallus* could reach more than 40ºC, and it could be associated with their high activity (endothermy, Amiot et al., 2017). In our study, the crocodilians from the late Miocene of the Solimões Formation (Brazil) showed body temperatures above the environmental ones, being an average of 29ºC of T_b in 20ºC of T_w. Recently, Gomes et al. (2021) reconstructed the paleotemperature of the Miocene using some boreholes of the Solimões Formation, estimating the mean annual temperature of 24.9ºC. Thalattosuchians have also demonstrated a higher T_b concerning the T_w (Séon et al., 2020), assuming the 2% of O-enrichment of the body water in crocodyliforms (Amiot et al., 2007). Also, the crocodilians of our study were demonstrated to have variable T_b values and greater ones than the previously studied crocodylomorphs. It is known that marine reptiles have a T_b lower than terrestrial or semi-aquatic ones (Seymour et al., 2004). According to Amiot et al. (2007), the semi-aquatic crocodilians get in contact with air by basking or cooling in the water, being more exposed to the sun, and body mass contributes greatly to this shuttling behavior, representing an interesting explanation for the high body temperatures seen in semi-aquatic crocodilians. In addition, the variations in body temperature found in each sample demonstrate that these crocodilians depended on the environment to thermoregulate. Furthermore, Amiot et al. (2007) mention that the values in each animal analyzed may vary due to differences in available resources/diet. Also, the authors emphasized that there is a probability that the tooth had a temperature different from the body temperature, but this hypothesis needs further investigation.

Living crocodilians show body temperatures ranging from 26ºC to 36ºC (Markwick 1998), with a critical maximum of 39ºC – 40ºC (Amiot et al., 2007). According to Brisbin et al. (1982), American alligators (*Alligator mississippiensis*) have a critical maximum of 38.5ºC and a minimum of 4.5ºC. Moreover, Seebacher et al. (2003) analyzed the body temperature of alligators in different seasons,

reaching almost 30ºC in summer and 15.6ºC in winter, the largest *A. mississippiensis* showing an average of 2ºC higher than the smallest. Additionally, Campos et al. (2005) showed T_b in *Caiman yacare* of the Brazilian Pantanal ranging between 16.9ºC and 37.4ºC. Our study seems to be consistent with these ranges, with an average of 29ºC for extinct crocodilians.

Crocodilians use thermoregulation strategies in their behavior, being an important physiologic factor. By coming out of the water to get warm and entering the water to cool down (Markwick, 1998; Amiot et al., 2007) to regulate T_b. Smith (1976) observed that *Alligator mississippiensis* were more active during the day in colder periods, and more active during the night in warmer periods to avoid overheating during the day; also, they were capable of heating up faster than they cooled down. These thermal strategies are more evident in larger crocodiles, which in winter spend more time on land than in the water, and more time in the water than on land in summer (Grigg et al., 1998). This can be explained by vasoconstriction in cold periods, reducing blood flow to the body surface, and thereby, reducing heat loss while in water or when exposed to cold air (Smith et al., 1984 *apud* Seebacher & Franklyn, 2007), keeping T_b less variable. Moreover, large crocodilians show fewer fluctuations in T_b due to a relatively smaller surface area, reducing heat loss or heat gain when compared to smaller animals with proportional larger surface area (Smith, 1976; Markwick, 1998; Seebacher et al., 1999).

According to Markwick (1998), Seebacher et al. (1999), and Grigg & Kirshner (2015), an increase of the body mass decreases the surface area of the crocodilian's body, providing less contact with the external environment, decreasing the magnitude of heat exchanges, maintaining body temperature for a long time even in cold periods. Grigg et al. (1998) observed that smaller *Crocodylus johnstoni* used behavioral thermal strategies more frequently to regulate body temperature, while the larger ones moved less in and out of the water, which can be explained by a slower heat exchange by the larger animals. Some authors mention that the osteoderms have an important role in the heat exchange since they are well vascularized and in close contact with the environment area absorbing heat (Seidel,

1979; Grigg & Kirshner, 2015), but this is not proven yet, and future studies analyzing these osteoderms can affirm this hypothesis. Seebacher et al. (1999) studied the thermoregulation of the *Crocodylus porosus* and those with more than 1,000 kg, kept T_b at about 30ºC, and the variations were few throughout the seasons of a year. Also, the authors estimated body temperature for a 10,000 kg 'crocodile-like dinosaur' and observed no circadian variation in T_b, with T_b being constant at 31ºC during winter and 36°C during summer. Assuming similar thermal relations, we can propose that giant extinct crocodilians, such as *Purussaurus* and *Mourasuchus*, could reach and maintain high body temperatures through different seasons, even with temperatures decreasing on a global scale during the late Miocene. From a thermal perspective, being a large crocodilian was advantageous during this epoch, because the low temperature could avoid high variations in the body temperature of huge crocodilians, keeping it more constant, and avoiding overheating. The case of ectothermic animals maintaining high body temperatures due to a large body mass was discussed in many studies. Paladino et al. (1990) proposed the term gigantothermy, in which large reptiles, especially the extinct ones (such as dinosaurs and crocodyliforms) with low metabolic rate maintain their heat due to a proportionally small surface area.

According to Aureliano et al. (2015), ectothermy could have precluded those caimans to reach much larger sizes, which could be advantageous because a high metabolic rate would increase their body temperature, guiding to overheating, and would need more food. Gillooly et al. (2006) analyzed growth rates in different fossil dinosaurs to estimate their T_b, which could reach 25ºC in 12 kg dinosaurs, while a 13,000 kg could reach 41ºC, inferring that they had homeothermic conditions with ectothermic metabolism. Nonetheless, Amiot et al. (2006) analyzed the $\delta^{18}O_p$ of small and large dinosaurs and concluded that they had a high and stable T_b, but a high metabolic rate was present in their ancestor. In other living reptiles, gigantothermy also is present, the primary example being the leatherback turtle, one of the largest reptiles that can maintain a T_b of about 20ºC to 30ºC in the sea (Paladino et al., 1990).

The evidence of an endothermic ancestral in the crocodyliforms lineage has long been debated (Seymour, 2013; 2016; Seymour et al., 2004; Cubo et al., 2020). Birds and crocodiles are the only living representatives in Archosauria, the first one with endothermic conditions, and the second one being ectothermic but probably with an endothermic stage during the lineage's evolution. The first who suggested this hypothesis was Bakker (1986), stating possible endothermy in an archosaurian lineage not only because of the crocodilian's physiology but also, because some anatomical features are quite similar to an endothermic animal, such as a four-chambered heart, which separates the high systemic blood pressures from low pulmonary blood pressures (Seymour et al., 2004). Also, the presence of a foramen of Panizza, which allows the shunting of blood between pulmonary and systemic circulations due to the connectivity of the left and right systemic aortas (Grigg & Kirshner, 2015), regulating oxygen delivery during diving, making them the only reptiles to acquire this feature. Seymour et al. (2004) stated that long dives and large body sizes are allometrically correlated. Another example is the unidirectional airflow in the lungs, which is also present in birds (Farmer & Sanders, 2010). Ectothermy probably became as energetic advantage in the aquatic environment for a sit-and-wait ambush predator (Seymour, 2016), and in crocodilians of the late Miocene is probable that they had a metabolic rate of an ectotherm (Grigg & Kirshner, 2015), and were homeothermic due to a great body mass (gigantothermic).

Relative metabolic rate decreases with increasing mass in animals, but ectotherms increase the metabolic rate with increasing body temperature (Seebacher et al., 1999; Makarieva et al., 2005; Grigg & Kirshner, 2015). Seymour et al. (2013) demonstrated that the metabolic rate in estuarine crocodiles, *Crocodylus porosus*, increases allometrically with body mass. Additionally, the food availability affects their sizes. Vertebrates with high metabolic rates and large sizes can search more for prey, increasing the chances of obtaining food (Scharf et al., 2006). Large body sizes imply niche partitioning (Farlow & Planka, 2002), providing good conditions and faster growth (Angilletta & Dunham, 2003).

An important survey, but still not inferred deeply in fossil crocodilians, is the analysis of their bone histology. Erickson & Brochu (1999) observed that *Deinosuchus* (a giant crocodyliform from the Cretaceous) showed a slow bone formation, such as extant crocodilians, characterized by a lamellar bone probably related to their physiology, allowing a prolonged growth to reach large sizes.

Thus, physiology is a very important factor for the growth and constancy of organisms, especially crocodyliforms. The metabolic rate of these animals, even if characterized by their low metabolism, deserves to be highlighted because it is an important agent of physiology and ecology, as it is reflected by an animal's behavior towards the environment in which it lives (Seymour et al., 2013). Seymour et al. (2012) studied nutritive foramen in long bones, being related to the bone tissue's metabolic activity (i.e., great oxygen transport linked with high metabolism) in endothermic animals, and they have large nutritive foramen, suggesting higher metabolic activity. The size of the foramen increases with increasing mass and is directly related to the metabolic capacity of these animals because the size of the blood vessels, that travel through the foramen, indicates oxygenation capacity and, consequently, the required blood flow, in which high activities proportionate good bone remodeling and large nutritive foramen (Seymour, 2016; Seymour et al., 2004, 2012).

Seymour et al. (2012) analyzed this condition in dinosaurs and noted that they also had high aerobic activities in long bone tissue. The blood flow alters heat transfer within the body, and changes in blood flow are an important thermoregulatory mechanism of vertebrates (Seebacher, 2000). Thinking about this scope, crocodilians with high body mass should have large nutritive foramina, and also considering that they possibly had an endothermic ancestor and some features in common. Paladino et al. (1990) suggested that the leatherback turtle changes its blood flow to regulate its heat and body temperature to avoid overheating and hypothermia. However, this needs to be more investigated, and nutritive foramina in fossil crocodilians have to be analyzed for this relation. If their foramina are small, the correlation made by Seymour et al. (2012) that large foramina are related to high activities is correct,

but if their nutritive foramina are large, the size of the nutritive foramina might not directly be related to high metabolic activity and neither with endothermy, but rather body size itself; or this condition was also another endothermic feature acquired by crocodilians.

Supplementary Material II

2.1 LIST OF TABLES

Table S6 Caimaninae specimens from the middle Miocene of Honda Group, Colombia. The skull measures available for them were dorsal cranial length (DCL) and orbito-dorsal cranial length (ODCL) in millimeters (mm). The measure of *Purussaurus neivensis* (ODCL) was made a proportion to get its DCL. The equation to predict body size was according to the skull measure available in Table 7 of the text.

Specimen	Number	Reference picture	Skull measure	Measure (mm)	Body size (mm)
Mourasuchus atopus	UCMP-38012	Cidade (2019)	DCL	712	6284
Purussaurus neivensis	UCMP-39704	Cidade (2019)	DCL	910	8056
P. neivensis	DHL-45	Aguilera et al. (2006)	ODCL/DCL	479	4209
Caiman sp	UCMP-39978	Cidade et al. (2019)	DCL	389	3409

Table S7 Caimaninae specimens from the middle Miocene of Pebas Formation, Peru. The skull measure available for them was the dorsal cranial length (DCL) in millimeters (mm). The equation to predict body size was according to the skull measure available in Table 7 of the text.

Species	Number	Reference picture	Skull measure	Measure (mm)	Body size (mm)
Caiman wannlangstoni	MUSM-2377	Cidade (2019)	DCL	357	3123
Gnatusuchus pebasensis	MUSM-990	Cidade (2019)	DCL	318	2783
Kuttanacaiman iquitosensis	MUSM-1490	Cidade (2019)	DCL	260	2264

Table S8 Caimaninae specimens from the late Miocene of Solimões Formation, Brazil. The skull measures available for them were dorsal cranial length (DCL) and head width (HW) in millimeters (mm). The equation to predict body size was according to the skull measure available in Table 7 of the text. The measure of *Caiman brevirostris* was taken in the literature itself.

Specimen	Number	Reference picture	Skull measure	Measure (mm)	Body size (mm)
Acresuchus pachytemporalis	UFAC-2505	Souza-Filho et al. (2018)	DCL	592	5208
Mourasuchus amazonensis	DGM-526-R	Cidade (2019)	DCL	1135	10069
Mourasuchus cf M. amazonensis	UFAC-1424	Cidade et al. (2019)	HW	692	4015
Purussaurus brasiliensis	UFAC-1118	Aguilera et al. (2006)	DCL	1387	12339
P. brasiliensis	UFAC-1403	Cidade (2019)	DCL	1406	12507
Caiman brevirostris	UFAC-5388	Fortier et al. (2014)	DCL	165	1428

Table S9 Caimaninae specimens from the late Miocene of Urumaco Formation, Venezuela. The skull measures available for them were dorsal cranial length (DCL) and head width (HW) in millimeters (mm). The equation to predict body size was according to the skull measure available in Table 7 of the text.

Specimen	Number	Reference picture	Skull measure	Measure (mm)	Body size (mm)
Mourasuchus arendsi	CIAAP-1297	Cidade (2019)	DCL	1085	9625
M. arendsi	MCNC-URU-110-72V	Scheyer & Delfino (2016)	DCL	1064	9434
M. pattersoni	MCNC-PAL-110-72V	Cidade et al. (2017)	DCL	1081	9587
Purussaurus mirandai	CIAAP-1369	Aguilera et al. (2006)	DCL	1228	10910
P. mirandai	AMU-CURS 1260	Aguilera et al. (2006)	HW	680	3956

P. mirandai	AMU-CURS 135	Scheyer & Delfino (2016)	DCL	1058	9379
Purussaurus cf. mirandai	UNEFM-CIAAP-1368	Souza-Filho & Guilerme (2011)	HW	551	3345
Purussaurus sp.	MCNC-PAL-112-72V		DCL	888	7854
Melanosuchus fisheri	AMU-CURS 234	Scheyer & Delfino (2016)	DCL	296	2583
M. fisheri	MCNC-243	Scheyer & Delfino (2016)	DCL	247	2150
Globydentosuchus brachyrostris	AMU-CURS 222	Scheyer et al. (2013)	DCL	288	2518
Caiman brevirostris	MCNC-1829	Scheyer & Delfino (2016)	DCL	255	2219

Table S10 Regression analysis of the Caimaninae from the Miocene of South America showing the correlation between maximum, mean, and minimum body sizes with oxygen isotopic $\delta^{18}O$ values of the data taken from Prokoph et al. (2008). There were used two different regressions: generalized least squares (GLS) and ordinary least squares (OLS). The values include the phi coefficient, intercept, and slope (being part of the curve), the Akaike Information Criterion (AIC), the coefficient of determination (R^2), and the p-value.

Data	**GLS**					**OLS**				
	Phi	Intercept	Slope	AIC	P-value	R^2	Intercept	Slope	AIC	P-value
Maximum size	0.61	5.477	1.894	5.426	0.33	0.32	5.659	2.126	4.177	0.42
Mean size	0.60	4.046	0.442	4.253	0.76	0.06	4.251	0.695	3.098	0.74
Minimum size	0.57	4.486	1.371	0.897	0.25	0.32	4.346	1.200	-0.300	0.43

Table S11 Regression analysis of the Caimaninae from the Miocene of South America showing the correlation between maximum, mean, and minimum body sizes with oxygen isotopic $\delta^{18}O$ values of the data taken from Zachos et al. (2008). There were used two different regressions: generalized least squares (GLS) and ordinary least squares (OLS). The values include the phi coefficient, intercept, and slope (being part of the curve), the Akaike Information Criterion (AIC), the coefficient of determination (R^2), and the p-value.

Data	**GLS**					**OLS**				
	Phi	Intercept	Slope	AIC	P-value	R^2	Intercept	Slope	AIC	P-value
Maximum size	-0.84	2.262	0.641	-2.375	0.02	0.81	2.104	0.695	-1.066	0.09
Mean size	-0.95	2.267	0.547	-15.570	9e-04	0.97	2.237	0.560	-10.788	0.01
Minimum size	-0.55	4.140	-0.302	0.554	0.22	0.40	4.054	-0.277	-0.800	0.36

Table S12 Complete data of the oxygen isotopic values extracted from tooth enamel ($\delta^{18}O_p$) of the crocodilians from the Solimoes Formation (late Miocene of Brazil) taken from Bissaro-Júnior (2019). Based on these values, the water (T_w) and body (T_b) temperatures were estimated according to the same equation adapted by Lécuyer et al. (2013). It was used the oxygen isotopic of body water value an independent organism (turtle shell) to have no bias, being that to estimate the T_b it was added 2% due to large crocodilians. Each letter from the same specimen (same number) represents the different region where the author extracted the $\delta^{18}O_p$. N = Niteroi site; T = Talismã site; and the others are unnamed.

Sample	**$\delta^{18}O_p$ (%)**	**T_w (ºC)**	**T_b (ºC)**
N102-B	18.66	12.9	21.9
N118-AR	14.43	31.9	40.9
N118-C	16.58	22.2	31.3
N118-DR	17.37	18.7	27.7
N118-DR2	17.41	18.5	27.5
N118-E	15.71	26.2	35.2
N118-G	12.78	39.4	48.4
N118-H	16.79	21.3	30.3
N118-I	14.98	29.5	38.5
N118-J	17.72	17.1	26.1
N118-KR	13.20	37.5	46.5
N118-L	13.66	35.4	44.4

N118-M	14.02	33.8	42.8
N118-P	15.94	25.1	34.1
N118-QR	17.68	17.3	26.3
N118-R	15.00	29.4	38.4
N118-T	17.69	17.3	26.3
N118-U	19.18	10.6	19.6
N118-W	19.09	11.0	20.0
N118-X	17.07	20.0	29.0
N118-Z11	14.53	31.5	40.5
N118-Z13	17.31	18.9	28.0
N118-Z1R	18.50	13.6	22.6
N118-Z4	20.69	3.8	12.8
N118-Z5	18.29	14.6	23.6
N128-A	15.52	27.0	36.0
N128-AR	18.66	12.9	21.9
N139-B	17.78	16.8	25.8
N144-BR	12.90	38.8	47.8
N144-D	14.53	31.5	40.5
N177-C	16.80	21.3	30.3
N17-B	15.77	25.9	34.9
N208-B	18.23	14.8	23.8
N211-HR	18.75	12.5	21.5
N211-OR	18.11	15.4	24.4
N214-A	19.05	11.1	20.1
N87-BR	16.41	23.0	32.0
N87-C	16.45	22.8	31.9
N87-D	16.16	24.2	33.2
NQ2R-D	17.25	19.2	28.2
T52-A	17.55	17.9	26.9
TSN3-B	17.55	17.9	26.9
TSN6-B	20.04	6.7	15.7
TSN5-A	19.87	7.5	16.5
TSN-4A	17.09	20.0	29.0
T177-AR	18.64	13.0	22.0
T52-B	18.69	12.8	21.8
T177-A	21.78	-1.1	7.8
J20-SN2-A	16.35	23.3	32.3
J20-4C	21.77	-1.0	7.9
J26-10B	17.25	19.2	28.2

J26-23B	14.85	30.0	39.0

2.2 R SCRIPT III

The first script of the correlation between body size and paleotemperature, using the maximum size of the Caimaninae from the Miocene of South America available in the previous literature for the correlation with oxygen isotopic values from that epoch, extracted in two different databases (Prokoph et al., 2008; Zachos et al., 2008).

```
# Set working directory
setwd("C:/Users/anapa/OneDrive/Desktop/data_max_size")

# Download packages
library(readxl)
library(esquisse)
library(ggplot2)
library(dplyr)
library(nlme)

#############################################################################
# USING MEAN PROKOPH ET AL. (2008) DATA
#############################################################################

# Downloading data
max_sizeP <- read_excel("temp_maxBS.xlsx", sheet = 1)

# Extract the columns that will gonna use and log body size
logdataP <- data.frame(max_sizeP$unit, max_sizeP$mean_age, max_sizeP$mean_temp,
log10(max_sizeP$max_BS))

# Rename columns
names(logdataP)[1] <- "unit"
names(logdataP)[2] <- "age"
names(logdataP)[3] <- "temp"
names(logdataP)[4] <- "Log_max_BS"
```

```
####### REGRESSION WITH d18O (PROXY FOR TEMPERATURE)

# Using GLS (generalized least squares) with autocorrelation
glsP <- gls(Log_max_BS ~ temp, correlation = corARMA(p = 1), data = logdataP, method = "ML")

# Results in console
summary(glsP)

# Confidence interval of GLS with autocorrelation
ci1 <- confint(glsP)
print(ci1)


# Using GLS without autocorrelation
ols_glsP <- gls(Log_max_BS ~ temp, data = logdataP, method = "ML")
summary(ols_glsP)

ci2 <- confint(ols_glsP)
print(ci2)

# Variance analysis
anova(glsP, ols_glsP)


plot(logdataP$temp, logdataP$Log_max_BS)
abline(lm(logdataP$Log_max_BS ~ logdataP$temp))


# PLOT THE REGRESSION
theme_update(plot.title = element_text(hjust = 0.5))
plot_regression <- ggplot(data = logdataP, aes(temp, Log_max_BS)) +
  geom_point(shape=16, colour = "#42C772", size = 6) +
  theme(panel.background = element_blank(),
        panel.grid.major.y = element_line(colour = "grey95"),
        panel.grid.major.x = element_line(colour = "grey95"),
        panel.grid.minor.y = element_blank(),
        panel.grid.minor.x = element_blank(),
        panel.border = element_rect(colour = "black", fill = NA),
        axis.text.y = element_text(size=8.5),
        axis.text.x = element_text(size=8.5),
        axis.title = element_text(size=9.5),
        title = element_text (size=15.5, face="bold"),
        legend.position="none",
        aspect.ratio=1) +
  geom_smooth(method="lm", se=FALSE, colour = "#BA4762") +
  labs(title = "", x = "temp", y = "BS")
plot_regression
```

```
# PLOT THE REGRESSION IN GGPLOT, WITHOUT THE LOG

max_sizeP %>%
 filter(!is.na(unit)) %>%
 ggplot() +
 aes(x = mean_age, y = mean_temp, colour = unit, size = max_BS) +
 geom_point() +
 scale_color_hue() +
 scale_x_continuous(trans = "reverse") +
 scale_y_continuous(trans = "reverse") +
 labs(x = "Age", y = "Paleotemperature (d18O)") +
 theme_minimal()


#############################################################################
# USING MEAN ZACHOS ET AL. (2008) DATA
#############################################################################


# Downloading data
max_sizeZ <- read_excel("temp_maxBS.xlsx", sheet = 2)

# Extract the columns that will gonna use and log body size
logdataZ <- data.frame(max_sizeZ$unit, max_sizeZ$mean_age, max_sizeZ$mean_temp,
log10(max_sizeZ$max_BS))

# Rename columns
names(logdataZ)[1] <- "unit"
names(logdataZ)[2] <- "age"
names(logdataZ)[3] <- "temp"
names(logdataZ)[4] <- "Log_max_BS"


####### REGRESSION WITH d18O (PROXY FOR TEMPERATURE)

# Using GLS (generalized least squares) with autocorrelation
glsZ <- gls(Log_max_BS ~ temp, correlation = corARMA(p = 1), data = logdataZ, method = "ML")

# Results in console
summary(glsZ)

# Confidence interval of GLS with autocorrelation
ci4 <- confint(glsZ)
print(ci4)


# Using GLS without autocorrelation
```

```
ols_glsZ <- gls(Log_max_BS ~ temp, data = logdataZ, method = "ML")
summary(ols_glsZ)

ci5 <- confint(ols_glsZ)
print(ci5)

# Variance analysis
anova(glsZ, ols_glsZ)


plot(logdataZ$temp, logdataZ$Log_max_BS)
abline(lm(logdataZ$Log_max_BS ~ logdataZ$temp))


# PLOT THE REGRESSION
theme_update(plot.title = element_text(hjust = 0.5))
plot_regression <- ggplot(data = logdataZ, aes(temp, Log_max_BS)) +
  geom_point(shape=16, colour = "#42C772", size = 6) +
  theme(panel.background = element_blank(),
        panel.grid.major.y = element_line(colour = "grey95"),
        panel.grid.major.x = element_line(colour = "grey95"),
        panel.grid.minor.y = element_blank(),
        panel.grid.minor.x = element_blank(),
        panel.border = element_rect(colour = "black", fill = NA),
        axis.text.y = element_text(size=8.5),
        axis.text.x = element_text(size=8.5),
        axis.title = element_text(size=9.5),
        title = element_text (size=15.5, face="bold"),
        legend.position="none",
        aspect.ratio=1) +
  geom_smooth(method="lm", se=FALSE, colour = "#BA4762") +
  labs(title = "", x = "temp", y = "BS")
plot_regression


# PLOT THE REGRESSION IN GGPLOT, WITHOUT THE LOG

max_sizeZ %>%
 filter(!is.na(unit)) %>%
 ggplot() +
 aes(x = mean_age, y = mean_temp, colour = unit, size = max_BS) +
 geom_point() +
 scale_color_hue() +
 scale_x_continuous(trans = "reverse") +
 scale_y_continuous(trans = "reverse") +
 labs(x = "Age", y = "Paleotemperature (d18O)") +
 theme_minimal()
```

Second script of the correlation between body size and paleotemperature, using mean size of the Caimaninae from the Miocene of South America available in the previous literature for the correlation with oxygen isotopic values from that epoch, extracted in two different databases (Prokoph et al., 2008; Zachos et al., 2008).

```
# Set working directory
setwd("C:/Users/anapa/OneDrive/Desktop/data_mean_size")

# Download packages
library(readxl)
library(esquisse)
library(ggplot2)
library(dplyr)
library(nlme)

##############################################################################
# USING MEAN PROKOPH ET AL. (2008) DATA
##############################################################################


# Downloading data
mean_sizeP <- read_excel("temp_meanBS.xlsx", sheet = 1)

# Extract the columns that will gonna use and log body size
logdataP <- data.frame(mean_sizeP$unit, mean_sizeP$mean_age, mean_sizeP$mean_temp, log10(mean_sizeP$mean_BS))

# Rename columns
names(logdataP)[1] <- "unit"
names(logdataP)[2] <- "age"
names(logdataP)[3] <- "temp"
names(logdataP)[4] <- "Log_mean_BS"


############# REGRESSION WITH d18O (PROXY FOR TEMPERATURE)

# Using GLS (generalized least squares) with autocorrelation
glsP <- gls(Log_mean_BS ~ temp, correlation = corARMA(p = 1), data = logdataP, method = "ML")

# Results in console
summary(glsP)
```

```
# Confidence interval of GLS with autocorrelation
ci1 <- confint(glsP)
print(ci1)


# Using GLS without autocorrelation
ols_glsP <- gls(Log_mean_BS ~ temp, data = logdataP, method = "ML")
summary(ols_glsP)

ci2 <- confint(ols_glsP)
print(ci2)

# Variance analysis
anova(glsP, ols_glsP)


plot(logdataP$temp, logdataP$Log_mean_BS)
abline(lm(logdataP$Log_mean_BS ~ logdataP$temp))


# PLOT THE REGRESSION
theme_update(plot.title = element_text(hjust = 0.5))
plot_regression <- ggplot(data = logdataP, aes(temp, Log_mean_BS)) +
  geom_point(shape=16, colour = "#42C772", size = 6) +
  theme(panel.background = element_blank(),
        panel.grid.major.y = element_line(colour = "grey95"),
        panel.grid.major.x = element_line(colour = "grey95"),
        panel.grid.minor.y = element_blank(),
        panel.grid.minor.x = element_blank(),
        panel.border = element_rect(colour = "black", fill = NA),
        axis.text.y = element_text(size=8.5),
        axis.text.x = element_text(size=8.5),
        axis.title = element_text(size=9.5),
        title = element_text (size=15.5, face="bold"),
        legend.position="none",
        aspect.ratio=1) +
  geom_smooth(method="lm", se=FALSE, colour = "#BA4762") +
  labs(title = "", x = "temp", y = "BS")
plot_regression


# PLOT THE REGRESSION IN GGPLOT, WITHOUT THE LOG

mean_sizeP %>%
 filter(!is.na(unit)) %>%
 ggplot() +
 aes(x = mean_age, y = mean_temp, colour = unit, size = mean_BS) +
```

```
 geom_point() +
 scale_color_hue() +
 scale_x_continuous(trans = "reverse") +
 scale_y_continuous(trans = "reverse") +
 labs(x = "Age", y = "Paleotemperature (d18O)") +
 theme_minimal()


##############################################################################
# USING MEAN ZACHOS ET AL. (2008) DATA
##############################################################################


# Downloading data
mean_sizeZ <- read_excel("temp_meanBS.xlsx", sheet = 2)

# Extract the columns that will gonna use and log body size
logdataZ <- data.frame(mean_sizeZ$unit, mean_sizeZ$mean_age, mean_sizeZ$mean_temp,
log10(mean_sizeZ$mean_BS))

# Rename columns
names(logdataZ)[1] <- "unit"
names(logdataZ)[2] <- "age"
names(logdataZ)[3] <- "temp"
names(logdataZ)[4] <- "Log_mean_BS"


############# REGRESSION WITH d18O (PROXY FOR TEMPERATURE)

# Using GLS (generalized least squares) with autocorrelation
glsZ <- gls(Log_mean_BS ~ temp, correlation = corARMA(p = 1), data = logdataZ, method = "ML")

# Results in console
summary(glsZ)

# Confidence interval of GLS with autocorrelation
ci4 <- confint(glsZ)
print(ci4)


# Using GLS without autocorrelation
ols_glsZ <- gls(Log_mean_BS ~ temp, data = logdataZ, method = "ML")
summary(ols_glsZ)

ci5 <- confint(ols_glsZ)
print(ci5)

# Variance analysis
```

```
anova(glsZ, ols_glsZ)


plot(logdataZ$temp, logdataZ$Log_mean_BS)
abline(lm(logdataZ$Log_mean_BS ~ logdataZ$temp))


# PLOT THE REGRESSION
theme_update(plot.title = element_text(hjust = 0.5))
plot_regression <- ggplot(data = logdataZ, aes(temp, Log_mean_BS)) +
  geom_point(shape=16, colour = "#42C772", size = 6) +
  theme(panel.background = element_blank(),
        panel.grid.major.y = element_line(colour = "grey95"),
        panel.grid.major.x = element_line(colour = "grey95"),
        panel.grid.minor.y = element_blank(),
        panel.grid.minor.x = element_blank(),
        panel.border = element_rect(colour = "black", fill = NA),
        axis.text.y = element_text(size=8.5),
        axis.text.x = element_text(size=8.5),
        axis.title = element_text(size=9.5),
        title = element_text (size=15.5, face="bold"),
        legend.position="none",
        aspect.ratio=1) +
  geom_smooth(method="lm", se=FALSE, colour = "#BA4762") +
  labs(title = "", x = "temp", y = "BS")
plot_regression


# PLOT THE REGRESSION IN GGPLOT, WITHOUT THE LOG

mean_sizeZ %>%
 filter(!is.na(unit)) %>%
 ggplot() +
 aes(x = mean_age, y = mean_temp, colour = unit, size = mean_BS) +
 geom_point() +
 scale_color_hue() +
 scale_x_continuous(trans = "reverse") +
 scale_y_continuous(trans = "reverse") +
 labs(x = "Age", y = "Paleotemperature (d18O)") +
 theme_minimal()
```

Third script of the correlation between body size and paleotemperature using minimum size of the Caimaninae from the Miocene of South America available in the previous literature for the

correlation with oxygen isotopic values from that epoch, extracted in two different databases (Prokoph et al., 2008; Zachos et al., 2008).

```
# Set working directory
setwd("C:/Users/anapa/OneDrive/Desktop/data_min_size")

# Download packages
library(readxl)
library(esquisse)
library(ggplot2)
library(dplyr)
library(nlme)

##############################################################################
# USING MEAN PROKOPH ET AL. (2008) DATA
##############################################################################


# Downloading data
min_sizeP <- read_excel("temp_minBS.xlsx", sheet = 1)

# Extract the columns that will gonna use and log body size
logdataP <- data.frame(min_sizeP$unit, min_sizeP$mean_age, min_sizeP$mean_temp, log10(min_sizeP$min_BS))

# Rename columns
names(logdataP)[1] <- "unit"
names(logdataP)[2] <- "age"
names(logdataP)[3] <- "temp"
names(logdataP)[4] <- "Log_min_BS"


############## REGRESSION WITH d18O (PROXY FOR TEMPERATURE)

# Using GLS (generalized least squares) with autocorrelation
glsP <- gls(Log_min_BS ~ temp, correlation = corARMA(p = 1), data = logdataP, method = "ML")

# Results in console
summary(glsP)

# Confidence interval of GLS with autocorrelation
ci1 <- confint(glsP)
print(ci1)
```

```
# Using GLS without autocorrelation
ols_glsP <- gls(Log_min_BS ~ temp, data = logdataP, method = "ML")
summary(ols_glsP)

ci2 <- confint(ols_glsP)
print(ci2)

# Variance analysis
anova(glsP, ols_glsP)


plot(logdataP$temp, logdataP$Log_min_BS)
abline(lm(logdataP$Log_min_BS ~ logdataP$temp))


# PLOT THE REGRESSION
theme_update(plot.title = element_text(hjust = 0.5))
plot_regression <- ggplot(data = logdataP, aes(temp, Log_min_BS)) +
  geom_point(shape=16, colour = "#42C772", size = 6) +
  theme(panel.background = element_blank(),
        panel.grid.major.y = element_line(colour = "grey95"),
        panel.grid.major.x = element_line(colour = "grey95"),
        panel.grid.minor.y = element_blank(),
        panel.grid.minor.x = element_blank(),
        panel.border = element_rect(colour = "black", fill = NA),
        axis.text.y = element_text(size=8.5),
        axis.text.x = element_text(size=8.5),
        axis.title = element_text(size=9.5),
        title = element_text (size=15.5, face="bold"),
        legend.position="none",
        aspect.ratio=1) +
  geom_smooth(method="lm", se=FALSE, colour = "#BA4762") +
  labs(title = "", x = "temp", y = "BS")
plot_regression


# PLOT THE REGRESSION IN GGPLOT, WITHOUT THE LOG

min_sizeP %>%
 filter(!is.na(unit)) %>%
 ggplot() +
 aes(x = mean_age, y = mean_temp, colour = unit, size = min_BS) +
 geom_point() +
 scale_color_hue() +
 scale_x_continuous(trans = "reverse") +
 scale_y_continuous(trans = "reverse") +
 labs(x = "Age", y = "Paleotemperature (d18O)") +
 theme_minimal()
```

```
##############################################################################
# USING MEAN ZACHOS ET AL. (2008) DATA
##############################################################################


# Downloading data
min_sizeZ <- read_excel("temp_minBS.xlsx", sheet = 2)

# Extract the columns that will going to use and log body size
logdataZ <- data.frame(min_sizeZ$unit, min_sizeZ$mean_age, min_sizeZ$mean_temp,
log10(min_sizeZ$min_BS))

# Rename columns
names(logdataZ)[1] <- "unit"
names(logdataZ)[2] <- "age"
names(logdataZ)[3] <- "temp"
names(logdataZ)[4] <- "Log_min_BS"


############# REGRESSION WITH d18O (PROXY FOR TEMPERATURE)

# Using GLS (generalized least squares) with autocorrelation
glsZ <- gls(Log_min_BS ~ temp, correlation = corARMA(p = 1), data = logdataZ, method = "ML")

# Results in console
summary(glsZ)

# Confidence interval of GLS with autocorrelation
ci4 <- confint(glsZ)
print(ci4)


# Using GLS without autocorrelation
ols_glsZ <- gls(Log_min_BS ~ temp, data = logdataZ, method = "ML")
summary(ols_glsZ)

ci5 <- confint(ols_glsZ)
print(ci5)

# Variance analysis
anova(glsZ, ols_glsZ)


plot(logdataZ$temp, logdataZ$Log_min_BS)
abline(lm(logdataZ$Log_min_BS ~ logdataZ$temp))
```

```
# PLOT THE REGRESSION
theme_update(plot.title = element_text(hjust = 0.5))
plot_regression <- ggplot(data = logdataZ, aes(temp, Log_min_BS)) +
  geom_point(shape=16, colour = "#42C772", size = 6) +
  theme(panel.background = element_blank(),
        panel.grid.major.y = element_line(colour = "grey95"),
        panel.grid.major.x = element_line(colour = "grey95"),
        panel.grid.minor.y = element_blank(),
        panel.grid.minor.x = element_blank(),
        panel.border = element_rect(colour = "black", fill = NA),
        axis.text.y = element_text(size=8.5),
        axis.text.x = element_text(size=8.5),
        axis.title = element_text(size=9.5),
        title = element_text (size=15.5, face="bold"),
        legend.position="none",
        aspect.ratio=1) +
  geom_smooth(method="lm", se=FALSE, colour = "#BA4762") +
  labs(title = "", x = "temp", y = "BS")
plot_regression


# PLOT THE REGRESSION IN GGPLOT, WITHOUT THE LOG

min_sizeZ %>%
 filter(!is.na(unit)) %>%
 ggplot() +
 aes(x = mean_age, y = mean_temp, colour = unit, size = min_BS) +
 geom_point() +
 scale_color_hue() +
 scale_x_continuous(trans = "reverse") +
 scale_y_continuous(trans = "reverse") +
 labs(x = "Age", y = "Paleotemperature (d18O)") +
 theme_minimal()
```

General conclusions

This study proportionated an accurate analysis of the body size and mass of living and extinct crocodilians. More specifically, we used a comparative analysis of different methods based on cranial measurements in Caimaninae. We used a larger database containing almost all living species, including juvenile and adult specimens. Also, this study focused on the body proportions of the crocodilians, making a comparative approach with other analyses discussed over the research, and debated about the importance of the exclusion of the juveniles' specimens. Other than that, this work presented some estimates for total length and body mass that it was not done before, such as *Acresuchus pachytemporalis*, *Purussaurus mirandai*, *P. neivensis,* and *Purussaurus* sp. Furthermore, it was the first to make estimations based on head width measures for the group.

Body size and mass were positively correlated, being estimated from different approaches put forward in this chapter. The estimates using DCL measurements were effective, though it is necessary the use of a database containing only adult living specimens, turning estimates to be more conservative. The HW measurements return lower values, as discussed above in other crocodyliforms lineage. Thus, *Acresuchus pachytemporalis* reached 4.5 m in length and 494 kg in mass. The *Mourasuchus* species, in turn, were bigger than the generalized caimanine, being the largest species (*M. amazonensis*) reaching a size of 8.7 m and a mass of 3.6 tons, and the smallest species (*M. atopus*) with 5.4 m and 876 kg. The other two gulp-feeders, *M. arendsi* and *M. pattersoni,* could have reached 8.3 m and more than 3 tons. On the other hand, *Purussaurus* was the largest species that crocodyliforms had ever recorded, with *P. brasiliensis* reaching a total size of 10.8 m and weighing 7.1 tons. *P. mirandai* could reach 9.4 m and 4.7 tons in size and mass, respectively. The other smaller species were estimated to reach 7 m and 1.8 tons, and 6.8 m and 1.7 tons for *P. neivensis* and *Purussaurus* sp., respectively. Among the three studied

caimanine, *Acresuchus* was the smallest species; however, it is larger than the largest living caiman. Another small species was *Mourasuchus atopus*, which might have been similar in size as the largest current crocodile. As the quantitative analysis and body dimensions are increasing in paleontology, accurate analysis of the head width and dorsal cranial length proportions is important to denote these influences on the rest of the body.

The middle Miocene was marked by high temperature levels (Methner et al., 2020), which have influenced the evolution of different ecomorphotypes in crocodilians, mainly body sizes. On the other hand, the late Miocene was characterized by global cooling, and this climatic change could have affected the crocodilians' lifestyle and environment dynamic. Paleotemperature influenced mean and maximum body sizes, which temperature decline correlated with larger sizes. We infer that paleotemperature was not a limiting factor for their evolution, since reduced temperatures reduced the risk of overheating and not to variate much in their body temperature, due to less contact with the surface area provided by an increase in mass. However, in a certain moment of the evolution, the temperature decline coincided with the disappearance of the Pebas System, restricting food, habitat, niches, body sizes resembling, and increased competition.

Estimating their body temperature demonstrated that the crocodilians have variations in it, suggesting an ectothermic lifestyle, and previous studies show that an increase in the body mass, greater body temperature, favoring their metabolic rate. Nevertheless, larger crocodilians with high body temperature had the advantage to keep it constant, being gigantothermic with homeothermic conditions, as demonstrated for living crocodilians and turtles, and extinct crocodylomorphs (Paladino et al., 1990; Seebacher et al., 1999; Séon et al., 2020). Future works might evidence a deep study in their metabolism and unravel the mystery of being a lentic animal, with a low metabolic rate but having conditions as endothermic ones.

It is known that body size is influenced by ecological and physiological factors, such as diet, habitat, resources, behavior, predation, thermoregulation, and metabolic demand. Living on land consumes more energy for locomotion than living in water, so maybe these gigantic semi-aquatic crocodilians lived most of their life in water and just went on land to lay eggs. Another important factor is climate, which might have favored their metabolism, but this topic is poorly understood, once they are extinct animals. It is important to note that the same factors that influenced their body size evolution, have also led to their extinction. The habitat where they lived, Pebas and Acre systems, provided a lot of resources that gave them the advantage of being large and surviving for millions of years. Once this mega wetland disappeared in the late Miocene, the place was not habitable. Future studies could take abiotic questions to the core, and also a deep study of their metabolism, to deeply understand the physiological constraints and what helped them to grow so big.

BIBLIOGRAPHY

Aguilera, O. A. (2004). Tesoros paleontológicos de Venezuela: Urumaco, patrimonio natural de la humanidad. *Caracas: Editorial Arte*.

Aguilera, O. A., Riff, D., & Bocquentin-Villanueva, J. (2006). A new giant *Purussaurus* (crocodyliformes, alligatoridae) from the upper Miocene Urumaco formation, Venezuela. *Journal of Systematic Palaeontology*, *4*(3), 221-232.

Alvim, A. M. V., Santos, R. V., Roddaz, M., Antoine, P., Ramos, M. I. F., Carmo, D. A., Linhares, A. P., Negri, F. R. (2021). Fossil isotopic constraints (C, O and 87Sr/86Sr) on Miocene shallow-marine incursions in Amazonia. *Palaeogeography, Palaeoclimatology, Palaeoecology*, 110422.

Amiot, R., Lécuyer, C., Buffetaut, E., Escarguel, G., Fluteau, F., & Martineau, F. (2006). Oxygen isotopes from biogenic apatites suggest widespread endothermy in Cretaceous dinosaurs. *Earth and Planetary Science Letters*, *246*(1-2), 41-54.

Amiot, R., Lécuyer, C., Escarguel, G., Billon-Bruyat, J. P., Buffetaut, E., Langlois, C., Martin, S., Martineau, F., & Mazin, J. M. (2007). Oxygen isotope fractionation between crocodilian phosphate and water. *Palaeogeography, Palaeoclimatology, Palaeoecology*, *243*(3-4), 412-420.

Amiot, R., Angst, D., Legendre, S., Buffetaut, E., Fourel, F., Adolfssen, J., André, A., Bojar, A. V., Canoville, A., Barral, A., Goedert, J., Halas, S., Kusuhashi, N., Pestchevitskaya, E., Rey, K., Royer, A., Saraiva, A. A. F., Savary-Sismondini, B., Siméon, J., Touzeau, A., Zhou, Z., & Lécuyer, C. (2017). Oxygen isotope fractionation between bird bone phosphate and drinking water. *The Science of Nature*, *104*(5-6), 47.

Angilletta, Jr, M. J., & Dunham, A. E. (2003). The temperature-size rule in ectotherms: simple evolutionary explanations may not be general. *The American Naturalist*, *162*(3), 332-342.

Antoine, P., Abellho, M. A., Adnet, S., Sierra, A. J. A., Baby, P., Billet, G., Boivin, M., Calderón, Y., Candela, A., Chabain, J., Corfu, F., Croft, D. A., Ganerod, M., Jaramillo, C., Klaus, S., Marivaux, L., Navarrete, R. E., Orliac, M. J., Parra, F., Pérez, M. E., Pujos, F., Rage, J., Ravel, A., Robinet, C., Roddaz, M., Tejada-Lara, J. V., Vélez-Juarbe, J., Wesselingh, F. P., Salas-Gismondi, R. (2016). A 60-million-year Cenozoic history of western Amazonian ecosystems in Contamana, eastern Peru. *Gondwana Research*, *31*, 30-59.

Aureliano, T., Ghilardi, A. M., Guilherme, E., Souza-Filho, J. P., Cavalcanti, M., & Riff, D. (2015). Morphometry, bite-force, and paleobiology of the Late Miocene Caiman *Purussaurus brasiliensis*. *PloS one*, *10*(2), e0117944.

Bakker, R. T. (1986). *The dinosaur heresies: new theories unlocking the mystery of the dinosaurs and their extinction*. William Morrow.

Barbosa-Rodrigues, B. (1892). Les Reptiles fossiles de la vallée del'Amazone. Vellosia 2: 41-46.

Bernard, A., Lécuyer, C., Vincent, P., Amiot, R., Bardet, N., Buffetaut, E., Cuny, G., Fourel, F., Martineau, F., Mazin, J., & Prieur, A. (2010). Regulation of body temperature by some Mesozoic marine reptiles. *Science*, *328*(5984), 1379-1382.

Bissaro-Júnior, M. C., Kerber, L., Crowley, J. L., Ribeiro, A. M., Ghilardi, R. P., Guilherme, E., Negri, F. R., Souza-Filho, J. P., Hsiou, A. S. (2019). Detrital zircon U–Pb geochronology constrains the age of Brazilian Neogene deposits from Western Amazonia. *Palaeogeography, Palaeoclimatology, Palaeoecology*, *516*, 64-70.

Blanckenhorn, W. U. (2000). The evolution of body size: what keeps organisms small?. *The quarterly review of biology*, *75*(4), 385-407.

Blanco, R. E., Jones, W. W., & Villamil, J. (2015). The 'death roll'of giant fossil crocodyliforms (Crocodylomorpha: Neosuchia): allometric and skull strength analysis. *Historical biology*, *27*(5), 514-524.

Bocquentin-Villanueva, J. (1984). Un nuevo Nettosuchidae (Crocodylia, Eusuchia) proveniente de la Formación Urumaco (Mioceno Superior), Venezuela. *Ameghiniana*, *21*(1), 3-8.

Bocquentin-Villanueva, J., & Buffetaut, E. (1981). *Hesperogavialis cruxenti* n. gen., n. sp., nouveau gavialide (Crocodylia, Eusuchia) du Miocene Superieur (Huayquerien) d'Urumaco (Venezuela). *Géobios*, *14*(3), 415-419.

Böhme, M. (2003). The Miocene climatic optimum: evidence from ectothermic vertebrates of Central Europe. *Palaeogeography, Palaeoclimatology, Palaeoecology*, *195*(3-4), 389-401.

Bona, P. (2007). Una nueva especie de *Eocaiman* Simpson (Crocodylia, Alligatoridae) del Paleoceno Inferior de Patagonia. *Ameghiniana*, *44*(2), 435-445.

Bona, P., Riff, D., & de Gasparini, Z. B. (2012). Late Miocene crocodylians from northeast Argentina: new approaches about the austral components of the Neogene South American crocodylian fauna. *Earth and Environmental Science Transactions of the Royal Society of Edinburgh*, *103*(3-4), 551-570.

Bona, P., & Carabajal, A. P. (2013). *Caiman gasparinae* sp. nov., a huge alligatorid (Caimaninae) from the late Miocene of Paraná, Argentina. *Alcheringa: An Australasian Journal of Palaeontology*, *37*(4), 462-473.

Bona, P., Degrange, F. J., & Fernández, M. S. (2013). Skull anatomy of the bizarre crocodylian *Mourasuchus nativus* (Alligatoridae, Caimaninae). *The Anatomical Record*, *296*(2), 227-239.

Bona, P., Carabajal, A. P., & Gasparini, Z. (2015). Neuroanatomy of *Gryposuchus neogaeus* (Crocodylia, Gavialoidea): a first integral description of the braincase and endocranial morphological variation in extinct and extant gavialoids. *Earth and Environmental Science Transactions of the Royal Society of Edinburgh*, *106*(4), 235-246.

Bona, P., Blanco, M. V. F., Schever, T. M., & Both, C. (2017). Shedding light on the taxonomic diversity of the South American Miocene caimans: the status of *Melanosuchus fisheri* (Crocodylia, Alligatoroidea). *Ameghiniana*, *54*(6), 681-687.

Bona, P., Ezcurra, M. D., Barrios, F., & Fernandez Blanco, M. V. (2018). A new Palaeocene crocodylian from southern Argentina sheds light on the early history of caimanines. *Proceedings of the Royal Society B*, *285*(1885), 20180843.

Brisbin Jr, I. L., Standora, E. A., & Vargo, M. J. (1982). Body temperatures and behavior of American alligators during cold winter weather. *American Midland Naturalist*, 209-218.

Britton, A. R., Whitaker, R., & Whitaker, N. I. K. H. I. L. (2012). Here be a dragon: exceptional size in a saltwater crocodile (*Crocodylus porosus*) from the Philippines. *Herpetological Review*, *43*(4), 541-546.

Brochu, C. A. (1996). New eusuchian crocodyliforms from the Paleocene of West Texas: biogeographic and phylogenetic implications. In *Geological Society of America Abstracts with Programs* (Vol. 28, No. 6).

Brochu, C. A. (1999). Phylogenetics, taxonomy, and historical biogeography of Alligatoroidea. *Journal of Vertebrate Paleontology*, *19*(S2), 9-100.

Brochu, C. A. (2003). Phylogenetic approaches toward crocodylian history. *Annual Review of Earth and Planetary Sciences*, *31*(1), 357-397.

Brochu, C. A. (2011). Phylogenetic relationships of *Necrosuchus ionensis* Simpson, 1937 and the early history of caimanines. *Zoological journal of the linnean society*, *163*(suppl_1), S228-S256.

Bronzati, M., Montefeltro, F. C., & Langer, M. C. (2015). Diversification events and the effects of mass extinctions on Crocodyliformes evolutionary history. *Royal Society open science*, *2*(5), 140385.

Buchardt, B. (1978). Oxygen isotope palaeotemperatures from the Tertiary period in the North Sea area. *Nature*, *275*(5676), 121-123.

Campione, N. E., & Evans, D. C. (2020). The accuracy and precision of body mass estimation in non-avian dinosaurs. *Biological Reviews*, *95*(6), 1759-1797.

Campos, Z., Coutinho, M., & Magnusson, W. E. (2005). Field body temperatures of caimans in the Pantanal, Brazil. *The Herpetological Journal*, *15*(2), 97-106.

Cidade, G. M. (2015). *Revisão sistemática do gênero* Mourasuchus *(Alligatoroidea, Caimaninae), com comentários sobre filogenia, biogeografia e paleoecologia de Caimaninae* (Doctoral dissertation, Universidade de São Paulo).

Cidade, G. M. (2019). *Revisão filogenética de Alligatoroidea (Crocodylia) e revisão taxonômica das espécies do clado Caimaninae* (Doctoral dissertation, Universidade de São Paulo).

Cidade, G. M., & Rincón, A. D. (2021). The first occurrence of *Acresuchus* (Alligatoroidea, Caimaninae) from the Urumaco Formation of Venezuela and the late Miocene crocodylian fauna of northern South America. *Journal of South American Earth Sciences*, 103344.

Cidade, G. M., Solórzano, A., Rincón, A. D., Riff, D., & Hsiou, A. S. (2017). A new *Mourasuchus* (Alligatoroidea, Caimaninae) from the late Miocene of Venezuela, the phylogeny of Caimaninae and considerations on the feeding habits of *Mourasuchus*. *PeerJ*, *5*, e3056.

Cidade, G. M., Fortier, D., & Hsiou, A. S. (2019). The crocodylomorph fauna of the Cenozoic of South America and its evolutionary history: a review. *Journal of South American Earth Sciences, 90*, 392-411.

Cidade, G. M., Fortier, D., & Hsiou, A. S. (2020a). Taxonomic and phylogenetic review of *Necrosuchus ionensis* (Alligatoroidea: Caimaninae) and the early evolution and radiation of caimanines. *Zoological Journal of the Linnean Society, 189*(2), 657-669.

Cidade, G. M., Rincón, A. D., & Solórzano, A. (2020b). New cranial and postcranial elements of *Mourasuchus* (Alligatoroidea: Caimaninae) from the late Miocene of Venezuela and their palaeobiological implications. *Historical Biology*, 1-13.

Cooper, J. A., Pimiento, C., Ferrón, H. G., & Benton, M. J. (2020). Body dimensions of the extinct giant shark *Otodus megalodon*: a 2D reconstruction. *Scientific reports, 10*(1), 1-9.

Cossette, A. P., & Brochu, C. A. (2018). A new specimen of the alligatoroid *Bottosaurus harlani* and the early history of character evolution in alligatorids. *Journal of Vertebrate Paleontology, 38*(4), 1-22.

Cozzuol, M. A. (2006). The Acre vertebrate fauna: age, diversity, and geography. *Journal of South American Earth Sciences, 21*(3), 185-203.

Cubo, J., Sena, M. V., Aubier, P., Houee, G., Claisse, P., Faure-Brac, M. G., Allain, R., Andrade, R. C. L. P., Sayão, J. M. & Oliveira, G. R. (2020). Were Notosuchia (Pseudosuchia: Crocodylomorpha) warm-blooded? A palaeohistological analysis suggests ectothermy. *Biological Journal of the Linnean Society*, *131*(1), 154-162.

Cunha, P.R.C. (2007). Bacia do Acre. Bol. Geociencias Petrobras 15, 207–215.

Deem, V. R., Letter, A. W., Woodward, A. R., Ford, R. M., & Moore, B. C. (2021). Maximum Size of Female American Alligators and a New Record Total Length and Weight. *Southeastern Naturalist*, *20*(1), N7.

Díaz de Gamero, M. L., & Linares, O. J. (1989). Estratigrafía y paleontología de la Formación Urumaco, del Mioceno tardío de Falcón noroccidental. In *VII Congreso Geológico Venezolano, Memorias* (Vol. 1, pp. 419-438).

Erickson, G. M., & Brochu, C. A. (1999). How the 'terror crocodile'grew so big. *Nature*, *398*(6724), 205-206.

Erickson, G. M., Gignac, P. M., Steppan, S. J., Lappin, A. K., Kent, A. V., Brueggen, J. D., Inouye, B. D., Kledzik, D., Webb, G. J. W. (2012). Insights into the ecology and evolutionary success of crocodilians revealed through bite-force and tooth-pressure experimentation. *PLoS One*, *7*(3), e31781.

Farlow, J. O., & Planka, E. R. (2002). Body size overlap, habitat partitioning and living space requirements of terrestrial vertebrate predators: implications for the paleoecology of large theropod dinosaurs. *Historical Biology*, *16*(1), 21-40.

Farlow, J. O., Hurlburt, G. R., Elsey, R. M., Britton, A. R., & Langston Jr, W. (2005). Femoral dimensions and body size of *Alligator mississippiensis*: estimating the size of extinct mesoeucrocodylians. *Journal of Vertebrate Paleontology*, *25*(2), 354-369.

Farmer, C. G., & Sanders, K. (2010). Unidirectional airflow in the lungs of alligators. *Science*, *327*(5963), 338-340.

Flower, B. P., & Kennett, J. P. (1994). The middle Miocene climatic transition: East Antarctic ice sheet development, deep ocean circulation and global carbon cycling. *Palaeogeography, palaeoclimatology, palaeoecology*, *108*(3-4), 537-555.

Foth, C., Bona, P., & Desojo, J. B. (2015). Intraspecific variation in the skull morphology of the black caiman *Melanosuchus niger* (Alligatoridae, Caimaninae). *Acta Zoologica*, *96*(1), 1-13.

Foth, C., Blanco, M. V. F., Bona, P., & Scheyer, T. M. (2018). Cranial shape variation in jacarean caimanines (Crocodylia, Alligatoroidea) and its implications in the taxonomic status of extinct species: the case of *Melanosuchus fisheri*. *Journal of Morphology*, *279*(2), 259-273.

Fortier, D. C. (2011). O Registro fóssil de Crocodilianos na América do Sul: estudo da arte, análise crítica e registro de novos materiais para o cenozóico.

Fortier, D. C., De Souza-Filho, J. P., Guilherme, E., Maciente, A. A., & Schultz, C. L. (2014). A new specimen of *Caiman brevirostris* (Crocodylia, Alligatoridae) from the Late Miocene of Brazil. *Journal of Vertebrate Paleontology*, *34*(4), 820-834.

Fox, J., & Weisberg, S. (2019). *An R companion to applied regression*. Third Edition. Sage publications.

Garnier, S. (2021) viridis: Colorblind-Friendly color maps for R.

Gearty, W., & Payne, J. L. (2020). Physiological constraints on body size distributions in Crocodyliformes. *Evolution*, *74*(2), 245-255.

Gignac, P., & O'Brien, H. (2016). Suchian feeding success at the interface of ontogeny and macroevolution. *Integrative and Comparative Biology*, *56*(3), 449-458.

Gillooly, J. F., Allen, A. P., & Charnov, E. L. (2006). Dinosaur fossils predict body temperatures. *PLoS biology*, *4*(8), e248.

Godoy, P. L. (2014). *Osteologia e filogenia de dois Crocodyliformes fósseis:* Aplestosuchus sordidus *do Cretáceo do Brasil e* Eocaiman cavernensis *do Eoceno da Argentina* (Doctoral dissertation, Universidade de São Paulo).

Godoy, P. L. (2020). Crocodylomorph cranial shape evolution and its relationship with body size and ecology. *Journal of evolutionary biology*, *33*(1), 4-21.

Godoy, P. L., & Turner, A. H. (2020) Body Size Evolution in Crocodylians and Their Extinct Relatives. *eLS*, *1*, 442-452.

Godoy, P. L., Benson, R. B., Bronzati, M., & Butler, R. J. (2019). The multi-peak adaptive landscape of crocodylomorph body size evolution. *BMC evolutionary biology*, *19*(1), 1-29.

Godoy, P. L., Cidade, G. M., Montefeltro, F. C., Langer, M. C., & Norell, M. A. (2021). Redescription and phylogenetic affinities of the caimanine *Eocaiman cavernensis* (Crocodylia, Alligatoroidea) from the Eocene of Argentina. *Papers in Palaeontology*.

Gomes, B. T., Absy, M. L., D'Apolito, C., Caballero-Rodríguez, D., Martínez, C., & Jaramillo, C. (2021). Miocene paleoenvironments and paleoclimatic reconstructions based on the palynology of the Solimões Formation of western Amazonia (Brazil). *Palynology*, (just-accepted), 1980129.

Grigg, G. & Kirshner, D. (2015). Biology and Evolution of Crocodylians.

Grigg, G. C., Seebacher, F., Beard, L. A., & Morris, D. (1998). Thermal relations of large crocodiles, *Crocodylus porosus*, free—ranging in a naturalistic situation. *Proceedings of the Royal Society of London. Series B: Biological Sciences*, *265*(1407), 1793-1799.

Guerrero, J. (1997). Stratigraophy, sedimentary environments, and the Miocene uplift of the Colombian Andes. *Vertebrate Paleontology in the Neotropics*, 15-43.

Hastings, A. K., Bloch, J. I., Jaramillo, C. A., Rincon, A. F., & MacFadden, B. J. (2013). Systematics and biogeography of crocodylians from the Miocene of Panama. *Journal of Vertebrate Paleontology*, *33*(2), 239-263.

Holbourn, A., Kuhnt, W., Kochhann, K. G., Andersen, N., & Sebastian Meier, K. J. (2015). Global perturbation of the carbon cycle at the onset of the Miocene Climatic Optimum. *Geology*, *43*(2), 123-126.

Holliday, C. M., & Gardner, N. M. (2012). A new eusuchian crocodyliform with novel cranial integument and its significance for the origin and evolution of Crocodylia. *PloS one*, *7*(1), e30471.

Hone, D. W., & Benton, M. J. (2005). The evolution of large size: how does Cope's Rule work?. *Trends in Ecology & Evolution*, *20*(1), 4-6.

Hoorn, C. (1993). Marine incursions and the influence of Andean tectonics on the Miocene depositional history of northwestern Amazonia: results of a palynostratigraphic study. *Palaeogeography, palaeoclimatology, palaeoecology*, *105*(3-4), 267-309.

Hoorn, C. (2006). The birth of the mighty Amazon. *Scientific American*, *294*(5), 52-59.

Hoorn, C., Wesselingh, F. P., Ter Steege, H., Bermudez, M. A., Mora, A., Sevink, J., Sanmartín, I., Sanchez-Meseguer, A., Anderson, C. L., Figueiredo, J. P., Jaramillo, C., Riff, D., Negri, F. R., Hooghiemstra, H., Lundberg, J., Stadler, T., Särkinen, T., & Antonelli, A. (2010a). Amazonia through time: Andean uplift, climate change, landscape evolution, and biodiversity. *science*, *330*(6006), 927-931.

Hoorn, C., Wesselingh, F. P., Hovikoski, J., & Guerrero, J. (2010b). The development of the amazonian mega-wetland (Miocene; Brazil, Colombia, Peru, Bolivia). *Amazonia, landscape and species evolution: a look into the past*, *123*, 142.

Hsiou, A. S. (2010). Lagartos e serpentes (Lepidosauria, Squamata) do Mioceno Médio-Superior da regiao norte da América do Sul.

Hurlburt, G. R., Heckert, A. B., & Farlow, J. O. (2003). Body mass estimates of phytosaurs (Archosauria: Parasuchidae) from the Petrified Forest Formation (Chinle Group: Revueltian) based on skull and limb bone measurements. *New Mex Mus Nat Hist Sci Bull*, *24*, 105-113.

Iijima, M., & Kubo, T. (2020). Vertebrae-based body length estimation in crocodylians and its implication for sexual maturity and the maximum sizes. *Integrative Organismal Biology*, *2*(1), obaa042.

Jaramillo, C., Romero, I., D'Apolito, C., Bayona, G., Duarte, E., Louwye, S., Escobar, J.; Luque, J.; Carrillo-Briceno, J. D.; Zapata, V.; Mora, A.; Schouten, S.; Zavada, M.; Harrington, G.; Ortiz, J.; Wesselingh, F. P. (2017). Miocene flooding events of western Amazonia. *Science advances*, *3*(5), e1601693.

Kaandorp, R. J., Vonhof, H. B., Wesselingh, F. P., Pittman, L. R., Kroon, D., & van Hinte, J. E. (2005). Seasonal Amazonian rainfall variation in the Miocene climate optimum. *Palaeogeography, Palaeoclimatology, Palaeoecology*, *221*(1-2), 1-6.

Lacerda, M. B. S., Souza, R. G., & Romano, P. S. R. (2017). Novos espécimes de Caimaninae (crocodylia, Alligatoroidea) do município de Sena madureira, formação Solimões (bacia do Acre). In *Anais do XXV Congresso Brasileiro de Paleontologia* (p. 160). Ribeirão Preto-São Paulo.

Lacerda, M. B. S., Souza, L. G., Lobo, L. S., Schaefer, C. E. G., & Romano, P. S. R. (2020). New outcrop with vertebrate remains from Solimões Formation (Eocene–Pliocene), Southern Solimões Basin, Acre State, Northern Brazil. *Journal of South American Earth Sciences*, *101*, 102588.

Langston, W. (1965). *Fossil crocodilians from Colombia and the Cenozoic history of the Crocodilia in South America* (Vol. 52). University of California press.

Langston, W. (2008). Notes on a partial skeleton of Mourasuchus (Crocodylia, Nettosuchidae) from the Upper Miocene of Venezuela. *Arquivos do Museu Nacional*, *66*(1), 125-143.

Langston, W., & Gasparini, Z. (1997). Crocodilians, *Gryposuchus*, and the south American gavials. *Vertebrate Paleontology in the Neotropics: the Mio− cene Fauna of La Venta, Colombia*, 113-154.

Latrubesse, E. M., Cozzuol, M., da Silva-Caminha, S. A., Rigsby, C. A., Absy, M. L., & Jaramillo, C. (2010). The Late Miocene paleogeography of the Amazon Basin and the evolution of the Amazon River system. *Earth-Science Reviews*, *99*(3-4), 99-124.

Lécuyer, C., Bogey, C., Garcia, J. P., Grandjean, P., Barrat, J. A., Floquet, M., Bardet, M., & Pereda-Superbiola, X. (2003). Stable isotope composition and rare earth element content of vertebrate remains from the Late Cretaceous of northern Spain (Laño): did the environmental record survive?. *Palaeogeography, Palaeoclimatology, Palaeoecology*, *193*(3-4), 457-471.

Lécuyer, C., Amiot, R., Touzeau, A., & Trotter, J. (2013). Calibration of the phosphate δ18O thermometer with carbonate–water oxygen isotope fractionation equations. *Chemical Geology*, *347*, 217-226.

Leite, F. P., Paz, J., do Carmo, D. A., & Silva-Caminha, S. A. (2017). The effects of the inception of Amazonian transcontinental drainage during the Neogene on the landscape and vegetation of the Solimões Basin, Brazil.

Linares, O. J. (2004). Bioestratigrafia de la fauna de mamíferos de las Formaciones Socorro, Urumaco y Codore (Mioceno medio-Plioceno temprano) de la región de Urumaco, Falcón, Venezuela. *Paleobiologia Neotropical*, *1*, 1-26.

Longinelli, A., & Nuti, S. (1973). Revised phosphate-water isotopic temperature scale. *Earth and Planetary Science Letters, 19*(3), 373-376.

Lyons, S. K., & Smith, F. A. (2010). Using macroecological approach to study geographic range, abundance and body size in the fossil record. *Quantitative methods in paleobiology. Paleontological Society Papers, 16*, 117-141.

Makarieva, A. M., Gorshkov, V. G., & Li, B. L. (2005). Gigantism, temperature and metabolic rate in terrestrial poikilotherms. *Proceedings of the Royal Society B: Biological Sciences*, *272*(1578), 2325-2328.

Mannion, P. D., Benson, R. B., Carrano, M. T., Tennant, J. P., Judd, J., & Butler, R. J. (2015). Climate constrains the evolutionary history and biodiversity of crocodylians. *Nature communications*, *6*(1), 1-9.

Mannion, P. D., Chiarenza, A. A., Godoy, P. L., & Cheah, Y. N. (2019). Spatiotemporal sampling patterns in the 230 million year fossil record of terrestrial crocodylomorphs and their impact on diversity. *Palaeontology*, *62*(4), 615-637.

Markwick, P. J. (1998). Fossil crocodilians as indicators of Late Cretaceous and Cenozoic climates: implications for using palaeontological data in reconstructing palaeoclimate. *Palaeogeography, Palaeoclimatology, Palaeoecology, 137*(3-4), 205-271.

Mateus, O., Puértolas-Pascual, E., & Callapez, P. M. (2019). A new eusuchian crocodylomorph from the Cenomanian (Late Cretaceous) of Portugal reveals novel implications on the origin of Crocodylia. *Zoological Journal of the Linnean Society*, *186*(2), 501-528.

McAliley, L. R., Willis, R. E., Ray, D. A., White, P. S., Brochu, C. A., & Densmore III, L. D. (2006). Are crocodiles really monophyletic?—Evidence for subdivisions from sequence and morphological data. *Molecular Phylogenetics and Evolution*, *39*(1), 16-32.

Methner, K., Campani, M., Fiebig, J., Löffler, N., Kempf, O., & Mulch, A. (2020). Middle Miocene long-term continental temperature change in and out of pace with marine climate records. *Scientific reports*, *10*(1), 1-10.

Meyer, F., & Perrier, V. (2020). esquisse: Explore and Visualize Your Data Interactively. *URL: https://github. com/dreamRs/esquisse/. R package version 0.3. 0.900. Accessed*, *21*.

Mook, C. C. (1942). A new fossil Crocodilian from Colombia. *Proceedings of the United States National Museum*.

Moreno-Bernal, J. W., Head, J., & Jaramillo, C. A. (2016). Fossil crocodilians from the High Guajira Peninsula of Colombia: Neogene faunal change in northernmost South America. *Journal of Vertebrate Paleontology*, *36*(3), e1110586.

Negri, F. R., Bocquentin-Villanueva, J., Ferigolo, J., & Antoine, P. O. (2009). A review of Tertiary mammal faunas and birds from western Amazonia. *Amazonia: Landscape and Species Evolution: A look into the past*, 243-258.

Nesbitt, S. J. (2009). *The early evolution of archosaurs: relationships and the origin of major clades*. Columbia University.

O'Brien, H. D., Lynch, L. M., Vliet, K. A., Brueggen, J., Erickson, G. M., & Gignac, P. M. (2019). Crocodylian head width allometry and phylogenetic prediction of body size in extinct crocodyliforms. *Integrative Organismal Biology*, *1*(1), obz006.

Paladino, F. V., O'Connor, M. P., & Spotila, J. R. (1990). Metabolism of leatherback turtles, gigantothermy, and thermoregulation of dinosaurs. *Nature*, *344*(6269), 858-860.

Paolillo, A., & Linares, O. J. (2007). Nuevos cocodrilos sebecosuchia del cenozoico suramericano (Mesosuchia: Crocodylia). *Paleobiologia Neotropical*, *3*, 1-25.

Peng, R. D. (2019). Simpleboot: simple bootstrap routines. *R package version*, *1*, 1-3.

Pinheiro, A. E., Fortier, D. C., Pol, D., Campos, D. A., & Bergqvist, L. P. (2013). A new *Eocaiman* (Alligatoridae, Crocodylia) from the Itaboraí Basin, Paleogene of Rio de Janeiro, Brazil. *Historical Biology*, *25*(3), 327-337.

Pinheiro, J., Bates, D., DebRoy, S., Sarkar, D., Heisterkamp, S., Van Willigen, B., & Ranke, J. (2021). Package 'nlme'. *Linear and nonlinear mixed effects models, version*, *3*(1).

Price, L. I. (1964). Sobre o cranio de um grande crocodilideo extinto do Alto Rio Jurua, Estado do Acre. *Anais da Academia Brasileira de Ciências*, *56*, 59-66. Pouech, J., Amiot, R., Lécuyer, C., Mazin, J. M., Martineau, F., & Fourel, F. (2014). Oxygen isotope composition of vertebrate phosphates from Cherves-de-Cognac (Berriasian, France): environmental and ecological significance. *Palaeogeography, Palaeoclimatology, Palaeoecology*, *410*, 290-299.

Price, L. I. (1967). Sobre a mandíbula de um gigantesco crocodilídeo extinto do alto Rio Juruá, Estado do Acre. *Atas Simpósio sobre a Biota Amazônica (Geociências). Belém: Sociedade Brasileira de Paleontologia*, *1*, 359-371.

Prokoph, A., Shields, G. A., & Veizer, J. (2008). Compilation and time-series analysis of a marine carbonate δ18O, δ13C, 87Sr/86Sr and δ34S database through Earth history. *Earth-Science Reviews*, *87*(3-4), 113-133.

Pucéat, E., Lécuyer, C., Sheppard, S. M., Dromart, G., Reboulet, S., & Grandjean, P. (2003). Thermal evolution of Cretaceous Tethyan marine waters inferred from oxygen isotope composition of fish tooth enamels. *Paleoceanography*, *18*(2).

R Core Team (2020). R: A language and environment for statistical computing.

Rey, K., Amiot, R., Lécuyer, C., Koufos, G. D., Martineau, F., Fourel, F., Kostopoulos, D. S., & Merceron, G. (2013). Late Miocene climatic and environmental variations in northern Greece inferred from stable isotope compositions (δ18O, δ13C) of equid teeth apatite. *Palaeogeography, Palaeoclimatology, Palaeoecology*, *388*, 48-57.

Riff, D., & Aguilera, O. A. (2008). The world's largest gharials *Gryposuchus*: description of *G. croizati* n. sp. (Crocodylia, Gavialidae) from the Upper Miocene Urumaco Formation, Venezuela. *Paläontologische zeitschrift*, *82*(2), 178-195.

Riff, D., R. Romano, P. S., Oliveira, G. R., & Aguilera, O. A. (2009). Neogene crocodile and turtle fauna in northern South America. *Amazonia: Landscape and Species Evolution: A look into the past*, 259-280.

Riff, D., Souza, R. G. D., Cidade, G. M., Martinelli, A. G., & Souza-Filho, J. P. (2012). Crocodilomorfos: a maior diversidade de répteis fósseis do Brasil. *Terræ*, *9* (1/2), 12-40.

Robinson, D., Hayes, A., Couch, S. (2021). broom: converting statistical analysis objects into tidy tibbles.

Royer, A., Lécuyer, C., Montuire, S., Amiot, R., Legendre, S., Cuenca-Bescós, G., Jeannet, M., & Martineau, F. (2013). What does the oxygen isotope composition of rodent teeth record?. *Earth and Planetary Science Letters*, *361*, 258-271.

Rusconi, C. (1931). Sobre un diente de un gigantesco cocodriliano extinguido, procedente de territorio boliviano. *La Semana Medica, Buenos Aires*, *38*, 531-533.

Rusconi, C. (1937). Nuevo aligatorino del Paleoceno argentino. *Boletin Paleontologico de Buenos Aires*, *8*, 1-5.

Sá, N. P., Carvalho, M. A. & Correia, G. C. (2020). Miocene paleoenvironmental changes in the Solimões Basin, western Amazon, Brazil: A reconstruction based on palynofacies analysis. *Palaeogeography, Palaeoclimatology, Palaeoecology*, *537*, 109450.

Salas-Gismondi, R., Antoine, P.-O., Baby, P., Brusset, S., Benammi, M., Espurt, N., de Franceschi, D., Pujos, F., Tejada, J., Urbina, M. (2007). Middle Miocene crocodiles from the Fitzcarrald Arch, Amazonian Peru. *Cuadernos del Museo Geominero*, *8*, 355-360.

Salas-Gismondi, R., Flynn, J. J., Baby, P., Tejada-Lara, J. V., Wesselingh, F. P., & Antoine, P. O. (2015). A Miocene hyperdiverse crocodylian community reveals peculiar trophic dynamics in proto-Amazonian mega-wetlands. *Proceedings of the Royal Society B: Biological Sciences*, *282*(1804), 20142490.

Sánchez-Villagra, M. R., & Aguilera, O. A. (2006). Neogene vertebrates from Urumaco, Falcón State, Venezuela: diversity and significance. *Journal of Systematic Palaeontology*, *4*(3), 213-220.

Scharf, I., Nulman, E., Ovadia, O., & Bouskila, A. (2006). Efficiency evaluation of two competing foraging modes under different conditions. *The American Naturalist*, *168*(3), 350-357.

Scheyer, T. M., & Delfino, M. (2016). The late Miocene caimanine fauna (Crocodylia: alligatoroidea) of the Urumaco Formation, Venezuela. *Palaeontologia Electronica*, *19*(3), 1-57.

Scheyer, T. M., Aguilera, O. A., Delfino, M., Fortier, D. C., Carlini, A. A., Sánchez, R., Carrillo-Briceño, J. D., Quiroz, L., Sánchez-Villagra, M. R. (2013). Crocodylian diversity peak and extinction in the late Cenozoic of the northern Neotropics. *Nature communications*, *4*(1), 1-9.

Schwimmer, D. R. (2002). *King of the crocodylians: the paleobiology of* Deinosuchus. Indiana University Press.

Seebacher, F. (2000). Heat transfer in a microvascular network: the effect of heart rate on heating and cooling in reptiles (Pogona barbata and Varanus varius). *Journal of Theoretical Biology*, *203*(2), 97-109.

Seebacher, F. (2003). Dinosaur body temperatures: the occurrence of endothermy and ectothermy. *Paleobiology*, *29*(1), 105-122.

Seebacher, F., & Franklin, C. E. (2007). Redistribution of blood within the body is important for thermoregulation in an ectothermic vertebrate (Crocodylus porosus). *Journal of Comparative Physiology B*, *177*(8), 841-848.

Seebacher, F., Grigg, G. C., & Beard, L. A. (1999). Crocodiles as dinosaurs: behavioural thermoregulation in very large ectotherms leads to high and stable body temperatures. *Journal of Experimental Biology*, *202*(1), 77-86.

Seebacher, F., Elsey, R. M., & Trosclair III, P. L. (2003). Body temperature null distributions in reptiles with nonzero heat capacity: seasonal thermoregulation in the American alligator (Alligator mississippiensis). *Physiological and Biochemical Zoology*, *76*(3), 348-359.

Seidel, M. R. (1979). The osteoderms of the American alligator and their functional significance. *Herpetologica*, 375-380.

Séon, N., Amiot, R., Martin, J. E., Young, M. T., Middleton, H., Fourel, F., Picot, L., Valentin, X. & Lécuyer, C. (2020). Thermophysiologies of Jurassic marine crocodylomorphs inferred from the oxygen isotope composition of their tooth apatite. *Philosophical Transactions of the Royal Society B*, *375*(1793), 20190139.

Sereno, P. C., Larsson, H. C., Sidor, C. A., & Gado, B. (2001). The giant crocodyliform *Sarcosuchus* from the Cretaceous of Africa. *Science*, *294*(5546), 1516-1519.

Seymour, R. S. (1987). Scaling of cardiovascular physiology in snakes. *American Zoologist*, *27*(1), 97-109.

Seymour, R. S. (2013). Maximal aerobic and anaerobic power generation in large crocodiles versus mammals: implications for dinosaur gigantothermy. *PLoS One*, *8*(7), e69361.

Seymour, R. S. (2016). Cardiovascular physiology of dinosaurs. *Physiology*, *31*(6), 430-441.

Seymour, R. S., Bennett-Stamper, C. L., Johnston, S. D., Carrier, D. R., & Grigg, G. C. (2004). Evidence for endothermic ancestors of crocodiles at the stem of archosaur evolution. *Physiological and Biochemical Zoology*, *77*(6), 1051-1067.

Seymour, R. S., Smith, S. L., White, C. R., Henderson, D. M., & Schwarz-Wings, D. (2012). Blood flow to long bones indicates activity metabolism in mammals, reptiles and dinosaurs. *Proceedings of the Royal Society B: Biological Sciences*, *279*(1728), 451-456.

Seymour, R. S., Gienger, C. M., Brien, M. L., Tracy, C. R., Manolis, S. C., Webb, G. J., & Christian, K. A. (2013). Scaling of standard metabolic rate in estuarine crocodiles *Crocodylus porosus*. *Journal of Comparative Physiology B*, *183*(4), 491-500.

Sievert, C., Parmer, C., Hocking T., Chamberlain, S., Ram, K., Corvellec, M., Despouy, P. (2021). Plotly: Create i*nteractive web graphs via "plotly.js"*.

Simpson, G. G. (1933). A new crocodilian from the Notostylops beds of Patagonia. American Museum novitates; no. 623.

Simpson, G. G. (1937). An ancient eusuchian crocodile from Patagonia. American Museum novitates; no. 965.

Singer, D., Bach, F., Bretschneider, H. J., & Kuhn, H. J. (1993). Metabolic size allometry and the limits to beneficial metabolic reduction: hypothesis of a uniform specific minimal metabolic rate. *Surviving Hypoxia Mechanisms of Control and Adaptation*, 447-458.

Smith, E. N. (1976). Heating and cooling rates of the American alligator, *Alligator mississippiensis*. *Physiological Zoology*, *49*(1), 37-48.

Solórzano, A., Rincón, A. D., Cidade, G. M., Núñez-Flores, M., & Sánchez, L. (2019). Lower Miocene alligatoroids (Crocodylia) from the Castillo Formation, northwest of Venezuela. *Palaeobiodiversity and Palaeoenvironments*, *99*(2), 241-259.

Solórzano, A., Núñez-Flores, M., Inostroza-Michael, O., & Hernández, C. E. (2020). Biotic and abiotic factors driving the diversification dynamics of Crocodylia. *Palaeontology*, *63*(3), 415-429.

Souza, R. G., Cidade, G. M., Campos, D. D. A., & Riff, D. (2016). New crocodylian remains from the Solimões Formation (lower eocene–pliocene), state of Acre, southwestern Brazilian Amazonia. *Revista brasileira de paleontologia*, *19*(2), 217-232.

Souza, L. G., Bandeira, K. L., Pêgas, R. V., Brum, A. S., Machado, R., Guilherme, E., Loboda, T., & SOUZA-FILHO, J. P. (2021). The history, importance and anatomy of the specimen that validated the giant Purussaurus brasiliensis Barbosa-Rodrigues 1892 (Crocodylia: Caimaninae). *Anais da Academia Brasileira de Ciências*, *93*.

Souza-Filho, J. P., & Guilherme, E. (2011). Ampliação da diagnose e primeiro registro de Mourasuchus arendsi (Crocodylia-Nettosuchidae) no Neógeno da Formação Solimões, Amazônia sul-ocidental. *Paleontologia: cenários de Vida*, *1*, 399-408.

Souza-Filho, J. P., Souza, R. G., Hsiou, A. S., Riff, D., Guilherme, E., Negri, F. R., & Cidade, G. M. (2018). A new caimanine (Crocodylia, Alligatoroidea) species from the Solimões Formation of Brazil and the phylogeny of Caimaninae. *Journal of Vertebrate Paleontology*, *38*(5), e1528450.

Souza-Filho, J. P., Guilherme, E., De Toledo, P. M., Carvalho, I. D. S., Negri, F. R., Maciente, A. A. D. R., Cidade, G. M., Lacerda, M. B. S., & De Souza, L. G. (2020). On a new Melanosuchus species (Alligatoroidea: Caimaninae) from Solimões Formation (Eocene-Pliocene), Northern Brazil, and evolution of Caimaninae. *Zootaxa*, *4894*(4), 561-593.

Spotila, J. R., Lommen, P. W., Bakken, G. S., & Gates, D. M. (1973). A mathematical model for body temperatures of large reptiles: implications for dinosaur ecology. *The American Naturalist*, *107*(955), 391-404.

Stanley, S. M. (1973). An explanation for Cope's rule. *Evolution*, 1-26.

Steinthorsdottir, M., Coxall, H. K., Boer, A. M., Huber, M., Barbolini, N., Bradshaw, C. D., Burls, N. J., Feakins, S. J., Gasson, E., Henderiks, J., Holbourn, A., Kiel, S., Kohn, M. J., Knorr, G., Kürschner, W. M., Lear, C. H., Liebrand, D., Lunt, D. J., Mörs, T., Pearson, P. N., Pound, M. J., Stoll, H., Strömberg, C. A. E. (2021). The Miocene: The future of the past. *Paleoceanography and Paleoclimatology*, *36*(4), e2020PA004037.

Stockdale, M. T., & Benton, M. J. (2021). Environmental drivers of body size evolution in crocodile-line archosaurs. *Communications biology*, *4*(1), 1-11.

Stocker, M. R., Brochu, C. A., & Kirk, E. C. (2021). A new caimanine alligatorid from the Middle Eocene of Southwest Texas and implications for spatial and temporal shifts in Paleogene crocodyliform diversity. *PeerJ*, *9*, e10665.

Stubbs, T. L., Pierce, S. E., Elsler, A., Anderson, P. S., Rayfield, E. J., & Benton, M. J. (2021). Ecological opportunity and the rise and fall of crocodylomorph evolutionary innovation. *Proceedings of the Royal Society B*, *288*(1947), 20210069.

Super, J. R., Thomas, E., Pagani, M., Huber, M., O'Brien, C., & Hull, P. M. (2018). North Atlantic temperature and pCO2 coupling in the early-middle Miocene. *Geology*, *46*(6), 519-522.

Thorbjarnarson, J. B. (2010). Black caiman *Melanosuchus niger*. *Crocodiles. Status survey and conservation action plan*, *3*, 29-39.

Tineo, D. E., Bona, P., Pérez, L. M., Vergani, G. D., González, G., Poiré, D. G., Gasparini Z., Legarreta, P. (2015). Palaeoenvironmental implications of the giant crocodylian *Mourasuchus* (Alligatoridae, Caimaninae) in the Yecua Formation (late Miocene) of Bolivia. *Alcheringa: An Australasian Journal of Palaeontology*, *39*(2), 224-235.

Tykoski, R. S., Rowe, T. B., Ketcham, R. A., & Colbert, M. W. (2002). *Calsoyasuchus valliceps*, a new crocodyliform from the Early Jurassic Kayenta Formation of Arizona. *Journal of Vertebrate Paleontology*, *22*(3), 593-611.

Verdade, L. M. (1995). Biologia reprodutiva do jacaré-de-papo-amarelo (*Caiman latirostris*) em São Paulo, Brasil. *Conservación y manejo de los Crocodylia de America Latina*, *1*, 57-79.

Verdade, L. M. (2000). Regression equations between body and head measurements in the broad-snouted caiman (*Caiman latirostris*). *Revista Brasileira de Biologia*, *60*(3), 469-482.

Verdade, L. M., & Piña, C. I. (2006). *Caiman latirostris*. *Catalogue of American Amphibians and Reptiles (CAAR)*.

Walter, J., Darlim, G., Massonne, T., Aase, A., Frey, E., & Rabi, M. (2021). On the origin of Caimaninae: insights from new fossils of Tsoabichi greenriverensis and a review of the evidence. *Historical Biology*, 1-16.

Webb, G. J. W., Messel, H., Crawford, J., & Yerbury, M. J. (1978). Growth rates of *Crocodylus porosus* (Reptilia: Crocodilia) from Arnhem Land, northern Australia. *Wildlife Research*, *5*(3), 385-399.v

Wesselingh, F. P., & Salo, J. A. (2006). A Miocene perspective on the evolution of the Amazonian biota. *Scripta Geologica*, *133*, 439-458.

Wesselingh, F. P., Guerrero, J., Räsänen, M. E., Romero Pittman, L., & Vonhof, H. B. (2006). Landscape evolution and depositional processes in the Miocene Amazonian Pebas lake/wetland system: evidence from exploratory boreholes in northeastern Peru. *0375-7587*.

Wickham, H. (2016). ggplot2: Elegant Graphics for Data Analysis. Springer-Verlag New York.

Wickham, H., & Bryan, J. (2019). Package 'readxl'.

Wilberg, E. W. (2017). Investigating patterns of crocodyliform cranial disparity through the Mesozoic and Cenozoic. *Zoological Journal of the Linnean Society*, *181*(1), 189-208.

Woodward, A. R., White, J. H., & Linda, S. B. (1995). Maximum size of the alligator (*Alligator mississippiensis*). *Journal of Herpetology*, 507-513.

Wu, X. B., Xue, H., Wu, L. S., Zhu, J. L., & Wang, R. P. (2006). Regression analysis between body and head measurements of Chinese alligators (Alligator sinensis) in the captive population. *Animal biodiversity and conservation*, *29*(1), 65-71.

Young, M. T., Rabi, M., Bell, M. A., Foffa, D., Steel, L., Sachs, S., & Peyer, K. (2016). Big-headed marine crocodyliforms and why we must be cautious when using extant species as body length proxies for long-extinct relatives. *Palaeontologia Electronica*, *19*(3), 1-14.

Zachos, J. C., Dickens, G. R., & Zeebe, R. E. (2008). An early Cenozoic perspective on greenhouse warming and carbon-cycle dynamics. *Nature*, *451*(7176), 279-283.